SAND2012-6020C

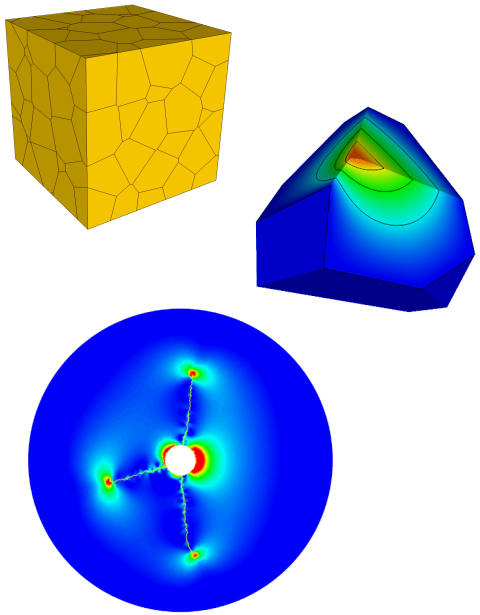

A Polyhedral Finite-Element Formulation using Harmonic Shape Functions with Applications to the Modeling of Multi-Physics Fracture Processes

Joe Bishop
Computational Structural Mechanics and Applications
Sandia National Laboratories
Albuquerque, NM

NSF Workshop on Barycentric Coordinates in Geometry Processing and Finite/Boundary Element Methods
Columbia University, New York, USA
July 25–27, 2012

This material is based upon work supported as part of the Center for Frontiers of Subsurface Energy Security, an Energy Frontier Research Center funded by the U.S. Department of Energy, Office of Science, Office of Basic Energy Sciences under Award Number DE-SC0001114.

Sandia National Laboratories

U.S. DEPARTMENT OF ENERGY

NNSA National Nuclear Security Administration

Sandia National Laboratories is a multi-program laboratory managed and operated by Sandia Corporation, a wholly owned subsidiary of Lockheed Martin Corporation, for the U.S. Department of Energy's National Nuclear Security Administration under contract DE-AC04-94AL85000.

Sandia National Laboratories

Outline

1. Pervasive fracture and fragmentation
2. Random meshes and a polyhedral finite-element formulation
3. Assessing mesh convergence in a probabilistic sense
4. Example of statistical convergence using dynamic ring expansion
5. What is material variability?
6. Summary

Pervasive Fracture

blast induced structural collapse

USS Cole

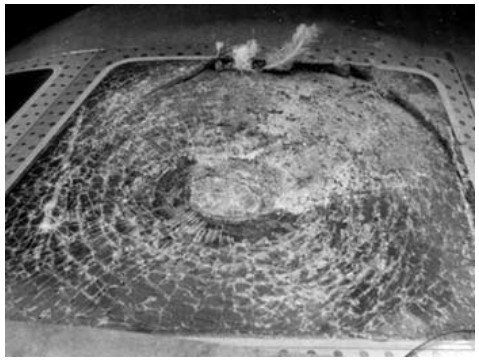

bird strike

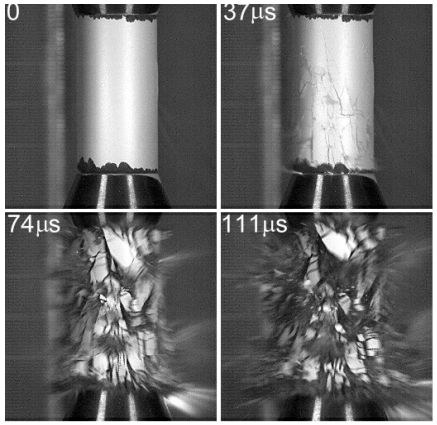

dynamic pervasive fracture

- crack branching
- crack coalescence
- tortuous crack paths
  (sensitivity to material heterogeneity)
- stochastic behavior

Geomechanics Applications

Sandia National Laboratories

Engineered Geothermal

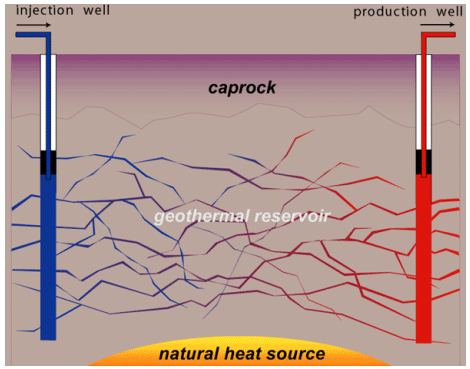

Nuclear Waste Isolation

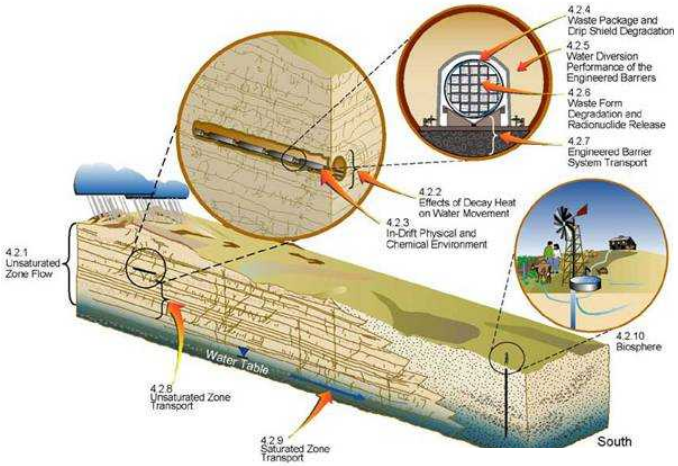

CO_2 Sequestration

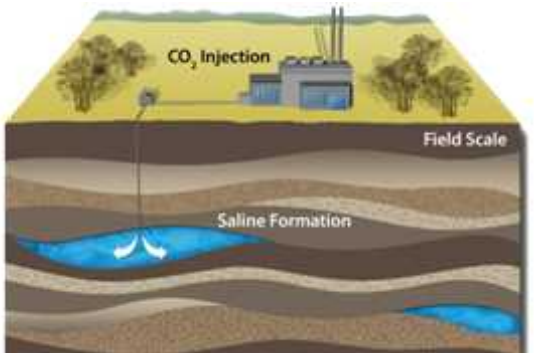

Compressed Air Energy Storage

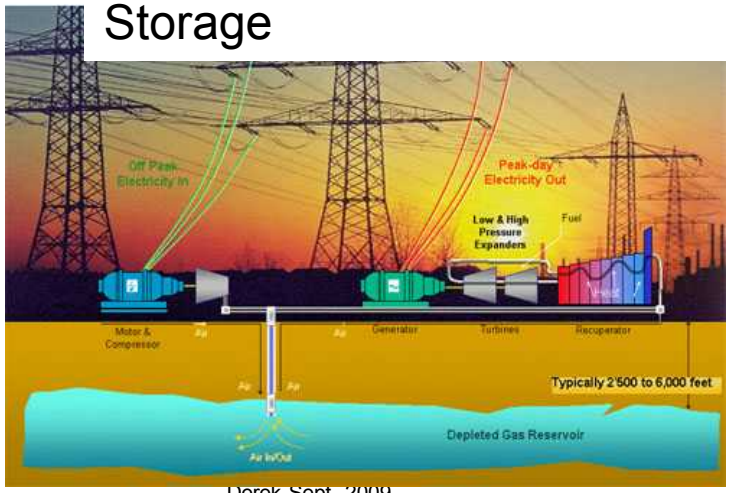

Hydraulic Fracturing

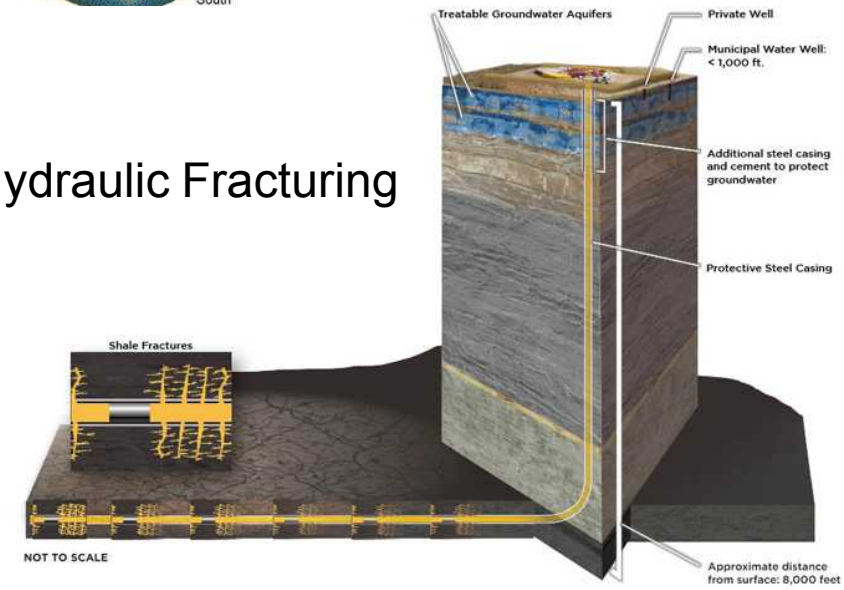

http://www.hydraulicfracturing.com

Spectrum of Fracture Problems

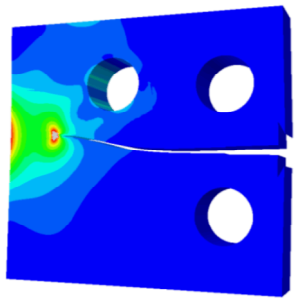

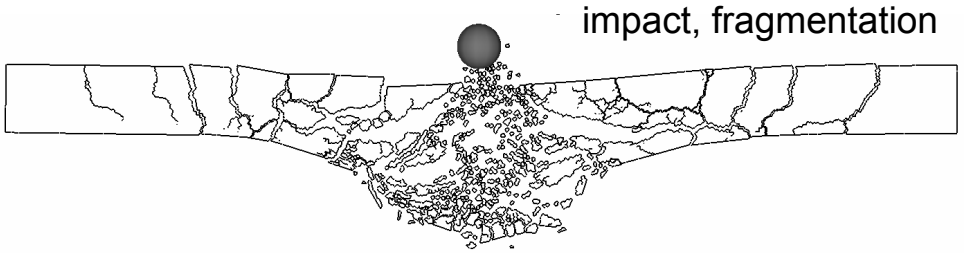

spectrum of fracture problems

single crack ⟷ pervasive fracture

- well defined deterministic propagation path
- analytical solutions
- enrichment methods (GFEM, XFEM, . . .)

- crack branching
- crack coalescence
- tortuous crack paths (sensitivity to material heterogeneity)
- stochastic behavior

How far can we extend the computational tools used for one end of the spectrum to the other?

Computational Challenges to Allowing Cracks to Grow Arbitrarily

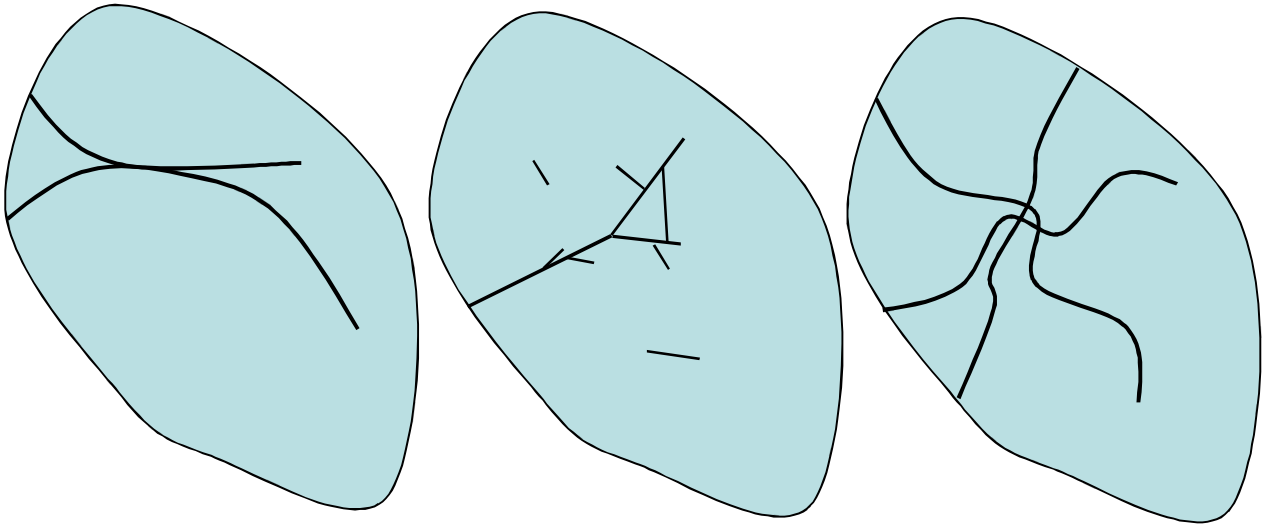

- Do we restrict branching?
- Do we restrict initiation?
  - from surface only?
  - from crack tips only?
  - from existing cracks only?
- Constraints on turning angles?
- Constraints on crossing angles?
- Constraints on minimum fragment size?

What about 3D?

Computational Approach

- Random Voronoi tessellation (mesh)
- Polyhedral finite-elements
- Fracture only allowed at element edges.
- *Dynamic* mesh connnectivity
- Insert cohesive tractions on new fracture surfaces (fracture energy).

Pandolfi, A. and M. Ortiz, 2002, *Engineering with Computers*, **18**: p. 148-159.

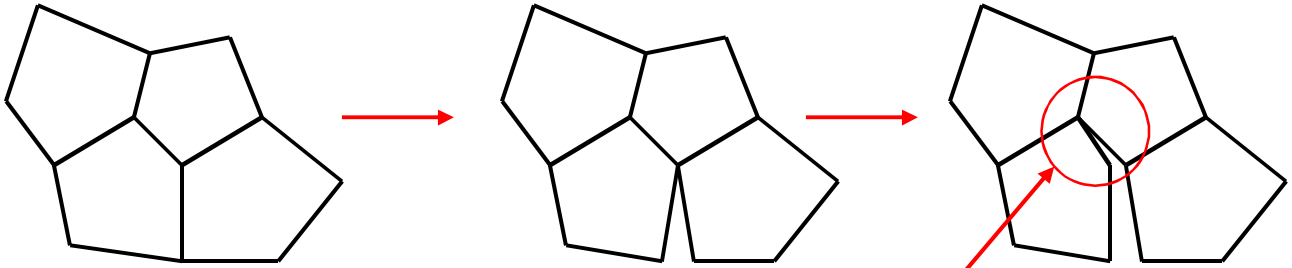

changing mesh connectivity

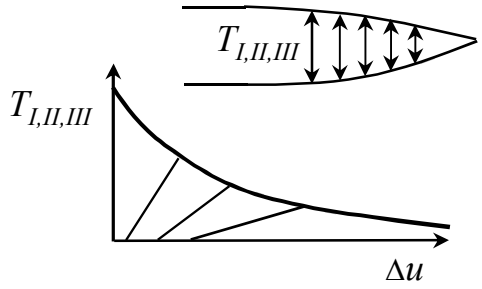

cohesive tractions at crack tip

Why a Random Voronoi Mesh?

Bolander, J.E. and S. Saito, 1998, *Fracture analyses using spring networks with random geometry.* Engineering Fracture Mechanics, **61**(5-6): p. 569-591.

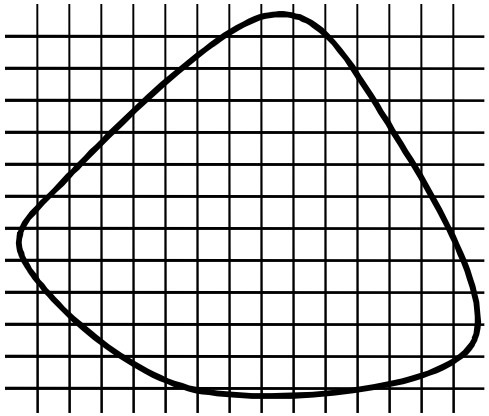

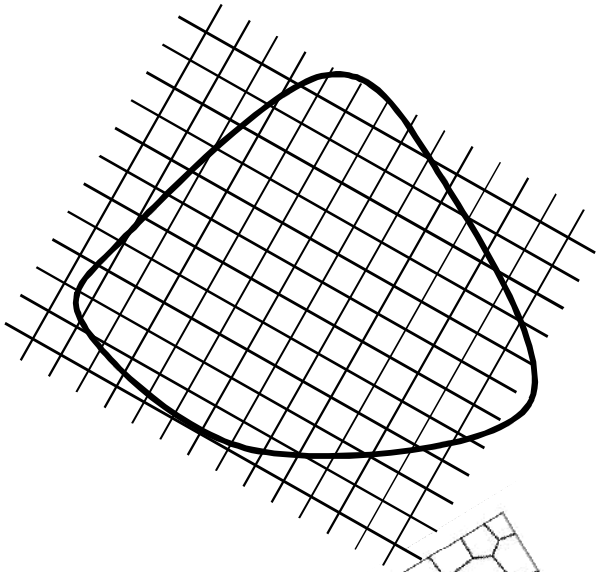

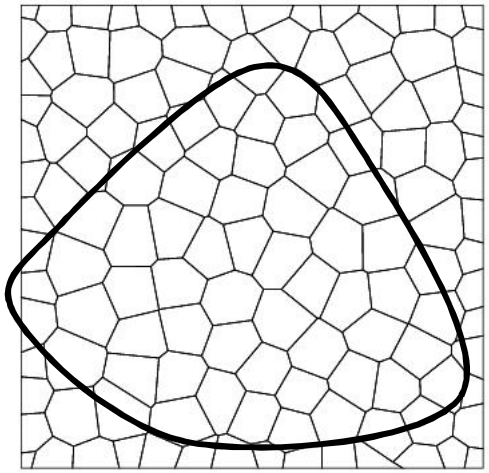

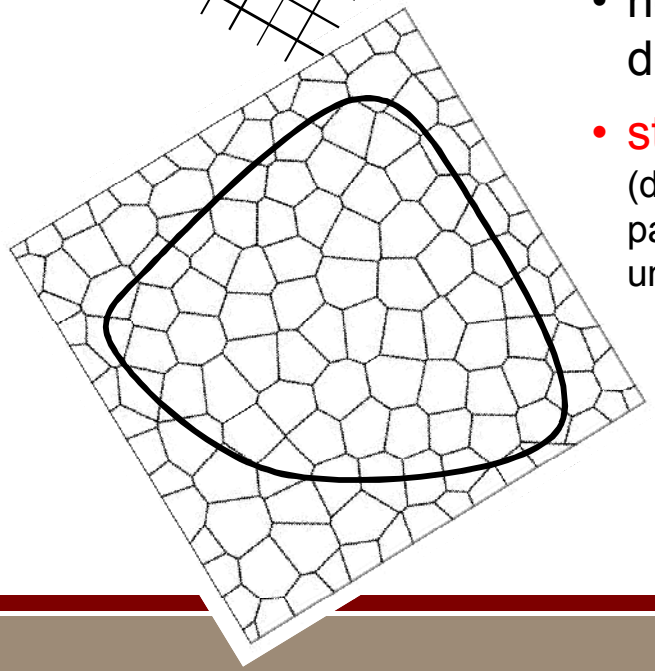

Voronoi tesselation of with random seeding

Structured grids can result in strong mesh induced bias (nonobjective).

- need to use ‘random’ discretizations
- statistically isotropic
  (distribution of edge orientations passes KS test against the uniform distribution)

Voronoi Texture Augments Material Variability

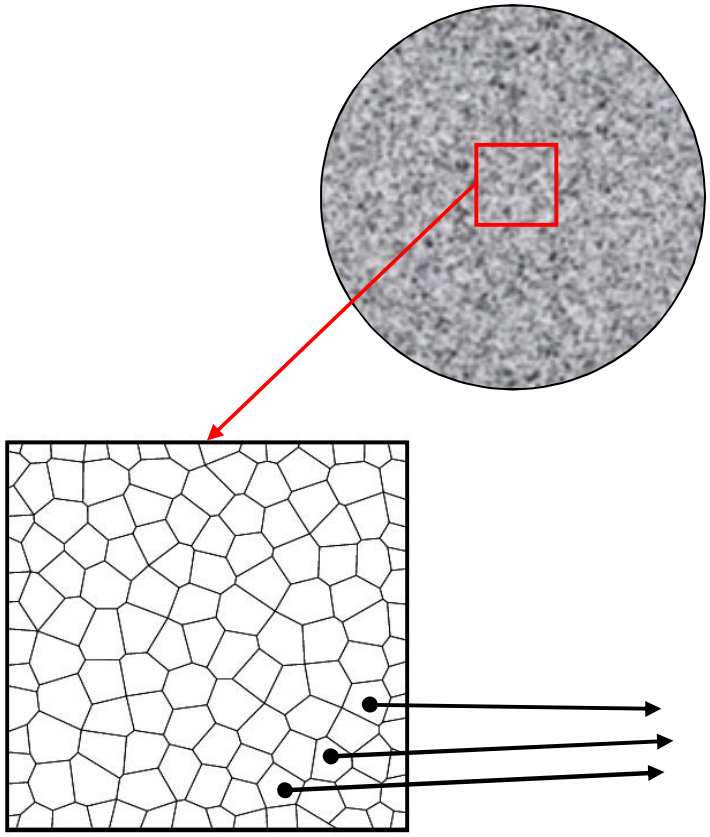

Probability Density

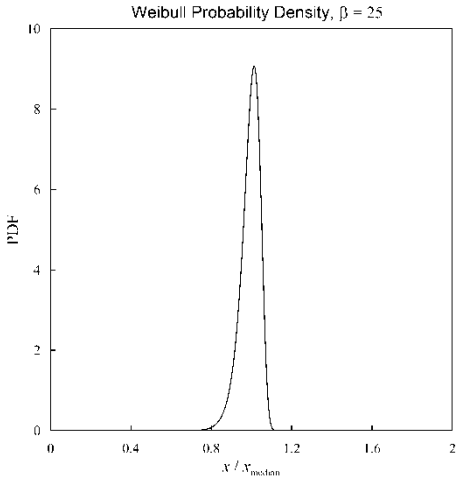

Voronoi Mesh Generation

Bolander, J., Saito, S., 1998, 'Fracture Analyses using Spring Networks with Random Geometry,' *Engineering Fracture Mechanics*, 61, 569-591

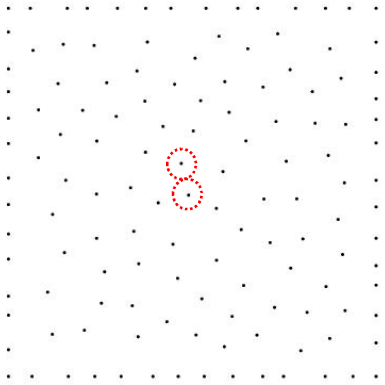

Poisson process

- constraint on min. dist.
- seed until 'max' packing

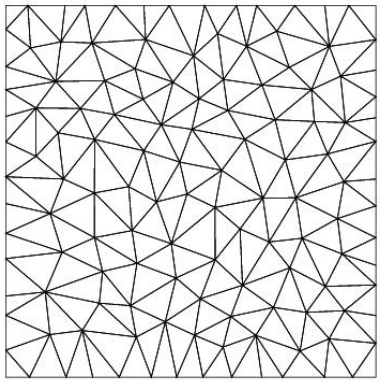

Delaunay triangulation

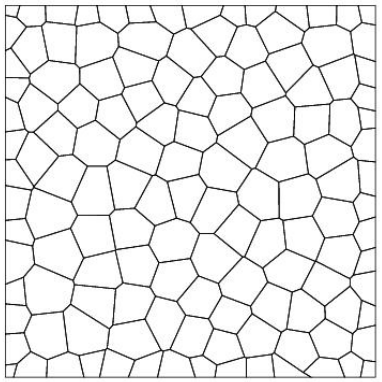

dual Voronoi

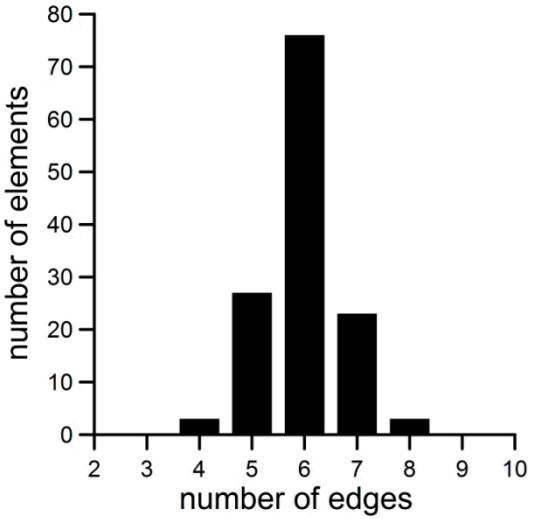

- Note that each Voronoi junction is randomly oriented.
- Most Voronoi junctions are triples.
- Average interior angles are 120°.

3D Element Formulation

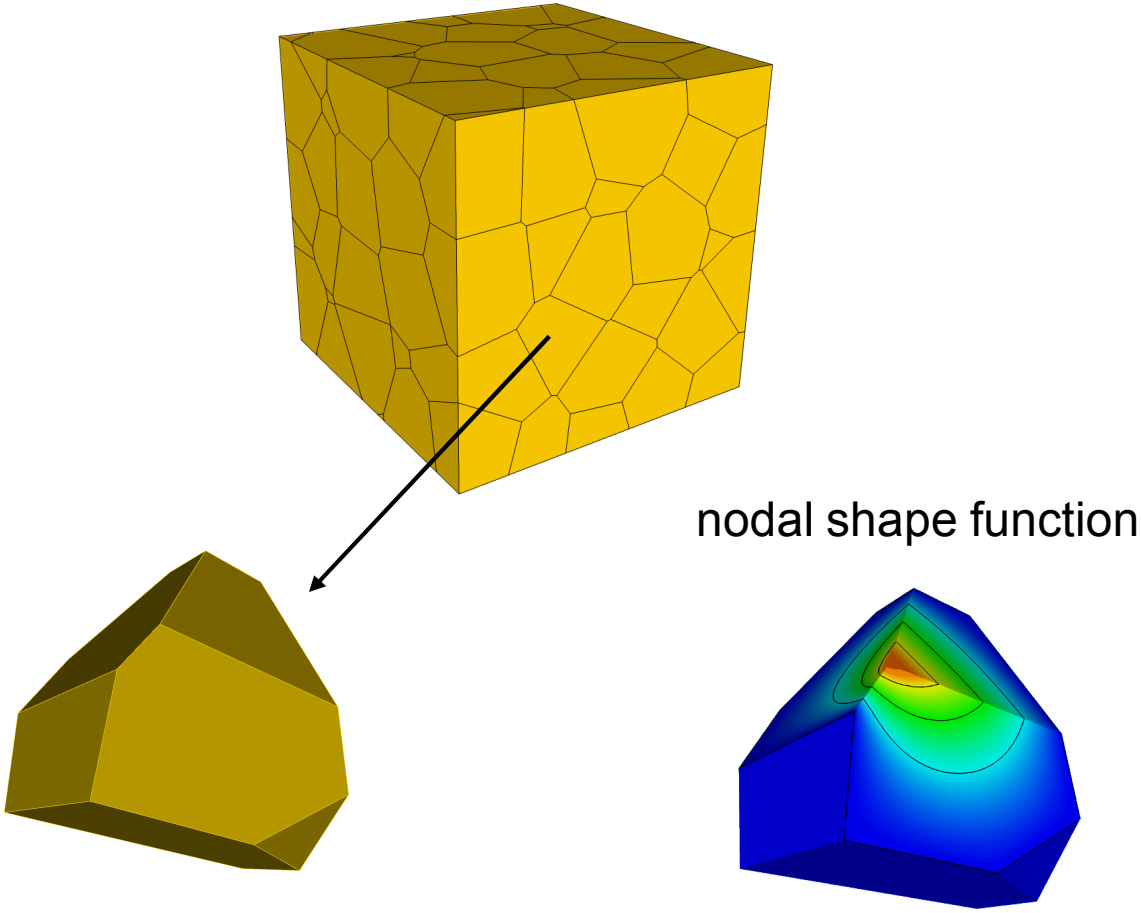

Harmonic Functions

A harmonic function is a solution of Laplace's equation.

$$\nabla^2 \varphi = 0 \quad \text{or} \quad \frac{\partial^2 \varphi}{\partial x^2} + \frac{\partial^2 \varphi}{\partial y^2} + \frac{\partial^2 \varphi}{\partial z^2} = 0$$

Can solve efficiently using BEM, or can just use FEM.

example in 2D

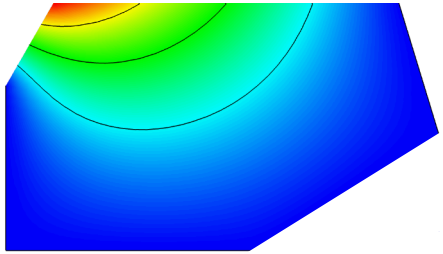

example in 3D

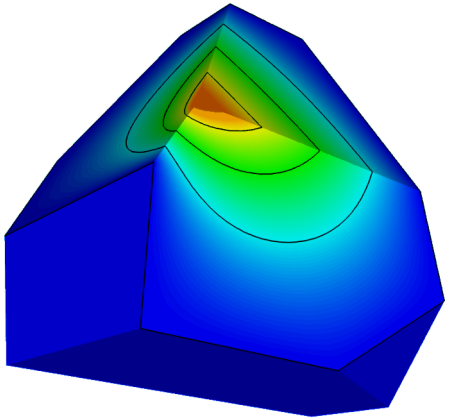

A subset of a broader notion of "energy minimizing" functions.

Construction of Harmonic Shape Functions in 3D

(Joshi, 2007, "Harmonic coordinates for character articulation")

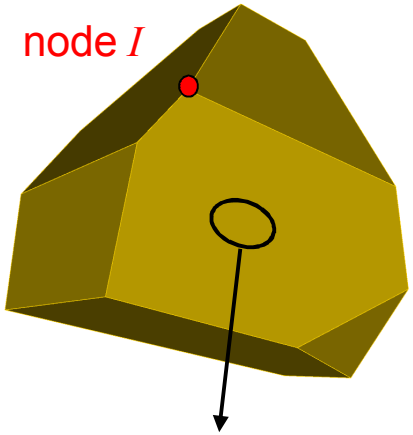

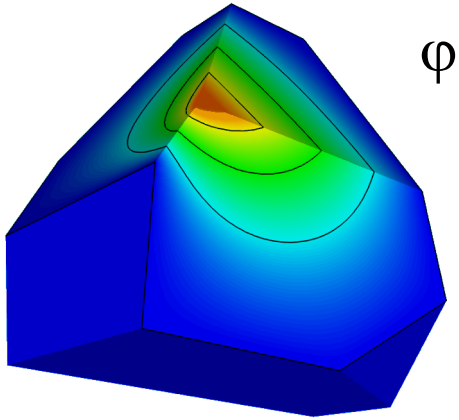

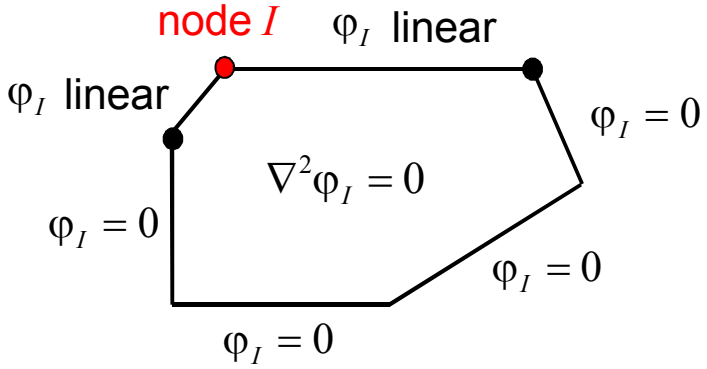

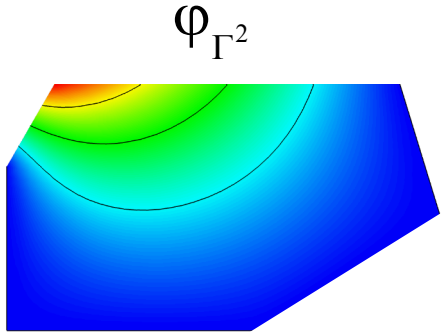

boundary conditions

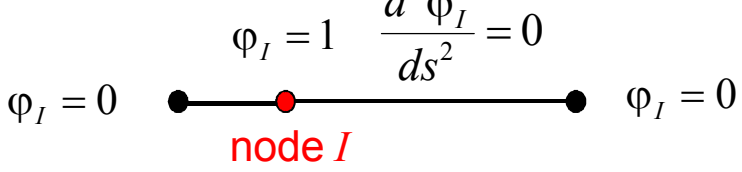

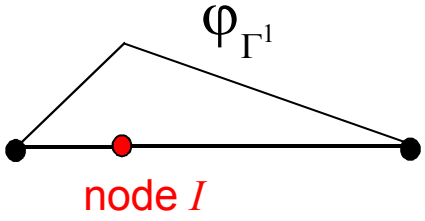

Harmonic Shape Function Properties

- partition of unity and reproduce space $\sum_I \psi_I(\mathbf{x}) = 1, \quad \sum_I \psi_I(\mathbf{x})\ \mathbf{x}_I = \mathbf{x}$

  even for the discrete harmonic solution $\sum_I \psi_I^h(\mathbf{x}) = 1, \quad \sum_I \psi_I^h(\mathbf{x})\ \mathbf{x}_I = \mathbf{x}$

- Kronecker delta property at nodes $\psi_I(\mathbf{x}_J) = \delta_{IJ}$
- linear on edges (low order)
- shape functions defined on original configuration (no mapping to 'parent' shape)

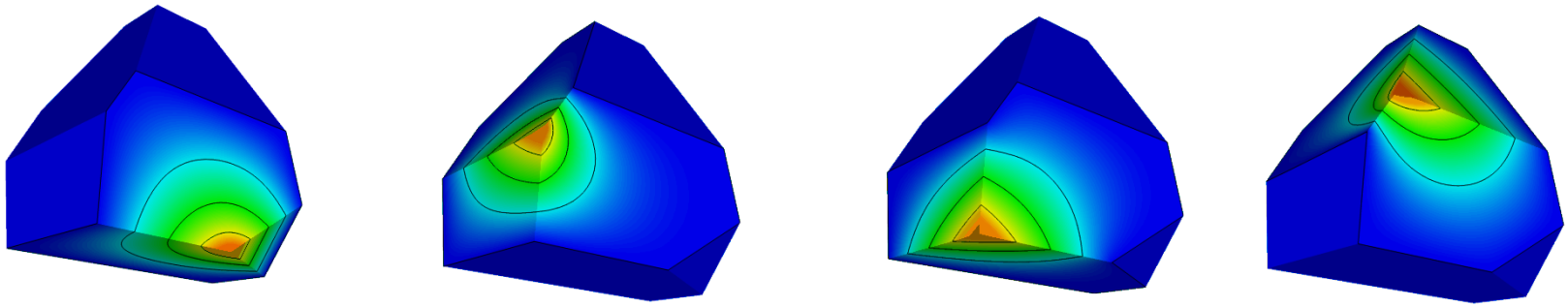

shape functions

Harmonic Shape Function Examples

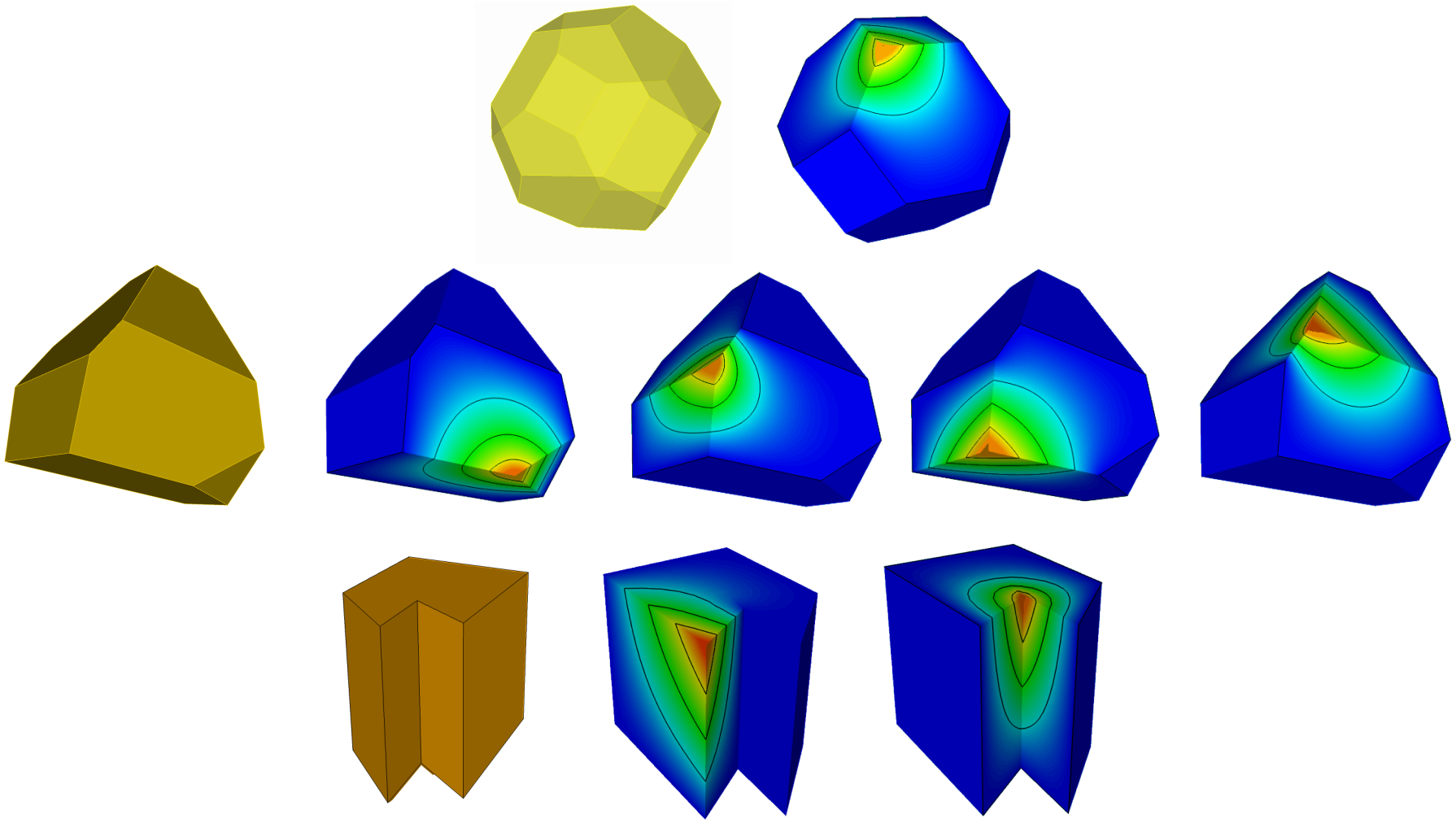

Only need to store shape functions and derivatives at integration points.

Discard everything else.

Element Integration

- Due to computational expense of plasticity models, want to minimize the number of integration points.
- Follow approach of Rashid and Selimotec, 2006.
- Each node is associated with a “tributary” volume, connected to the centroid.
- Number of integration points is equal to the number of vertices.

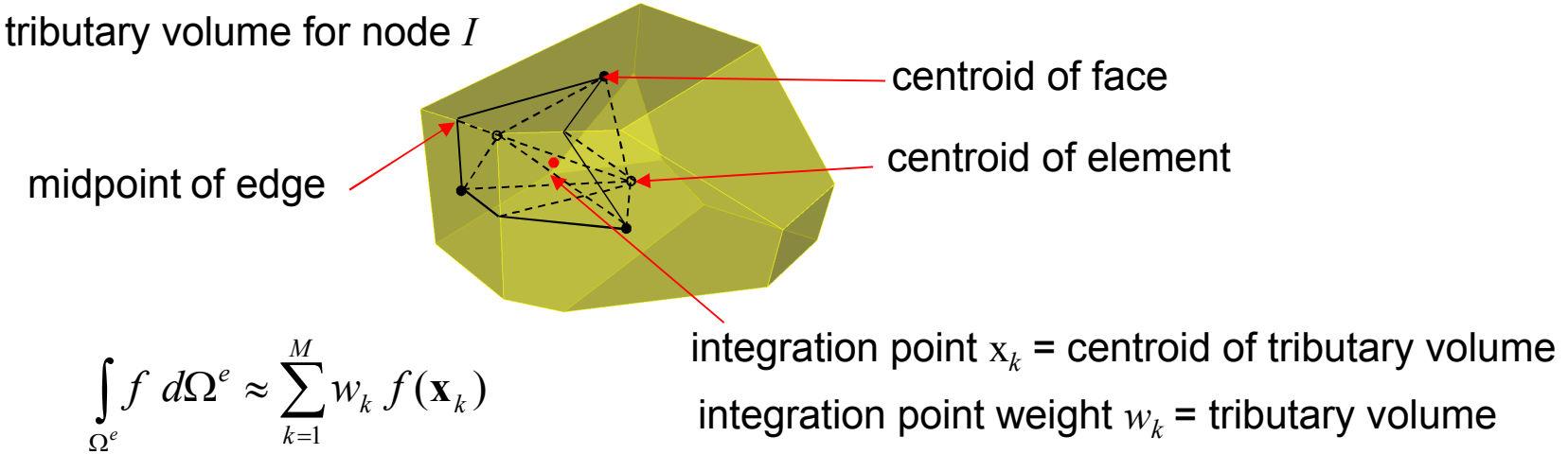

$$\int_{\Omega^e} f \, d\Omega^e \approx \sum_{k=1}^{M} w_k \, f(\mathbf{x}_k)$$

- Integration is only first order accurate.
- Sufficient to eliminate any zero energy modes.

“Engineering” Patch Test

The patch test verifies “completeness”, a necessary condition for convergence.

(Displacement field can represent rigid body motions and a constant strain state.)

On an “arbitrary” patch of elements, a linear displacement field should be produced on interior nodes when such a field is prescribed on the boundary nodes.

and, stress field should be constant.

Conversely, a constant stress field should be produced within each element when such a field is prescribed on the boundary surface.

and, strain field should be constant.

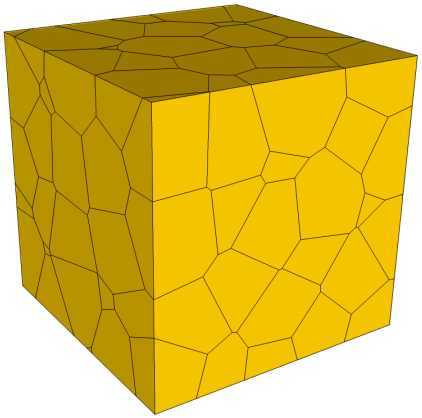

patch of elements

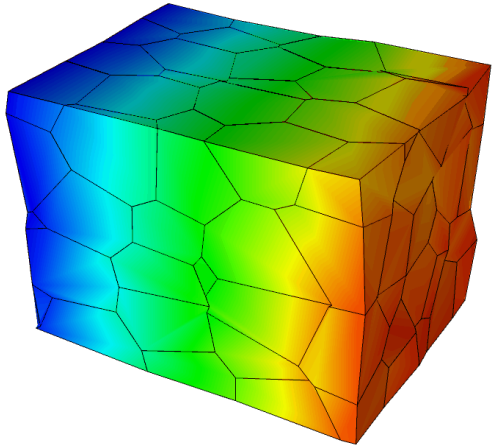

Failed patch test!

(result of low-order integration)

Element Stiffness Matrix (Linear Example)

From the weak form we get the element stiffness matrix

$$\mathbf{k}^e = \int_{\Omega^e} \mathbf{B}^T \mathbf{D} \mathbf{B} \, d\Omega$$

D contains elastic material constants.

$$\mathbf{B} = \begin{bmatrix} \mathbf{B}_1 & \mathbf{B}_2 & \cdots & \mathbf{B}_I & \cdots & \mathbf{B}_{N_{en}} \end{bmatrix}$$

$$\mathbf{B}_I = \begin{bmatrix} \varphi_{I,x} & 0 & 0 \\ 0 & \varphi_{I,y} & 0 \\ 0 & 0 & \varphi_{I,z} \\ 0 & \varphi_{I,z} & \varphi_{I,y} \\ \varphi_{I,z} & 0 & \varphi_{I,x} \\ \varphi_{I,y} & \varphi_{I,x} & 0 \end{bmatrix}$$

N_{en} = number of element nodes

$$\underbrace{\mathbf{k}^e}_{3N_{en} \times 3N_{en}} = \begin{bmatrix} \mathbf{k}^e_{11} & \mathbf{k}^e_{12} & \cdots \\ \mathbf{k}^e_{21} & \mathbf{k}^e_{22} & \cdots \\ \vdots & \vdots & \ddots \end{bmatrix}$$

nodal submatrix

$$\underbrace{\mathbf{k}^e_{IJ}}_{3\times 3} = \int_{\Omega^e} \mathbf{B}_I^T \mathbf{D} \mathbf{B}_J \, d\Omega$$

Contains terms like: $\int_{\Omega^e} \varphi_{I,x} \varphi_{J,x} \, d\Omega$, $\int_{\Omega^e} \varphi_{I,x} \varphi_{J,y} \, d\Omega$, $\int_{\Omega^e} \varphi_{I,x} \varphi_{J,z} \, d\Omega$, $\cdots$

But $\int_{\Omega^e} f \, d\Omega^e \approx \sum_{k=1}^{M} w_k \, f(\mathbf{x}_k)$ What's the effect of this approx.?

Requirements to Pass the Patch Test

(Krongauz and Belytschko, 1997)

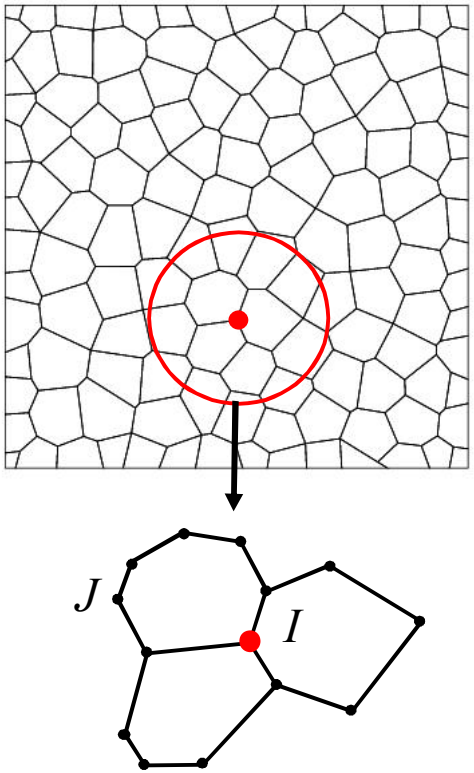

Ω_I = support of node I

global equilibrium equations: $\sum_J \mathbf{K}_{IJ}\mathbf{u}_J = \mathbf{F}_I$

K_{IJ} = global stiffness matrix

For patch test, need

$$u_x(x,y,z) = a_1 x + a_2 y + a_3 z + a_4$$
$$u_y(x,y,z) = b_1 x + b_2 y + b_3 z + b_4$$
$$u_z(x,y,z) = c_1 x + c_2 y + c_3 z + c_4$$

to be a solution of $\mathrm{Ku} = \mathrm{F}$ when applied as boundary conditions.

For interior nodes I need $\sum_J \mathbf{K}_{IJ}\mathbf{u}_J^{\text{linear}} = \mathbf{0}$ $\quad (\mathbf{F}_I = 0)$

Row I column J of K_{IJ} contains terms like:

$$\int_{\Omega_I} \varphi_{I,x}\varphi_{J,x}\, d\Omega\,, \quad \int_{\Omega_I} \varphi_{I,x}\varphi_{J,y}\, d\Omega\,, \quad \int_{\Omega_I} \varphi_{I,x}\varphi_{J,z}\, d\Omega\,, \quad \cdots$$

For example, need $\sum_J \int_{\Omega_I} \varphi_{I,x}\varphi_{J,z}\overbrace{(a_1 x_J + a_2 y_J + a_3 z_J + a_4)}\, d\Omega = 0$

Requirements to Pass the Patch Test

(Krongauz and Belytschko, 1997)

$$\sum_J \int_{\Omega_I} \varphi_{I,x}\varphi_{J,z}\left(a_1 x_J + a_2 y_J + a_3 z_J + a_4\right) d\Omega = 0$$

$$\int_{\Omega_I} \varphi_{I,x} \sum_J \varphi_{J,z}\left(a_1 x_J + a_2 y_J + a_3 z_J + a_4\right) d\Omega = 0$$

recall $\sum_{J=1}^{N} x_J \varphi_{J,z} = 0$ $\sum_{J=1}^{N} y_J \varphi_{J,z} = 0$ $\sum_{J=1}^{N} z_J \varphi_{J,z} = 1$ and $\sum_{J=1}^{N} \varphi_{J,z} = 0$

$$\int_{\Omega_I} \varphi_{I,x}\, d\Omega = 0$$

These integration properties of the shape function derivatives must hold in order to pass the patch test.

similarly $\int_{\Omega_I} \varphi_{I,y}\, d\Omega = 0$ $\int_{\Omega_I} \varphi_{I,z}\, d\Omega = 0$

But what about numerical integration? $\int_{\Omega_I} \varphi_{I,x}\, d\Omega \approx \sum_{k=1}^{N_{ip}} w_k\, \varphi_{I,x}(\mathbf{x}_k)$

w_k = integration weight

x_k = integration point

Integration Consistency

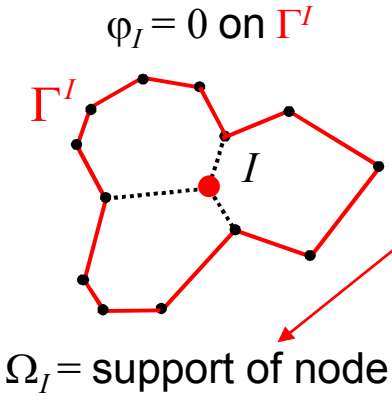

$$\int_{\Omega_I} \varphi_{I,x}\, d\Omega = 0$$

is equivalent to

Divergence Theorem

$$\int_{\Omega^e} \varphi_{I,x}\, d\Omega = \int_{\Gamma^e} \varphi_I\, n_x\, d\Gamma$$

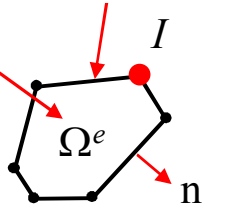

$$\int_{\Omega^e} \varphi_{I,x}\, d\Omega = \int_{\Gamma^e} \varphi_I\, n_x\, d\Gamma$$

Satisfaction of discrete form of Divergence Theorem requires "="

$$\sum_{k=1}^{M} w_k\, \varphi_{I,x}(\mathbf{x}_k) \cong \sum_{j=1}^{M_\Gamma} w_j^\Gamma\, \varphi_I(\mathbf{x}_j)\, n_x(\mathbf{x}_j)$$

volume integration point at x_k with weight w_k

surface integration point at x_j with weight w^Γ_j

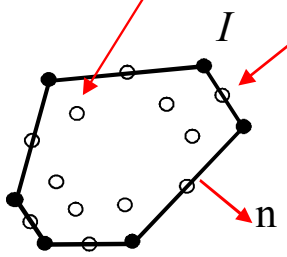

Approximate integration will cause failure of patch test for first-order integration.

Would need a large number of integration points to satisfy patch test.

. . . too expensive!

Instead, let's "tweak" the shape function derivatives to satisfy the patch test.

Let's "tweak" the Shape Function Derivatives

discrete form of Divergence Theorem

$$\sum_{k=1}^{M} w_k \, a_x^{I,k} - \sum_{j=1}^{M_\Gamma} w_j^\Gamma \, \varphi_I(\mathbf{x}_j) \, n_x(\mathbf{x}_j) = 0 \qquad I = 1, \ldots, N_{en}$$

$$\sum_{k=1}^{M} w_k \, a_y^{I,k} - \sum_{j=1}^{M_\Gamma} w_j^\Gamma \, \varphi_I(\mathbf{x}_j) \, n_y(\mathbf{x}_j) = 0 \qquad I = 1, \ldots, N_{en}$$

$$\sum_{k=1}^{M} w_k \, a_z^{I,k} - \sum_{j=1}^{M_\Gamma} w_j^\Gamma \, \varphi_I(\mathbf{x}_j) \, n_z(\mathbf{x}_j) = 0 \qquad I = 1, \ldots, N_{en}$$

$a_x^{I,k}, a_y^{I,k}, a_z^{I,k}$ are the new shape function derivatives for the I-th shape function at integration point k.

How to calculate $a_x^{I,k}, a_y^{I,k}, a_z^{I,k}$?

Minimize the sum of the squares of the difference w.r.t to the original derivatives.

$$L = \sum_{I=1}^{N_{en}} \sum_{k=1}^{M} \left(\varphi_{I,x}(\mathbf{x}_k) - a_x^{I,k} \right)^2$$

with "integration constraints"

$$\sum_{k=1}^{M} w_k \, a_x^{I,k} - \sum_{j=1}^{M_\Gamma} w_j^\Gamma \, \varphi_I(\mathbf{x}_j) \, n_x(\mathbf{x}_j) = 0 \qquad I = 1, \ldots, N_{en}$$

} solve use Lagrange multipliers

Modified Shape Function Derivatives

Introduce Lagrange multipliers λ_I, $I = 1, \ldots, N_{en}$ and form the augmented Lagrangian L_A

$$L_A = \sum_{I=1}^{N_{en}} \sum_{k=1}^{M} \left(\varphi_{I,x}(\mathbf{x}_k) - a_x^{I,k} \right)^2 + \sum_{i=1}^{N_{en}} \lambda_I \left[\sum_{k=1}^{M} w_k \, a_x^{I,k} - \sum_{j=1}^{M_\Gamma} w_j^\Gamma \, \varphi_I(\mathbf{x}_j) \, n_x(\mathbf{x}_j) \right]$$

necessary condition for local minimum

$$\frac{\partial L_A}{\partial a_x^{I,k}} = 0 , \quad I = 1, \cdots, N_{en} , \quad k = 1, \cdots, M$$

$$\frac{\partial L_A}{\partial \lambda_I} = 0 , \quad I = 1, \cdots, N_{en}$$

$$\begin{bmatrix} \mathbf{A} & \mathbf{L}^T \\ \mathbf{L} & 0 \end{bmatrix} \begin{bmatrix} \boldsymbol{a}_x \\ \boldsymbol{\lambda} \end{bmatrix} = \begin{bmatrix} \mathbf{b}_x \\ \mathbf{c}_x \end{bmatrix}$$

same for $(\,)_y$ and $(\,)_z$, only need to factor once for each element

3D Verification: Engineering Patch Test

Sandia National Laboratories

random patch

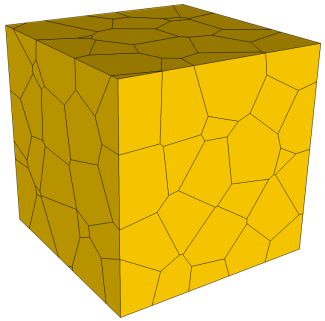

without derivative correction

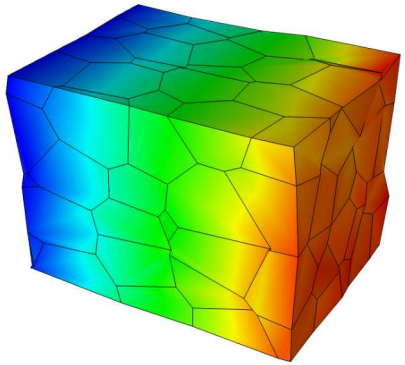

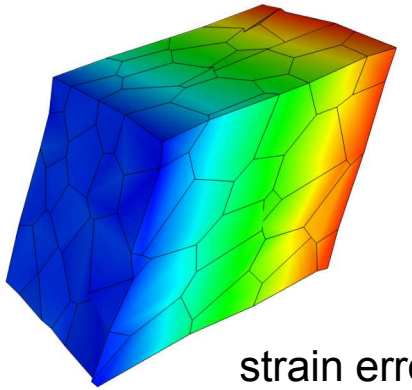

strain error = $O(10^{-1})$

with derivative correction

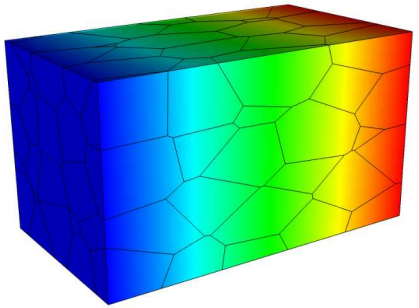

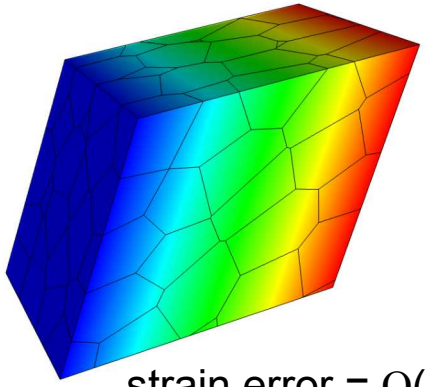

strain error = $O(10^{-5})$

Patch Test with Nonconvex Elements

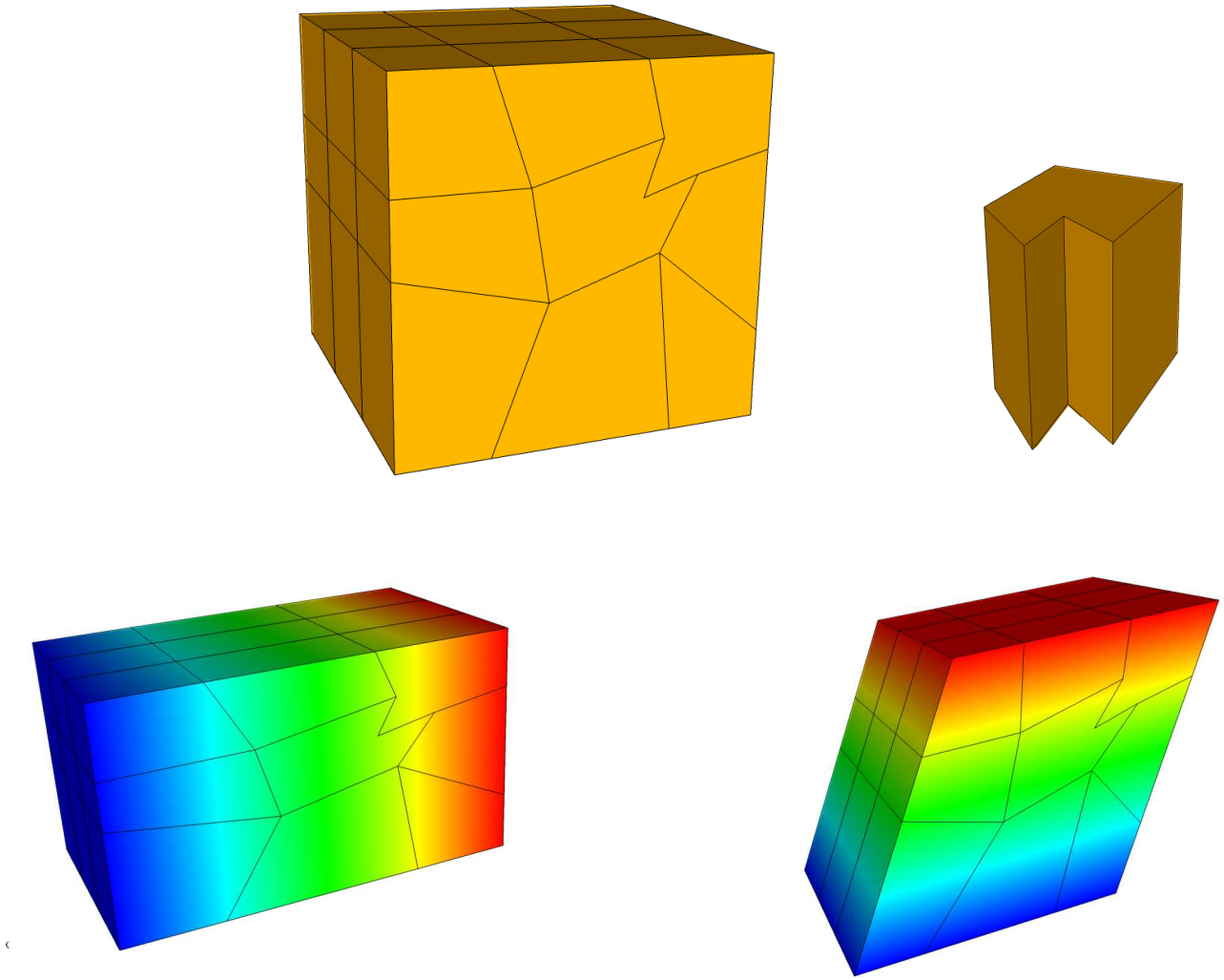

Verification Test: Beam with a Transverse End-Load

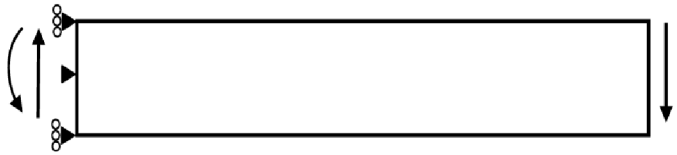

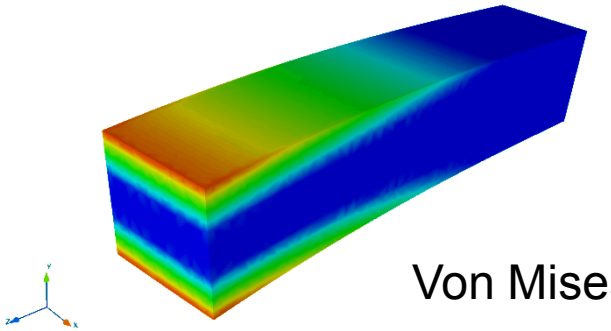

Von Mises stress field

3D exact linear elasticity solution, (Barber, 2010)

$$
\begin{aligned}
\sigma_{xx} &= \sigma_{yy} = \sigma_{xy} = 0 \\
\sigma_{zz} &= \frac{F_y}{I_x} yz \\
\sigma_{xz} &= \frac{2F_y a^2}{\pi^2 I_x} \frac{\nu}{1+\nu} \sum_{n=1}^{\infty} \frac{(-1)^n}{n^2} \sin\left(\frac{n\pi x}{a}\right) \frac{\sinh\left(\frac{n\pi y}{a}\right)}{\cosh\left(\frac{n\pi b}{a}\right)} \\
\sigma_{yz} &= \frac{F_y}{I_x} \left\{ \frac{1}{2}(b^2 - y^2) + \frac{1}{6}(3x^2 - a^2) \frac{\nu}{1+\nu} - \frac{2a^2}{\pi^2} \frac{\nu}{1+\nu} \sum_{n=1}^{\infty} \frac{(-1)^n}{n^2} \sin\left(\frac{n\pi x}{a}\right) \frac{\sinh\left(\frac{n\pi y}{a}\right)}{\cosh\left(\frac{n\pi b}{a}\right)} \right\}
\end{aligned}
$$

From this stress field → strain field → integrate to get displacement field using compatibility equations.

Randomly Close-Packed Voronoi Meshes

beam dimension
= 1 × 1 × 5

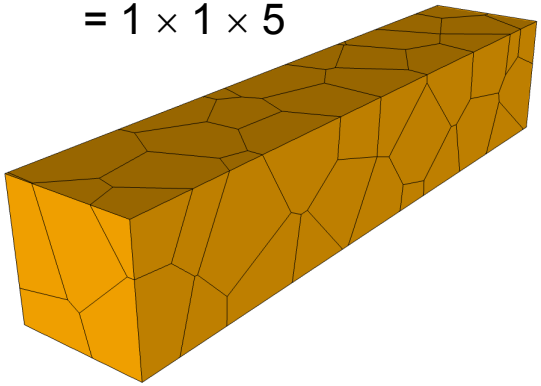

point spacing = 0.5

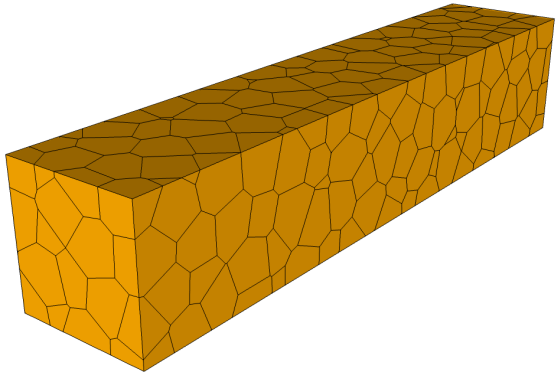

point spacing = 0.25

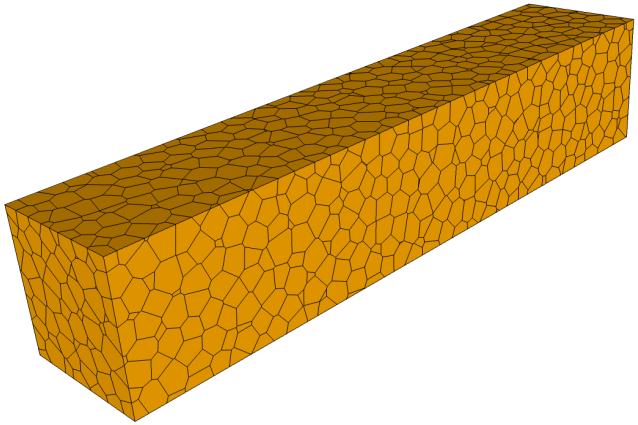

point spacing = 0.125

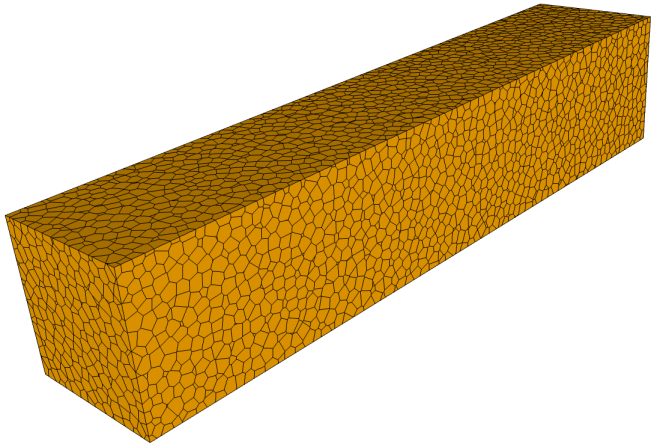

point spacing = 0.0625

minimum edge
to diameter
ratio = 10^{-4}

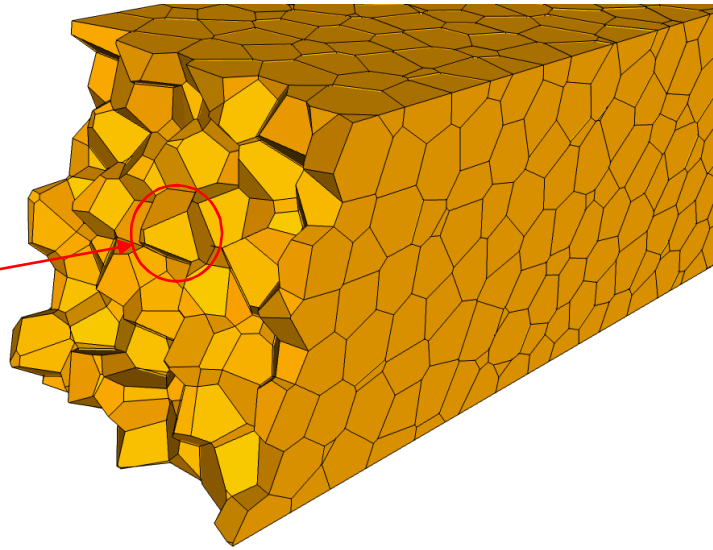

Randomly Close-Packed Voronoi Meshes

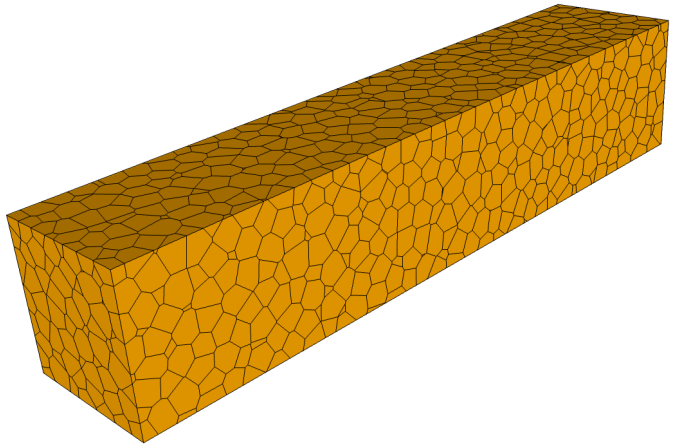

mesh statistics

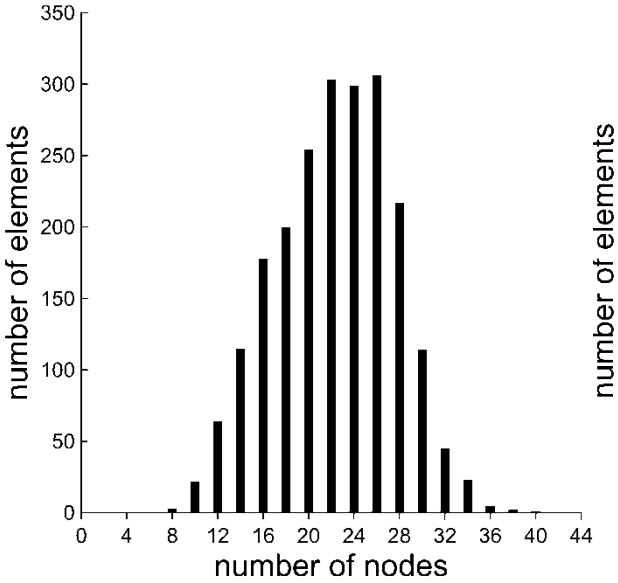

median 24 nodes per element

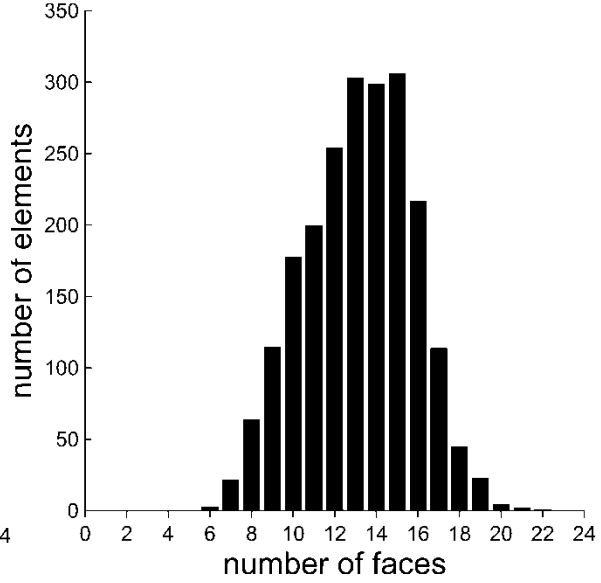

median 14 faces per element

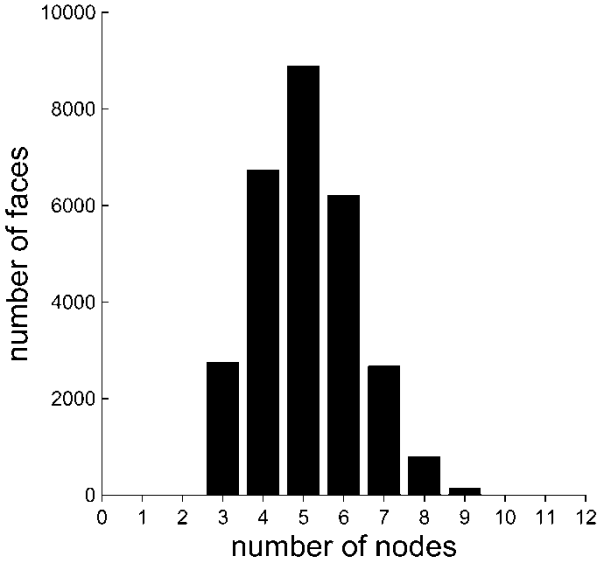

median 5 nodes per face

Verification Test: Beam with a Transverse End-Load

Randomly Close-Packed Voronoi

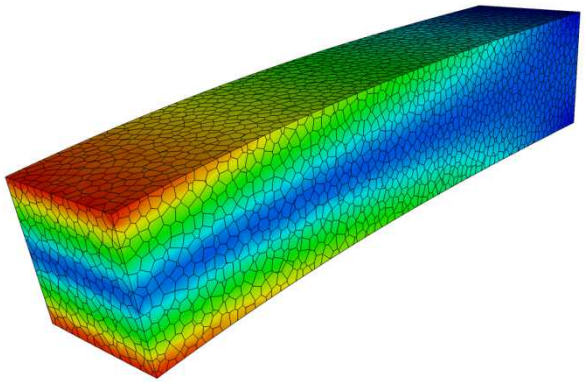

deformed shape, Von Mises stress

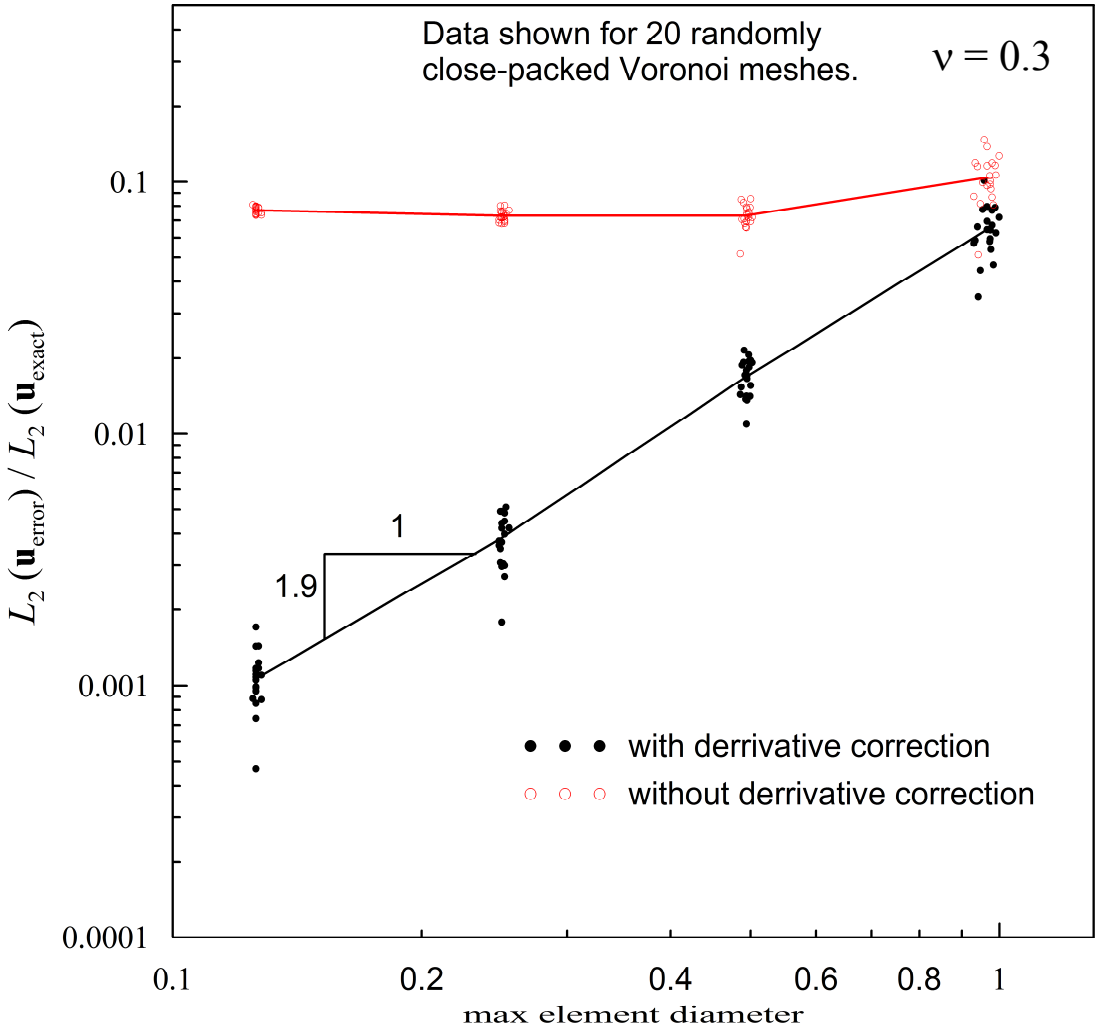

Verification Test: Beam with a Transverse End-Load

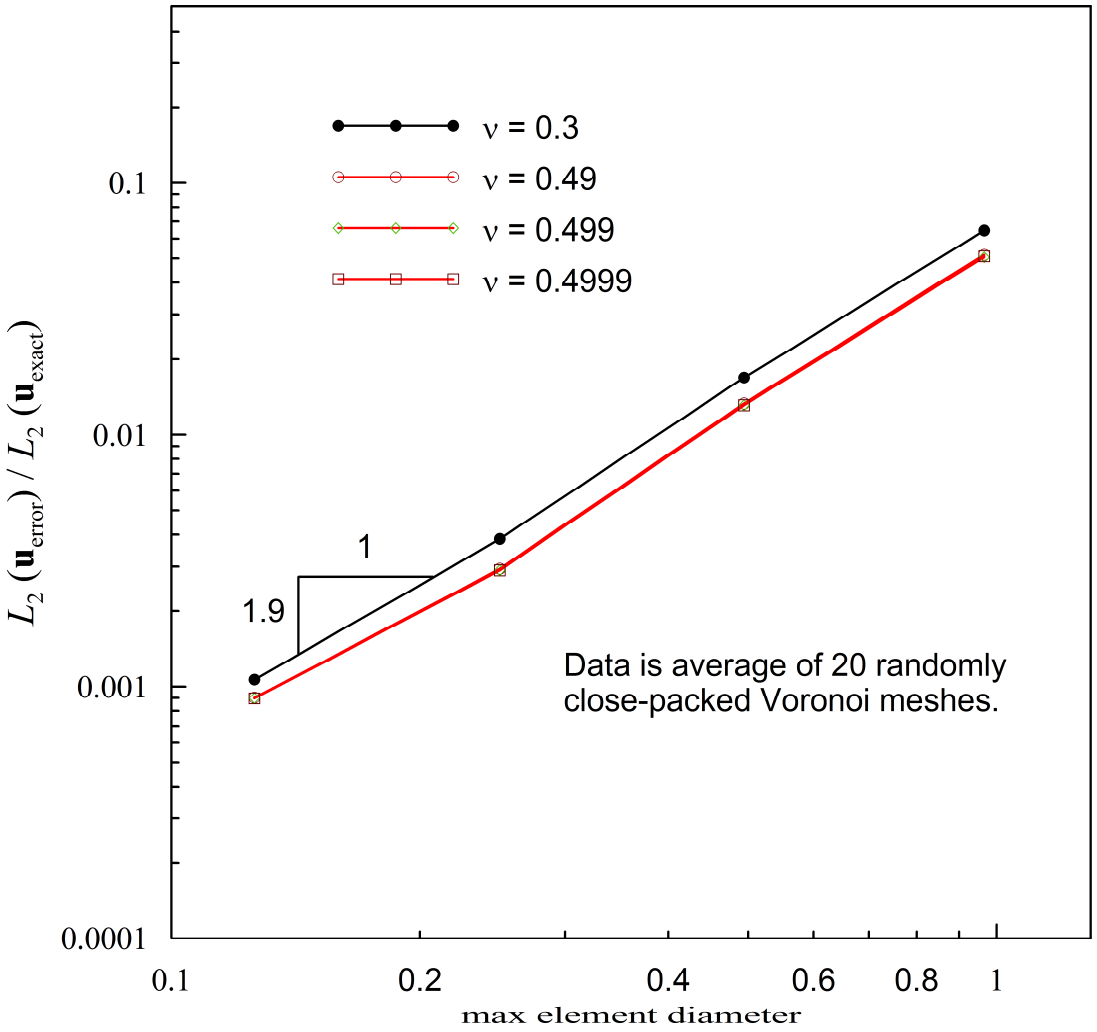

Standard mean-dilation formulation for nearly incompressible behavior (Nagtegaal, 1974)

No reduction in convergence rate as $\nu \rightarrow 1/2$.

Dynamic Mesh Connectivity

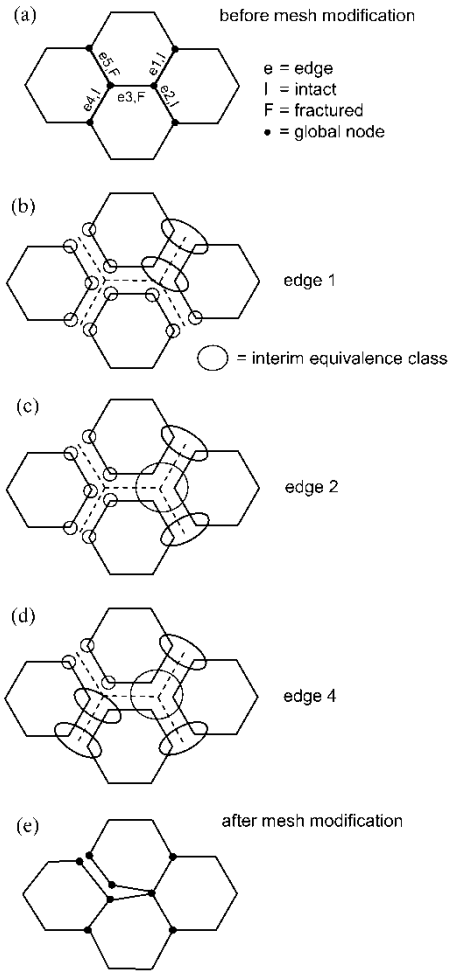

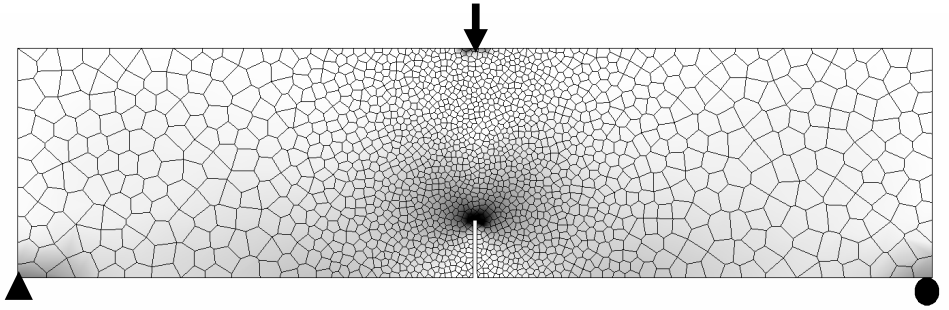

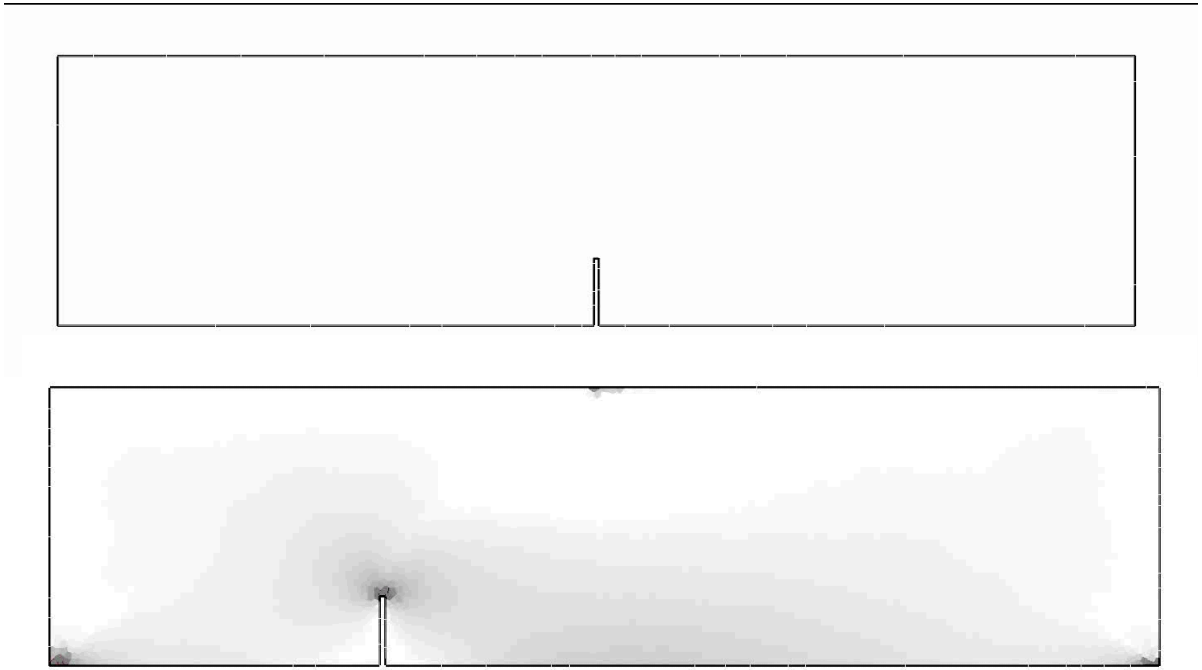

Quasi-Brittle Material Impact

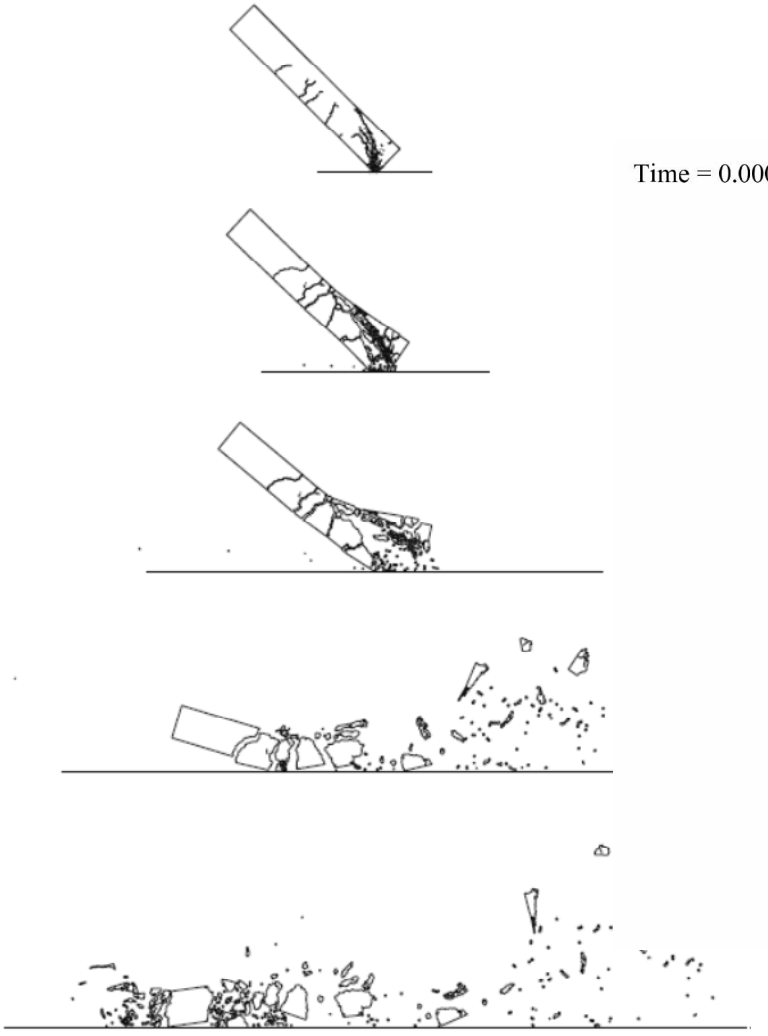

Time = 0.0000

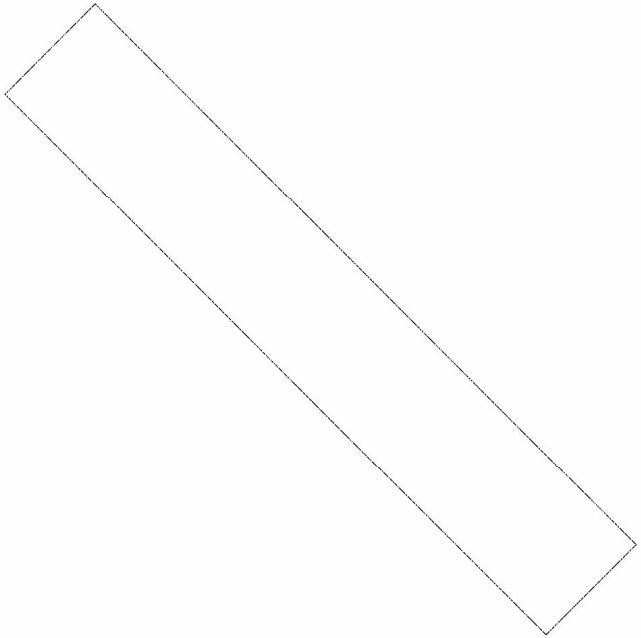

Impact Example

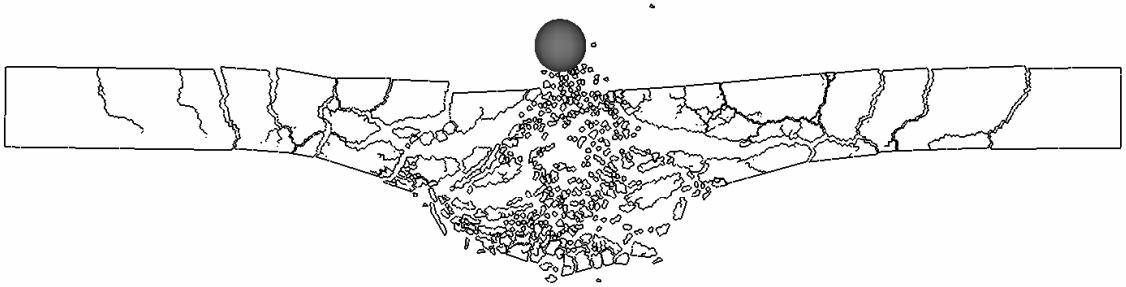

Time = 0.00000

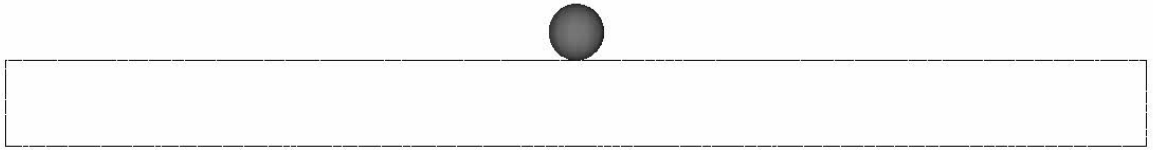

CFSES: Center for Subsurface Energy Security

Sandia National Laboratories

(www.utcfses.org)

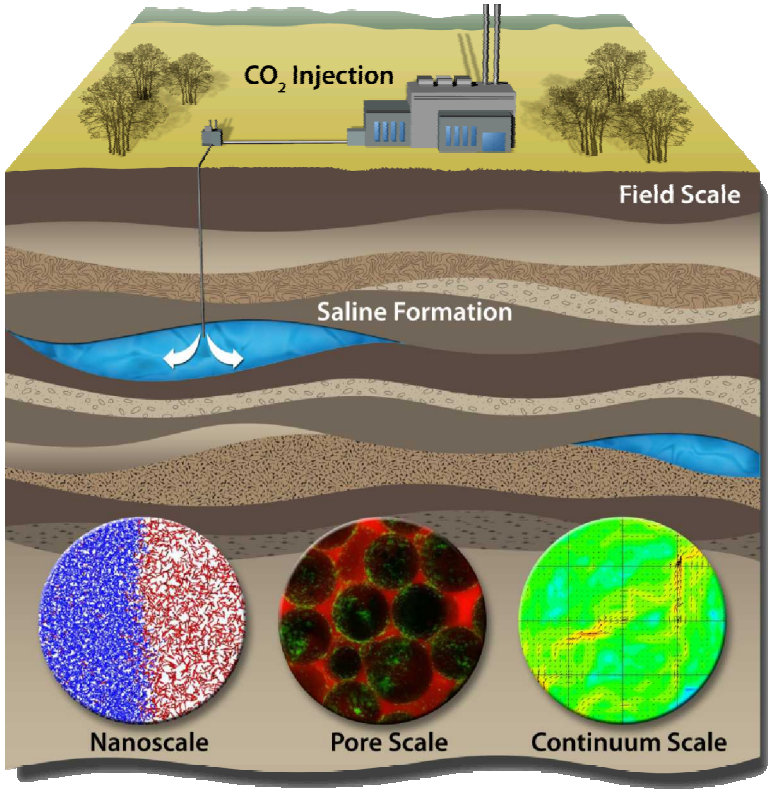

10^{3} years (or more)

Time

10^{-15} second

10^{-9} m | 10^{-5} m | 10^{-1} m | 10^{2} m

Focus Area 1 | **Focus Area 2** | **Focus Area 3** | **Focus Area 4**

Nanoscale | **Pore Scale** | **Continuum Scale** | **Field Scale**

Potential Leakage Paths for CO_2

Primary CO_2 trapping mechanism is structural.

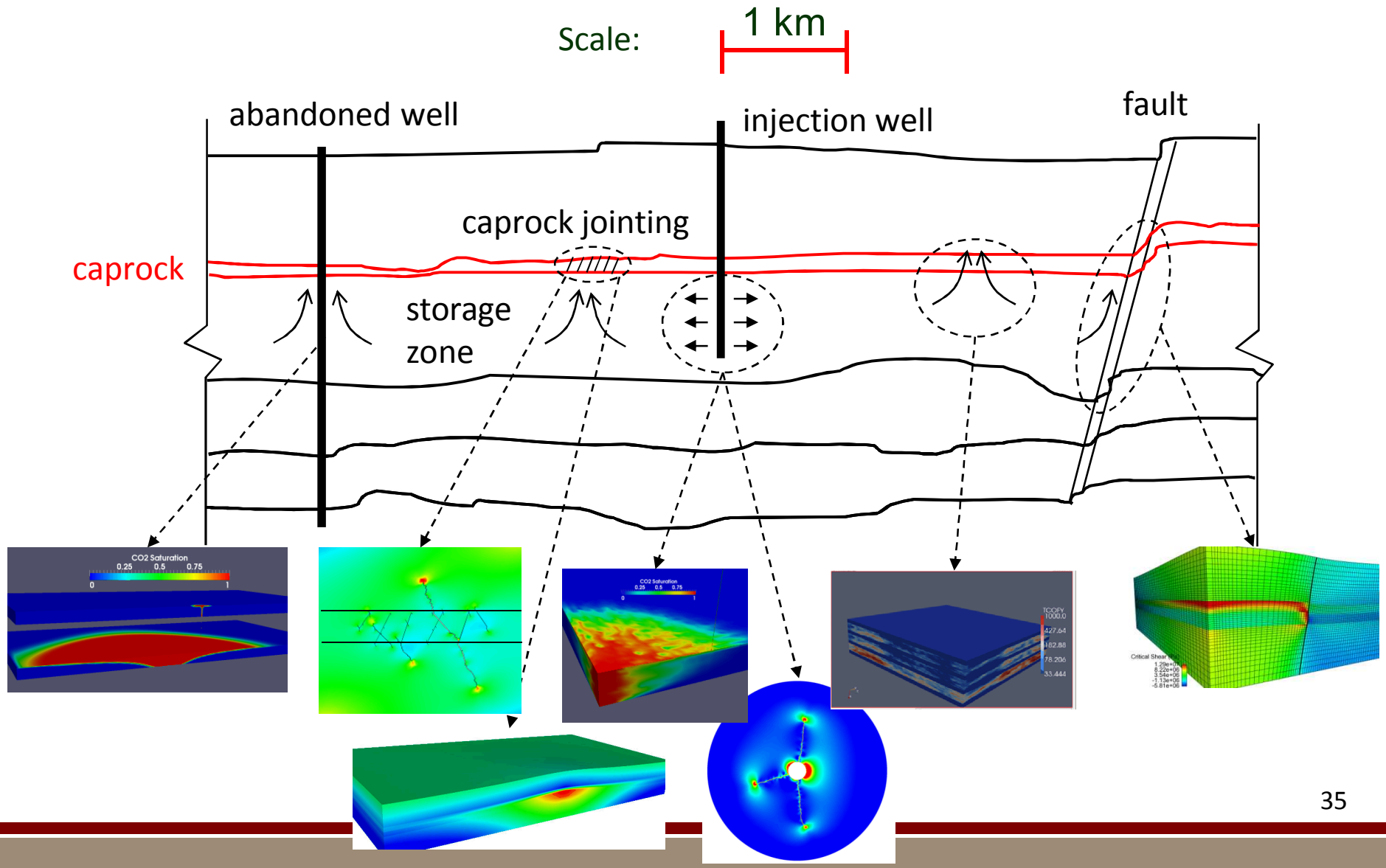

Hydromechanical Coupling in Fractured Rock

Fractured Porous Rock

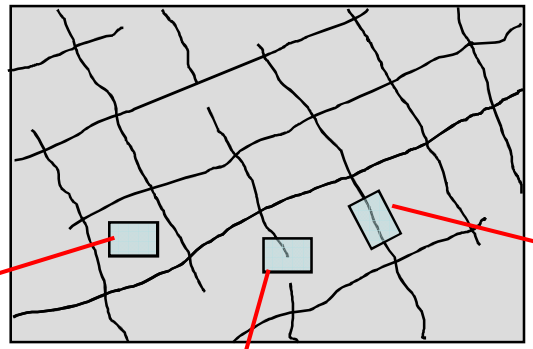

bulk constitutive properties

(Sandia GeoModel
Fossum & Brannon, 2004)

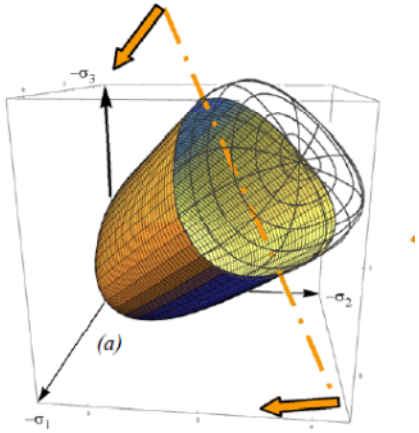

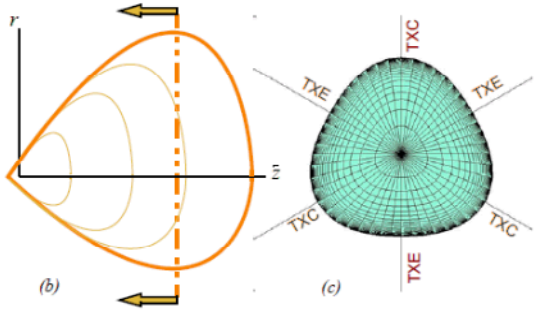

fracture contact properties

$$\sigma'_n = \sigma_n - p$$

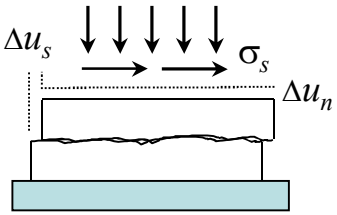

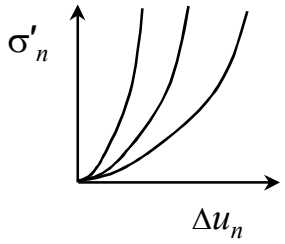

$$\sigma_s = \sigma_s\{\Delta u_s, \Delta u_n\}$$
$$\sigma'_n = \sigma'_n\{\Delta u_s, \Delta u_n\}$$

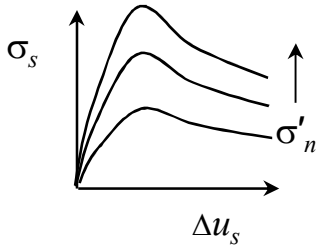

crack-tip cohesive properties

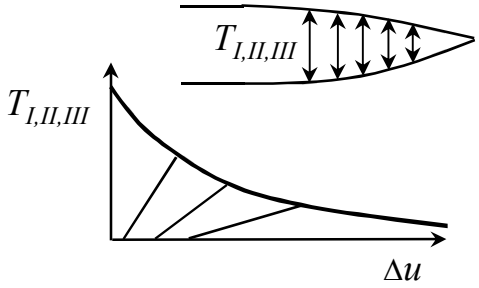

additional challenges

- scale dependence
- history dependence
- precipitation
- dissolution

MeshingGenie (Trilinos)

(Ebeida, M., Knupp, P., Vitus Leung, Sandia National Laboratories)

Fractured Rock

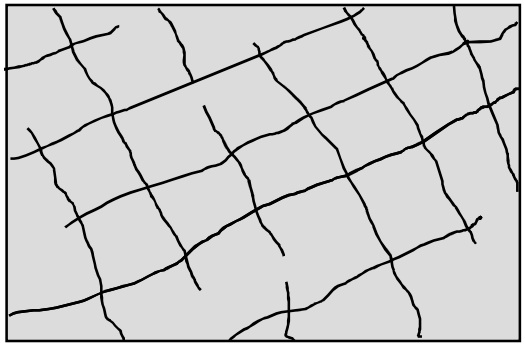

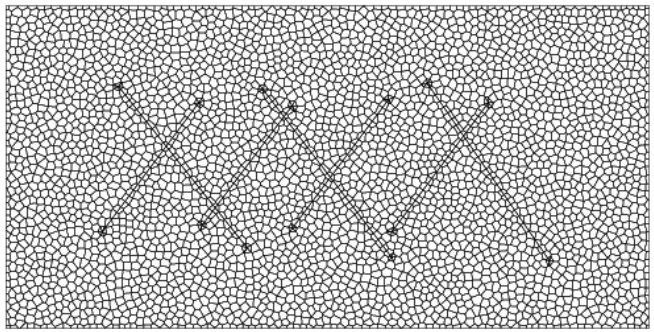

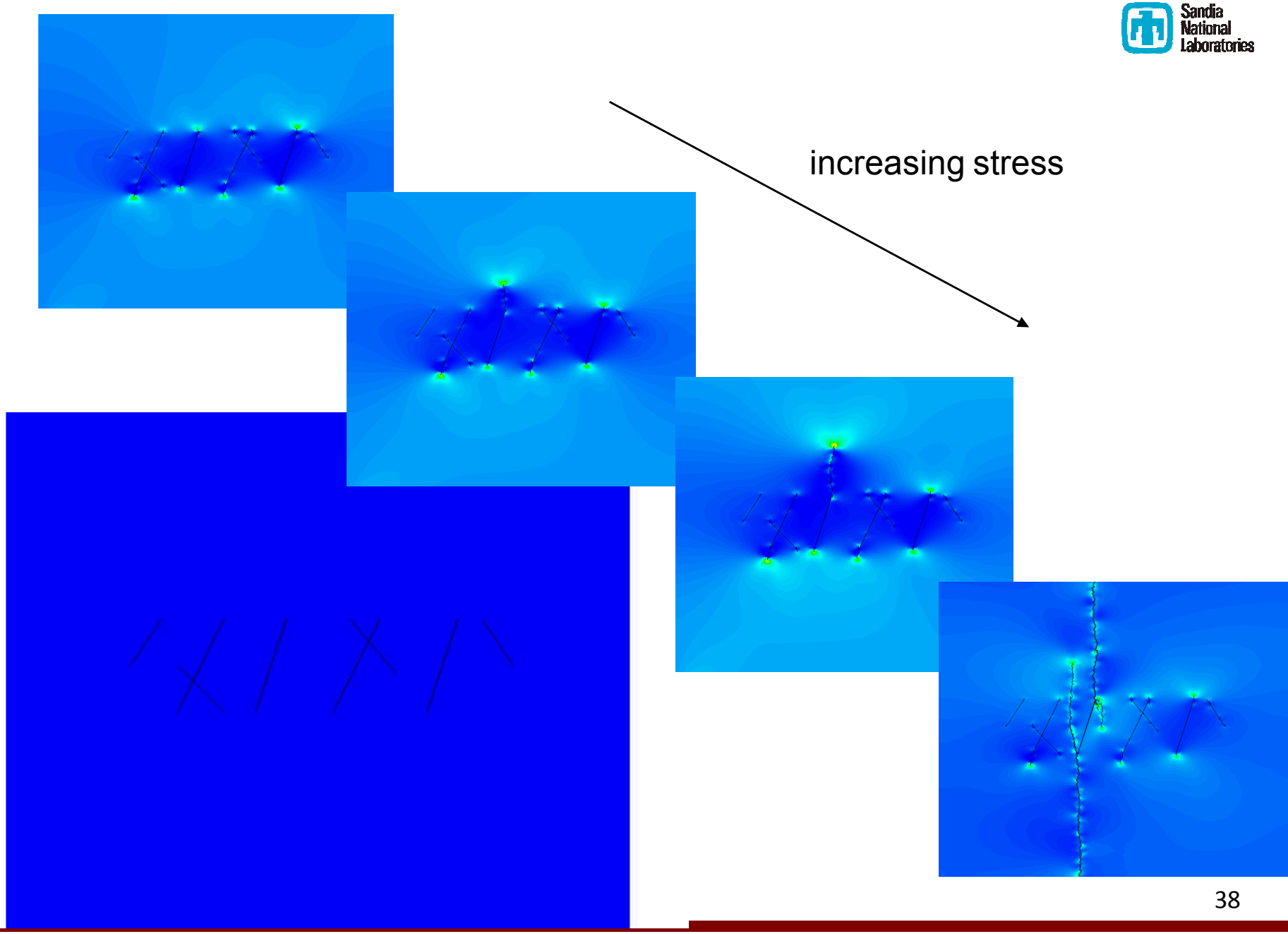
increasing stress

Fluid Flow in 2D Discrete Fracture Networks

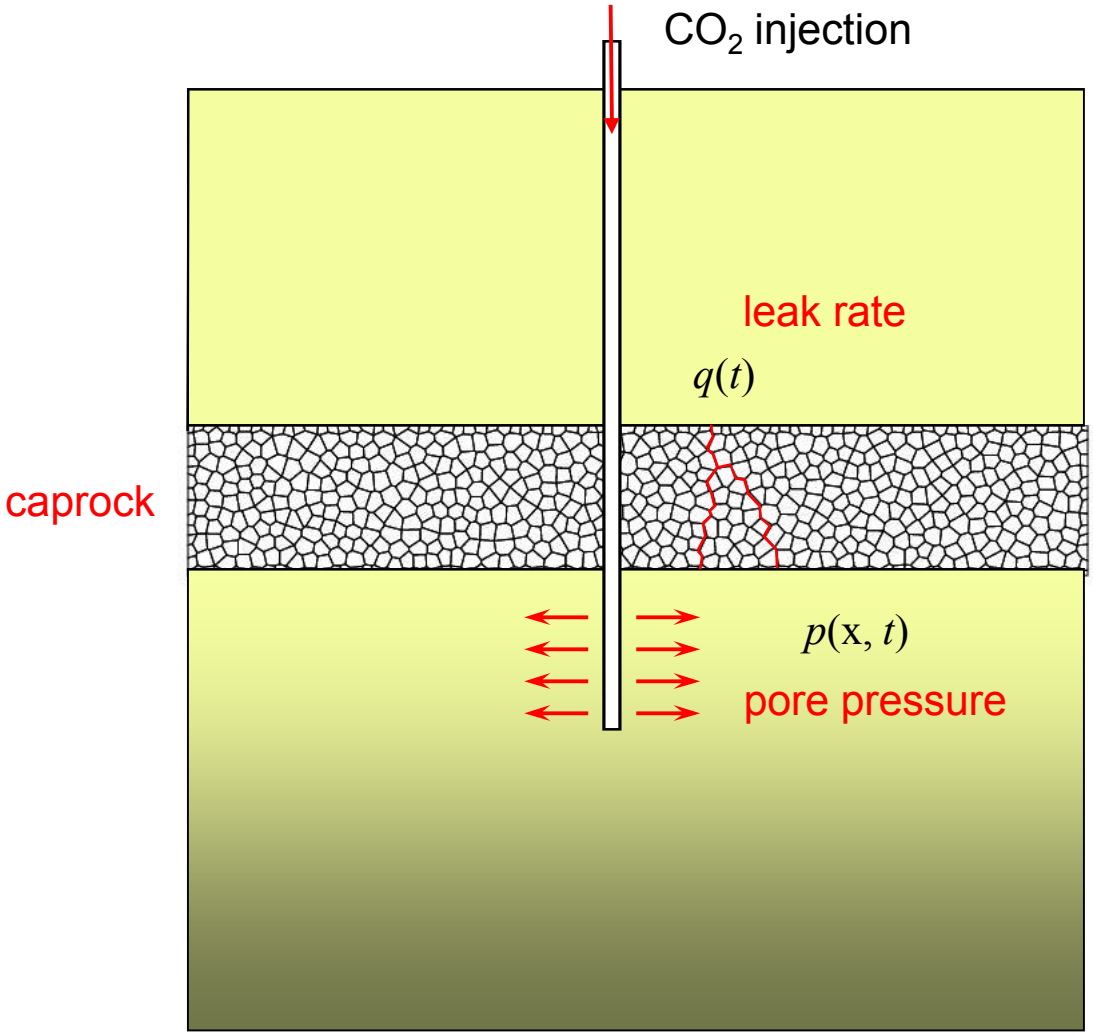

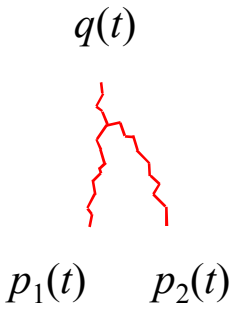

Fluid Flow in 2D Discrete Fracture Networks

Solve fluid network to get nodal pressures and flow rates.

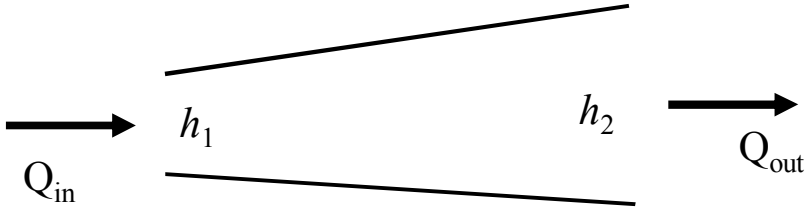

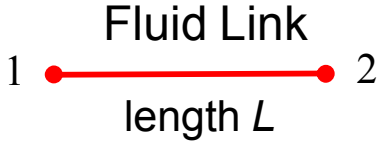

$$\begin{Bmatrix} Q_1 \\ Q_2 \end{Bmatrix} = \frac{T}{\mu} \begin{bmatrix} 1 & -1 \\ -1 & 1 \end{bmatrix} \begin{Bmatrix} P_1 \\ P_2 \end{Bmatrix}$$

Reynold's lubrication equation

$$\nabla(\rho \mathbf{Q}) = 0$$

$$\mathbf{Q} = -\frac{h^3}{12\mu}(\nabla p - \rho g h)$$

$$T = \frac{h_1^2 h_2^2}{6L} \frac{1}{h_1 + h_2}$$

Q = flow rate
P = pressure
μ = viscosity
T = transmissibility

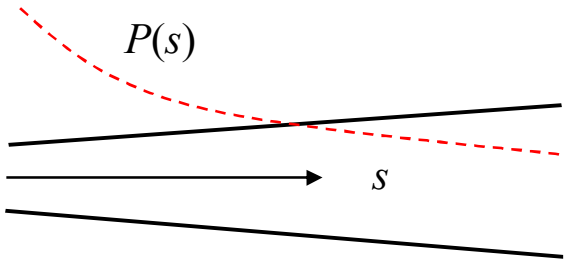

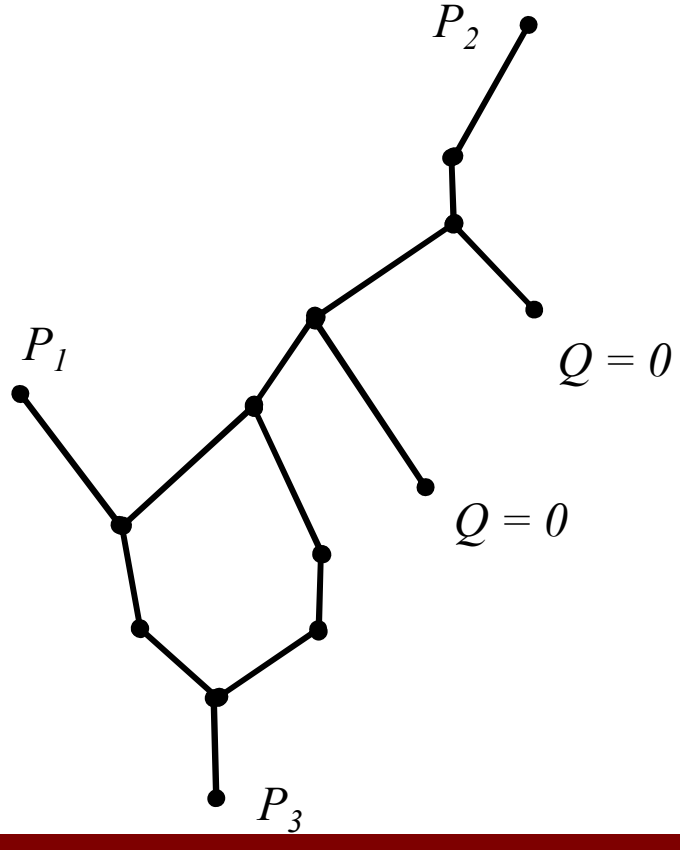

Fluid Flow in Discrete Fracture Networks

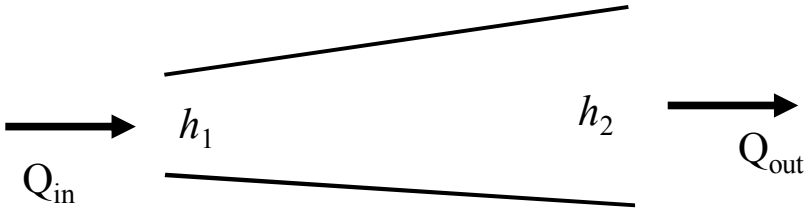

Reynold's lubrication equation

$$\nabla(\rho \mathbf{Q}) = 0$$

$$\mathbf{Q} = -\frac{h^3}{12\mu}(\nabla p - \rho g h)$$

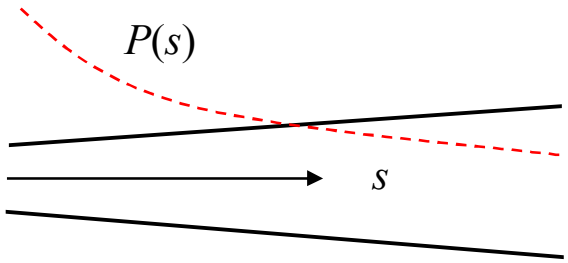

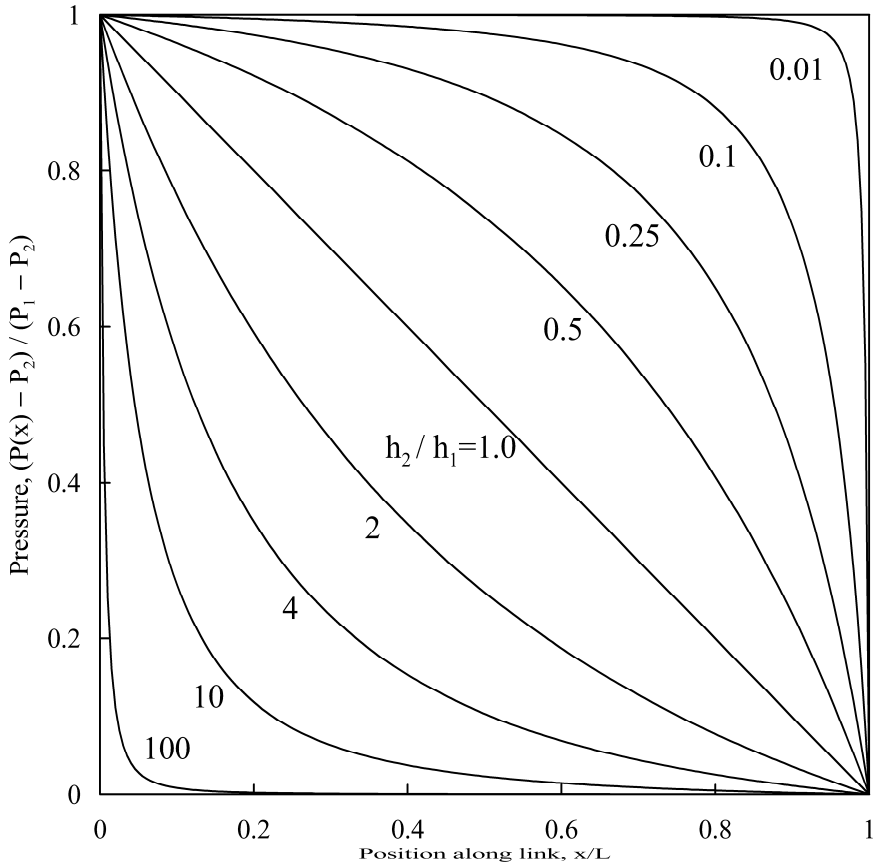

Hydraulic Fracture Simulation

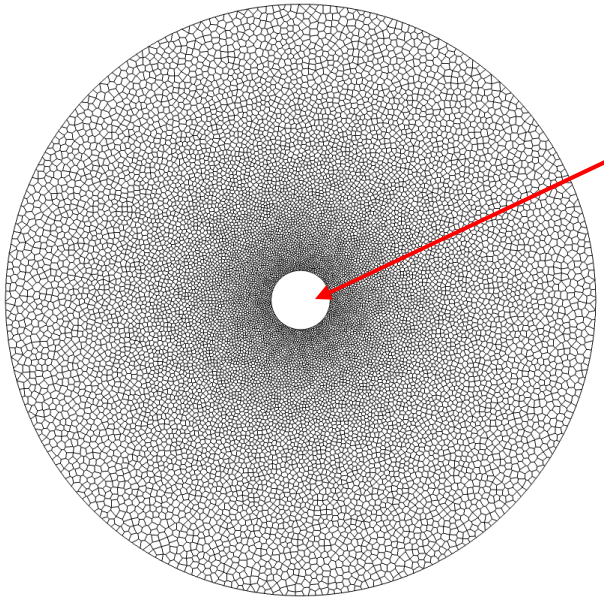

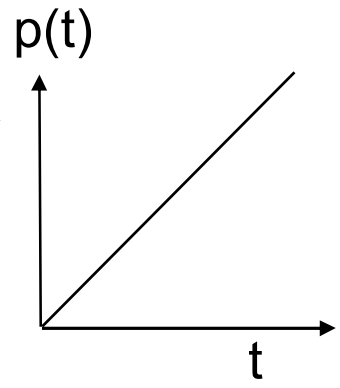

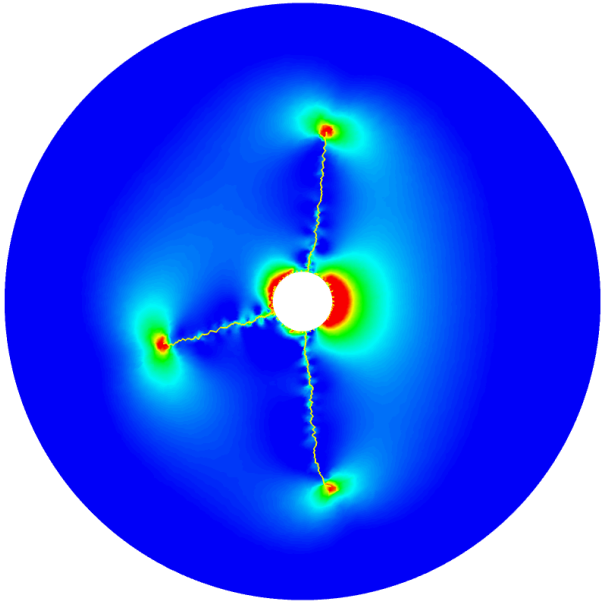

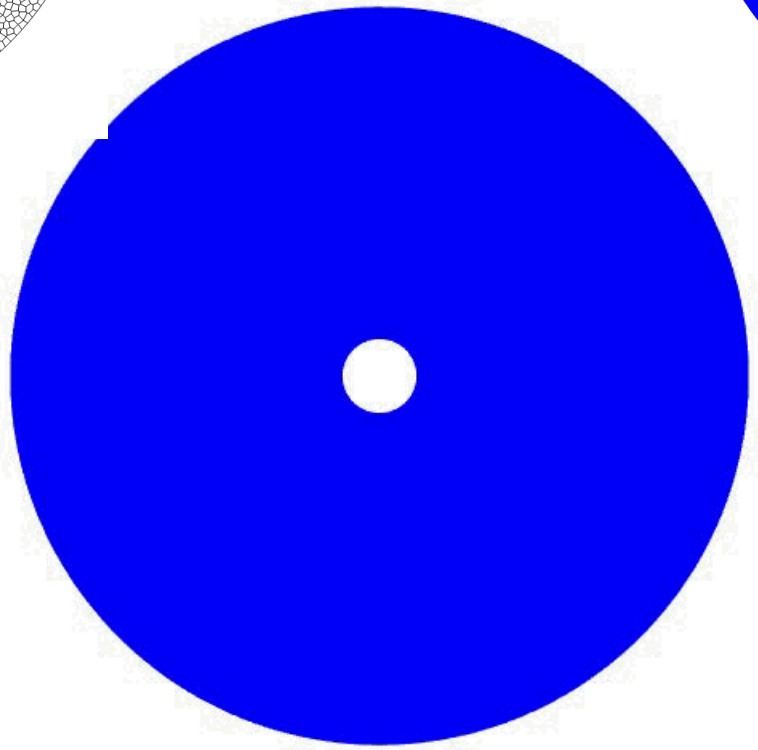

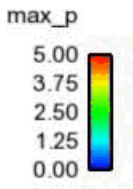

Hydraulic Fracture Simulation

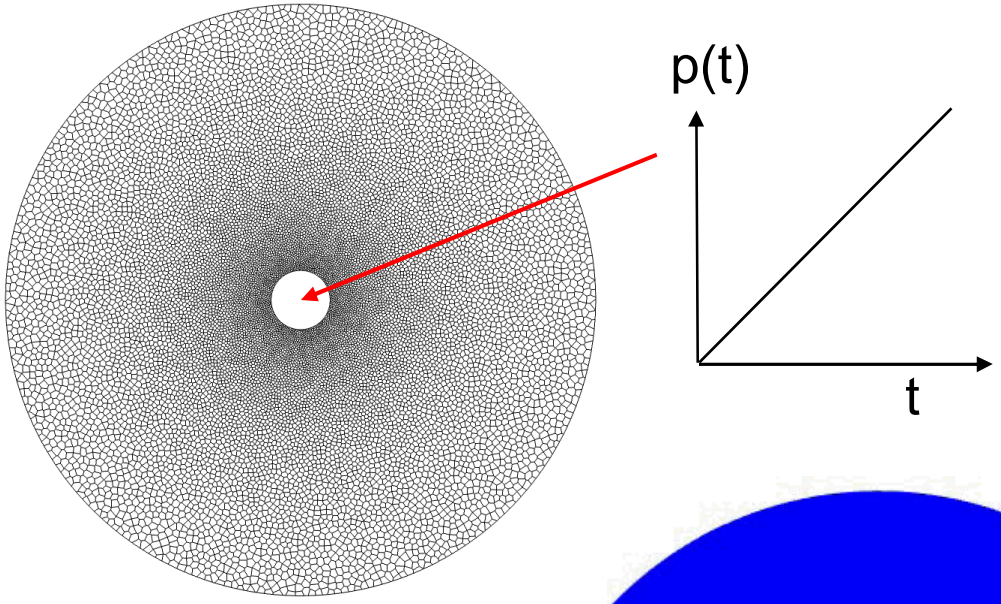

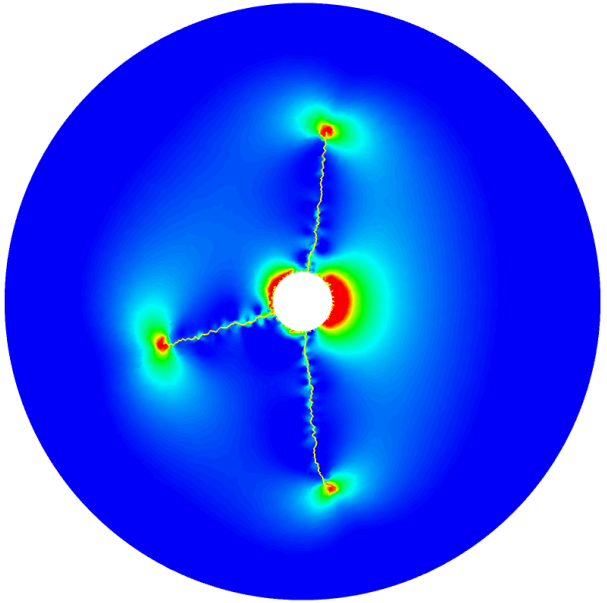

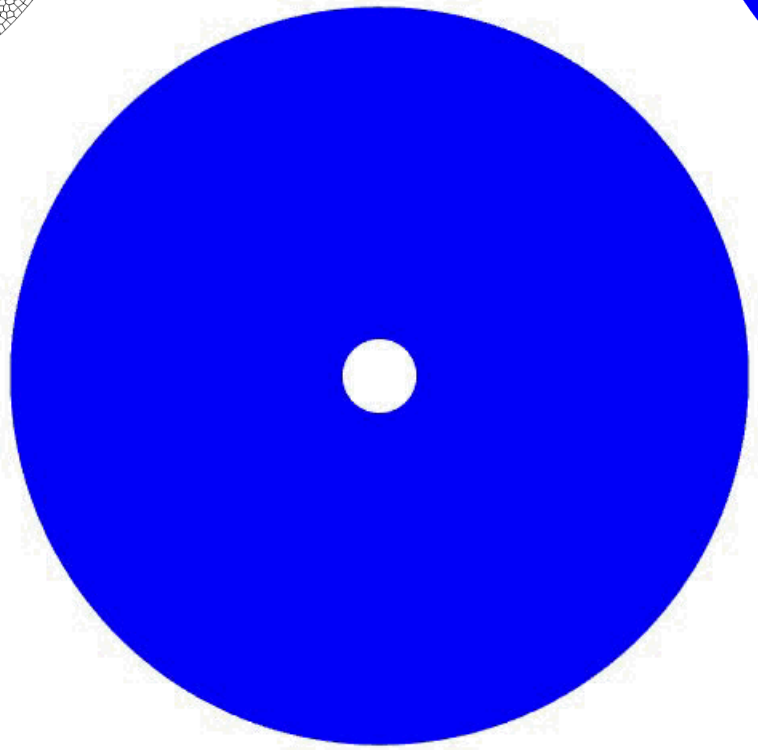

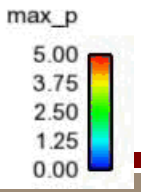

Coupled fluid flow in fracture networks

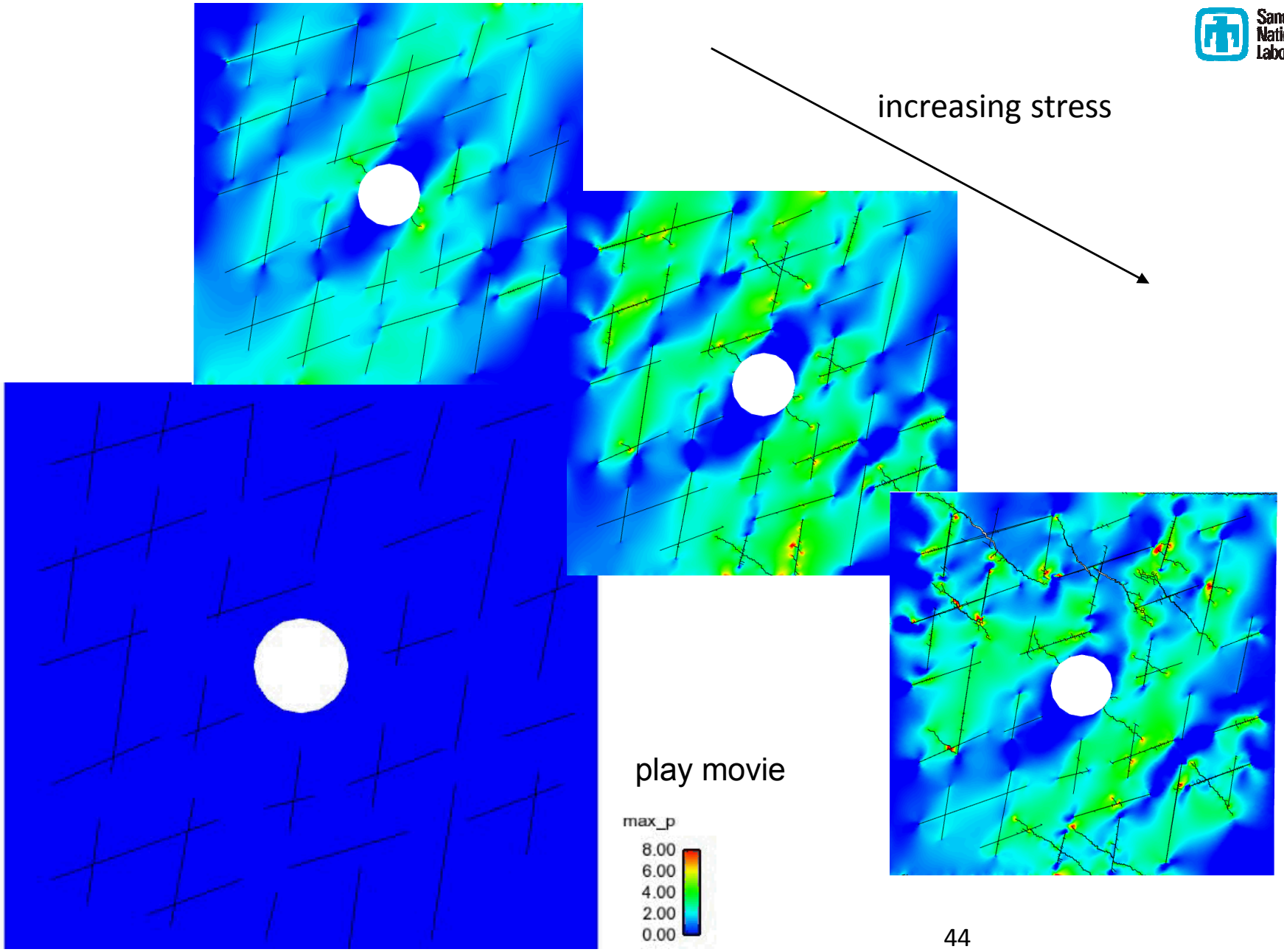

44

Sandia National Laboratories

Outline

1. Pervasive fracture and fragmentation
2. Random meshes and a polyhedral finite-element formulation
3. Assessing mesh convergence in a probabilistic sense
4. Example of statistical convergence using dynamic ring expansion
5. What is material variability?
6. Summary

Example: Explosively Loaded Cylinder

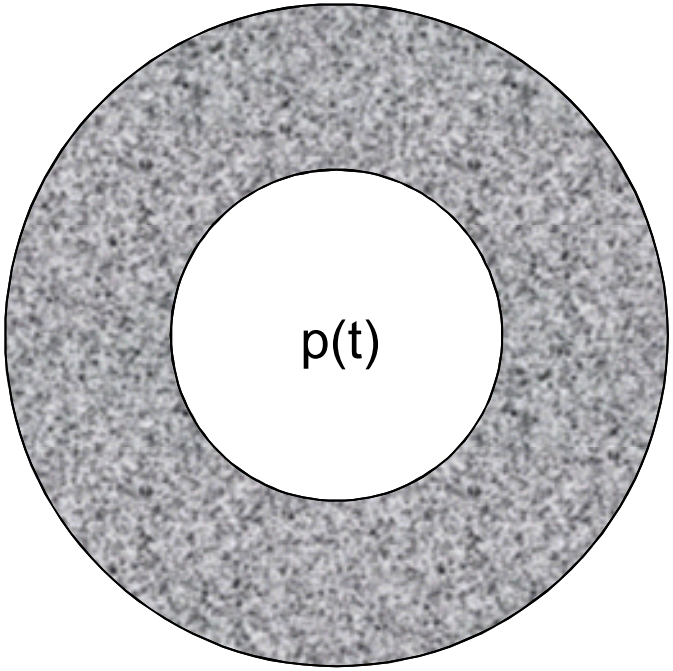

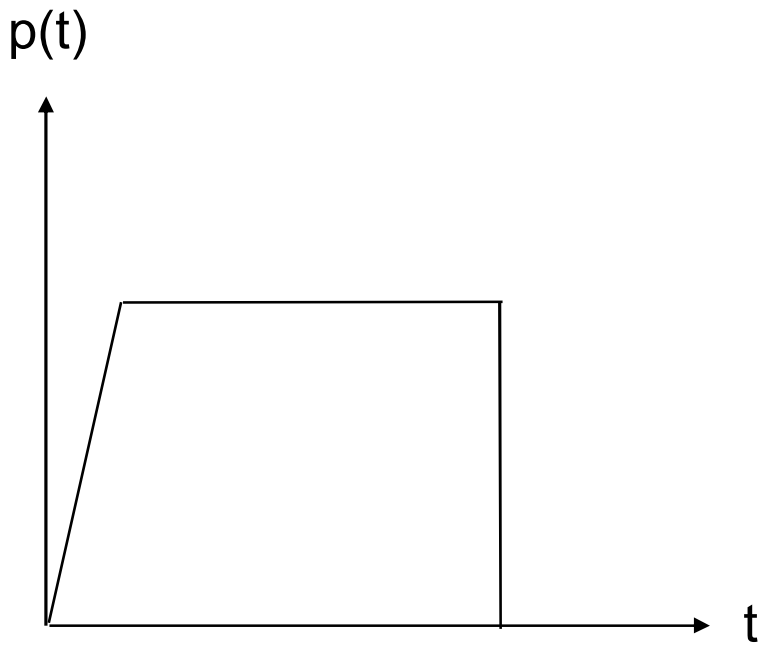

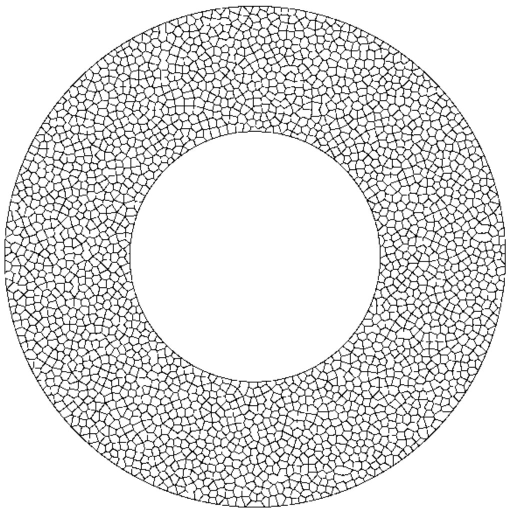

t = 0

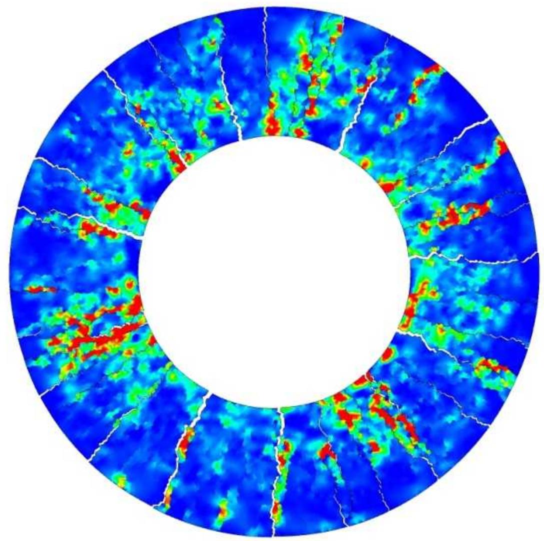

t = 2 ms

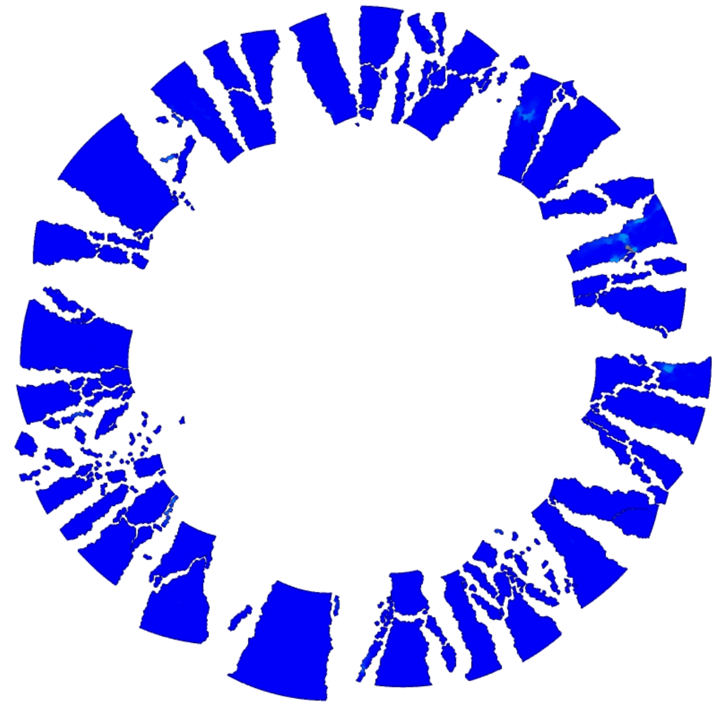

t = 20 ms

Short Time View, 2ms

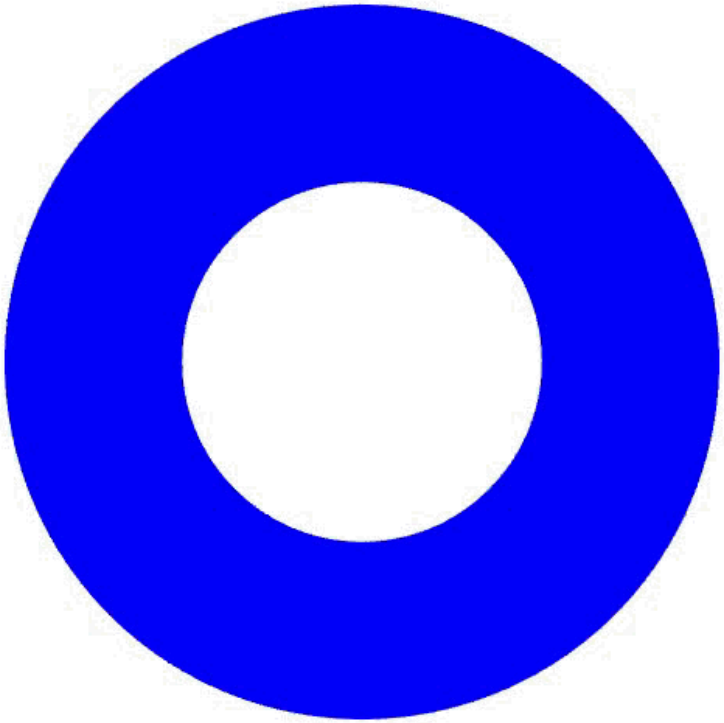

Long Time View, 20ms

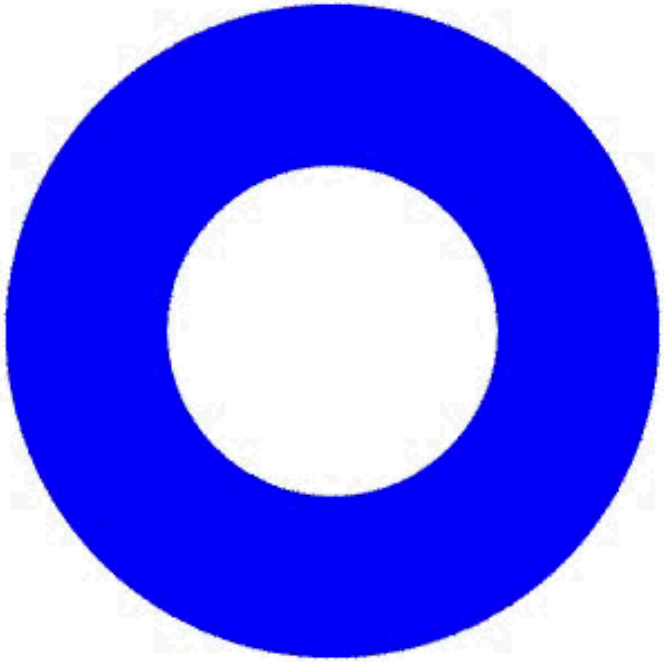

realization 1

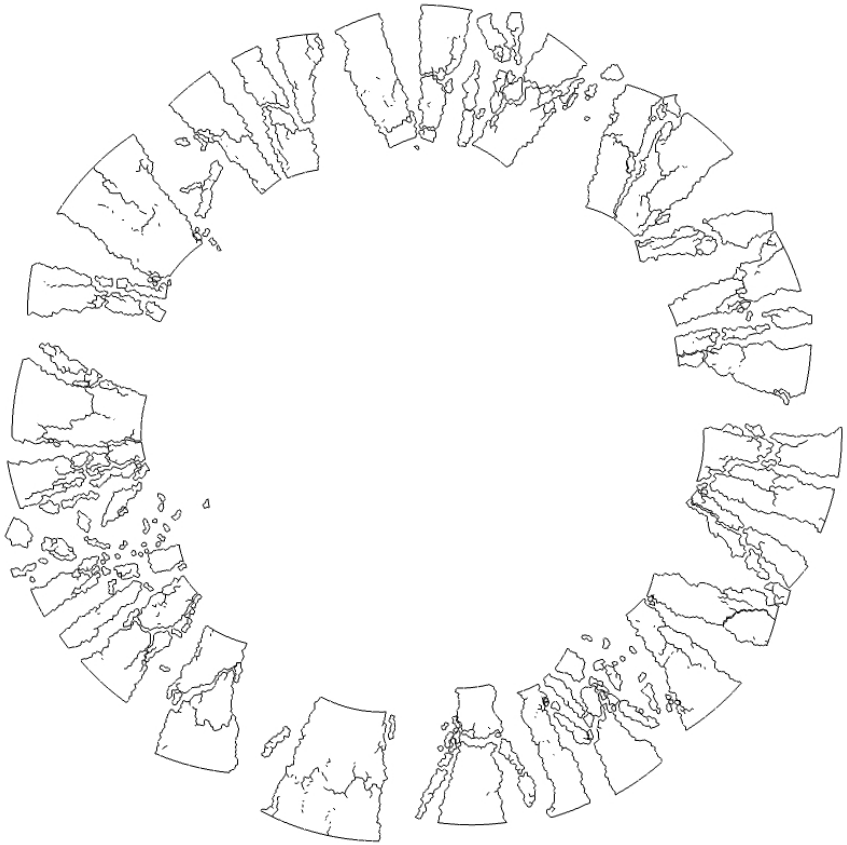

realization 2

Mesh Convergence?

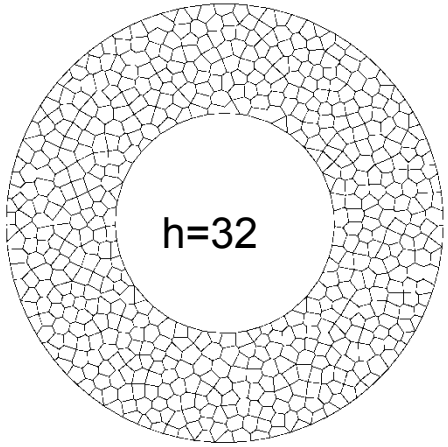

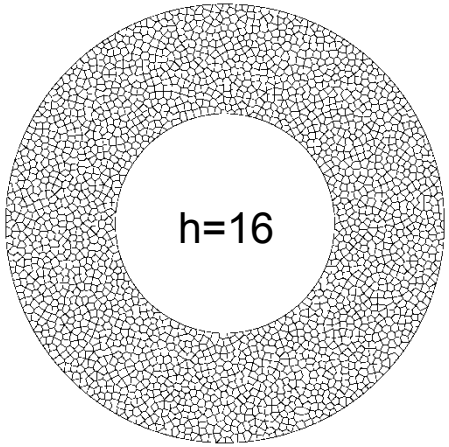

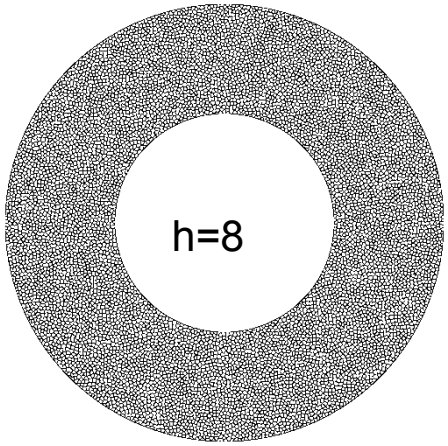

converging ?

Extreme Sensitivity to Initial Conditions

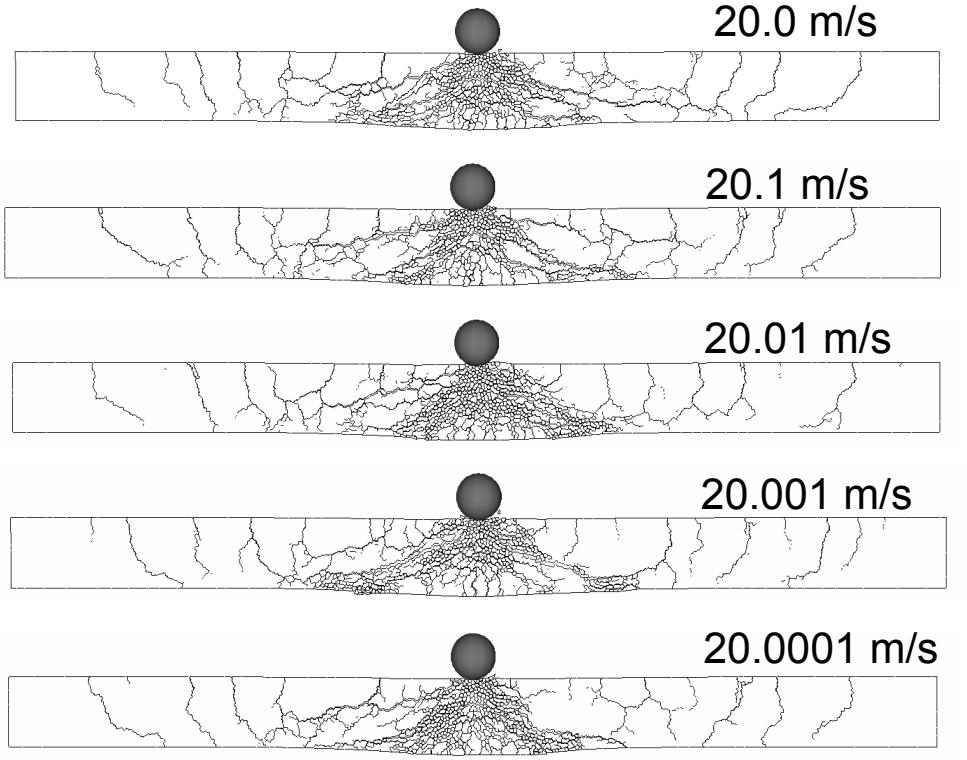

Crack patterns are qualitatively similar but distinctly different.

Nonlinear Dynamical Systems

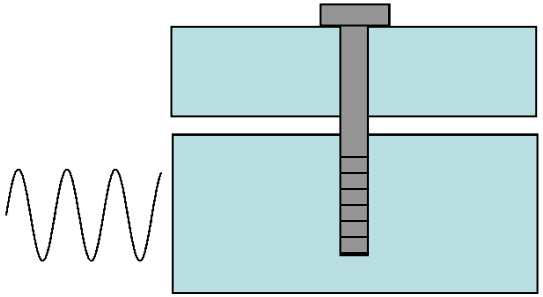

piecewise-smooth dynamical systems
- stick-slip
- contact-impact

buckling

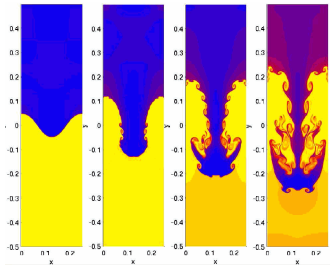

Rayleigh-Taylor instability

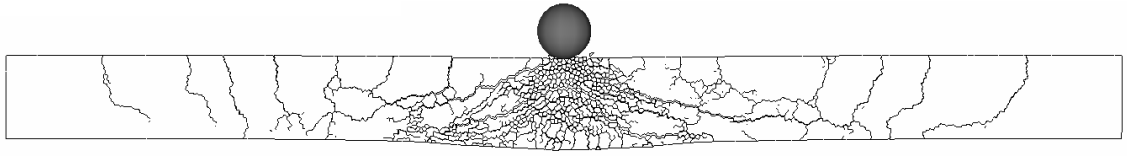

pervasive fracture

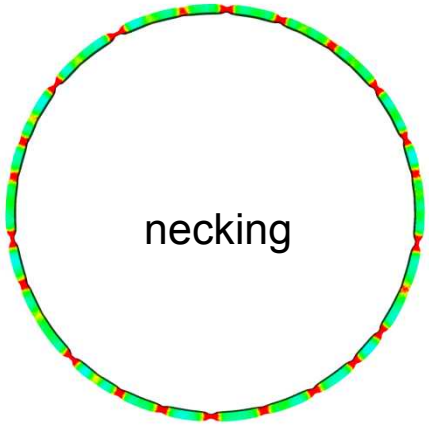

necking

shear banding

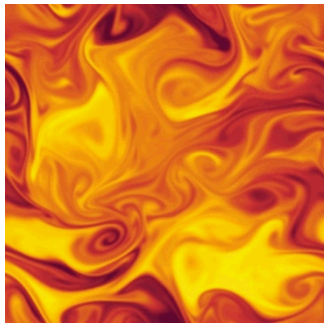

turbulence

- These deterministic systems can exhibit extreme sensitivity to initial conditions and system parameters.
- What about verification of mesh convergence?
- Need a way to quantify convergence in a statistical sense using random sampling.

Deterministic Horizon (Predictability Horizon)

result of extreme sensitivity to initial conditions

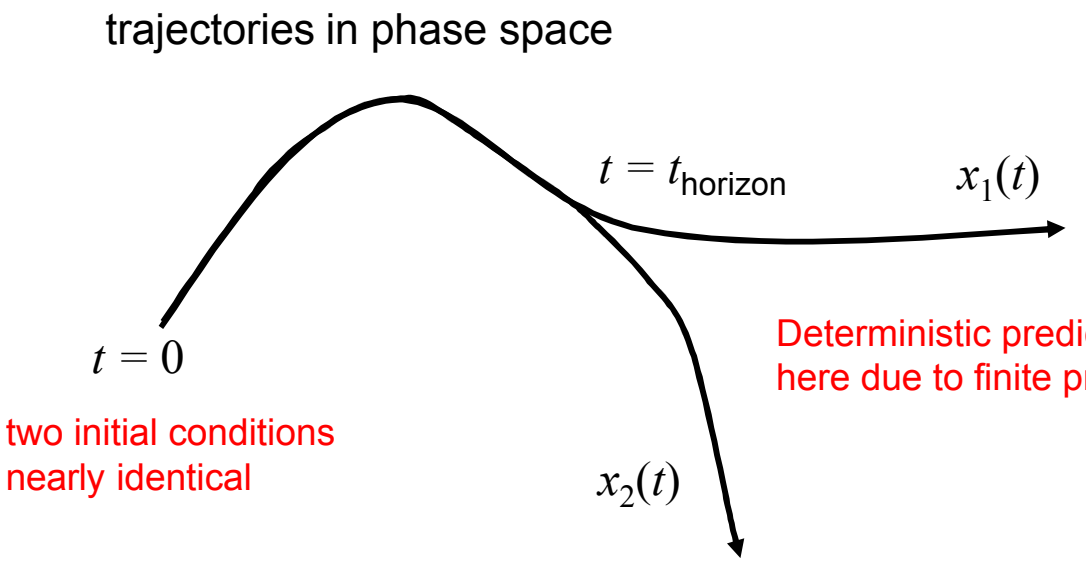

$$\delta(t) = x_1(t) - x_2(t)$$

$$\|\boldsymbol{\delta}(t)\| \sim \|\boldsymbol{\delta}_0\| e^{\lambda t}$$

$$t_{\text{horizon}} \sim O\left(\frac{1}{\lambda} \ln \frac{a}{\|\boldsymbol{\delta}_0\|}\right)$$

λ = Liapunov exponent

a = acceptable accuracy

Example: A Contact-Impact System, (Bouncing Ball)

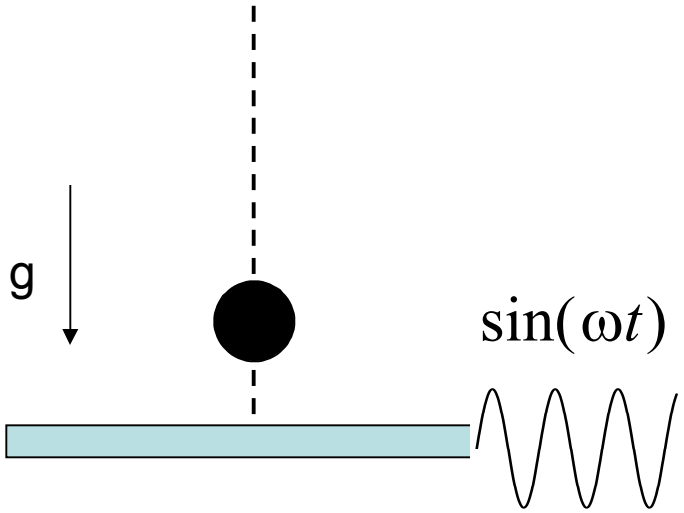

1 degree of freedom (up and down)

initial drop height

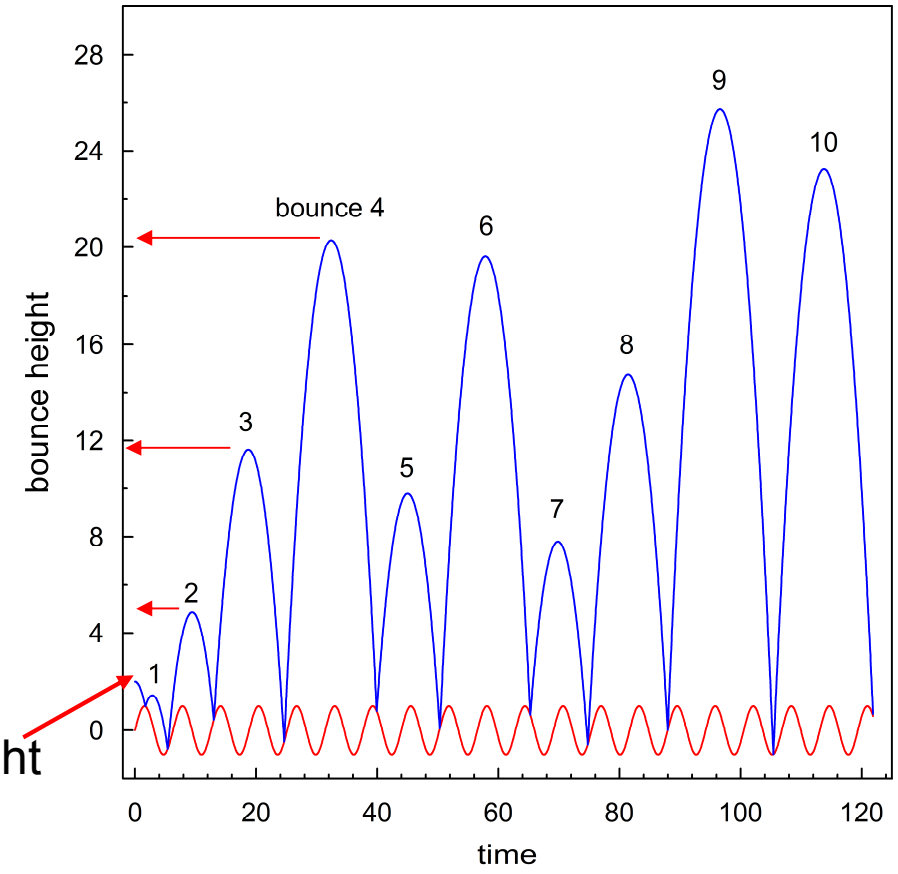

Sensitivity to Initial Conditions

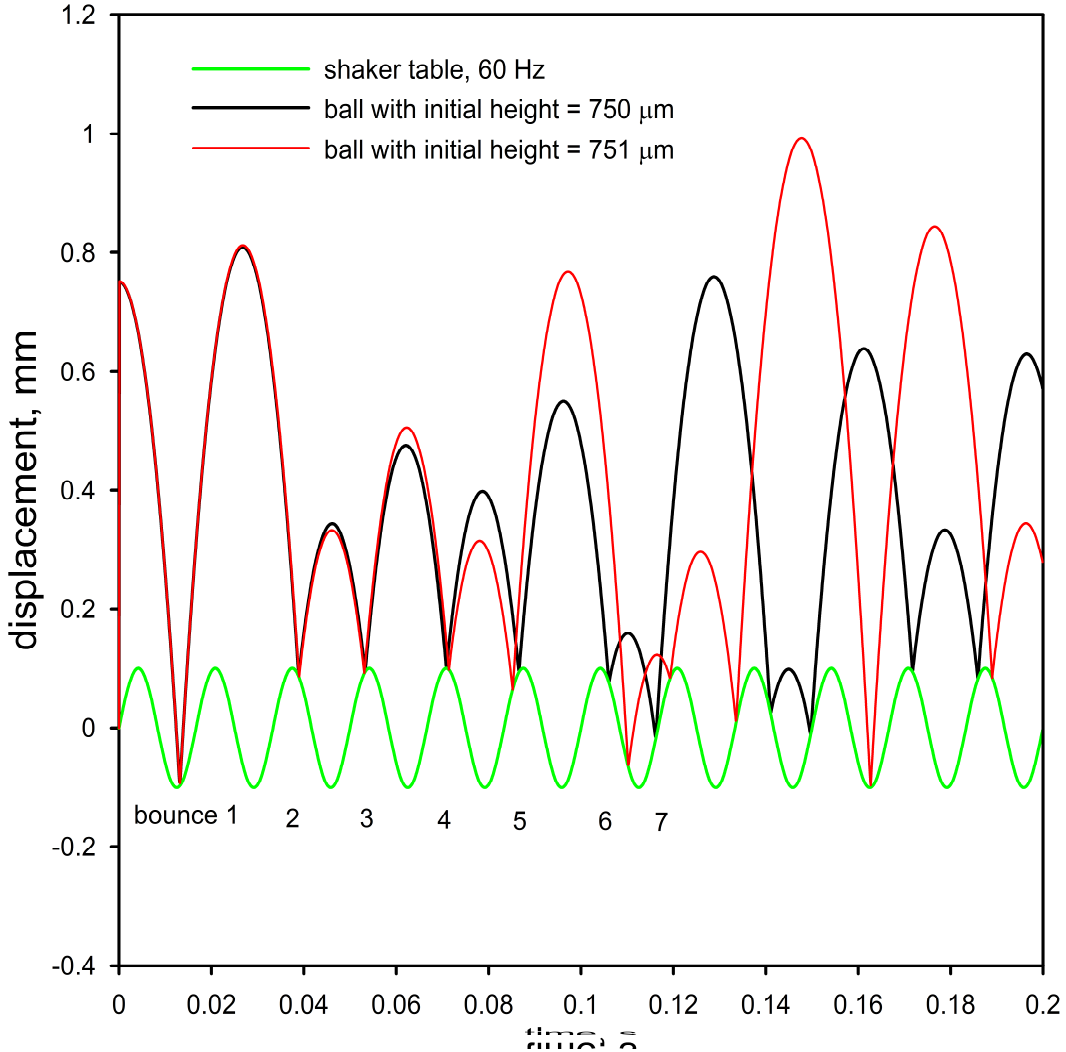

Sensitivity to Initial Conditions

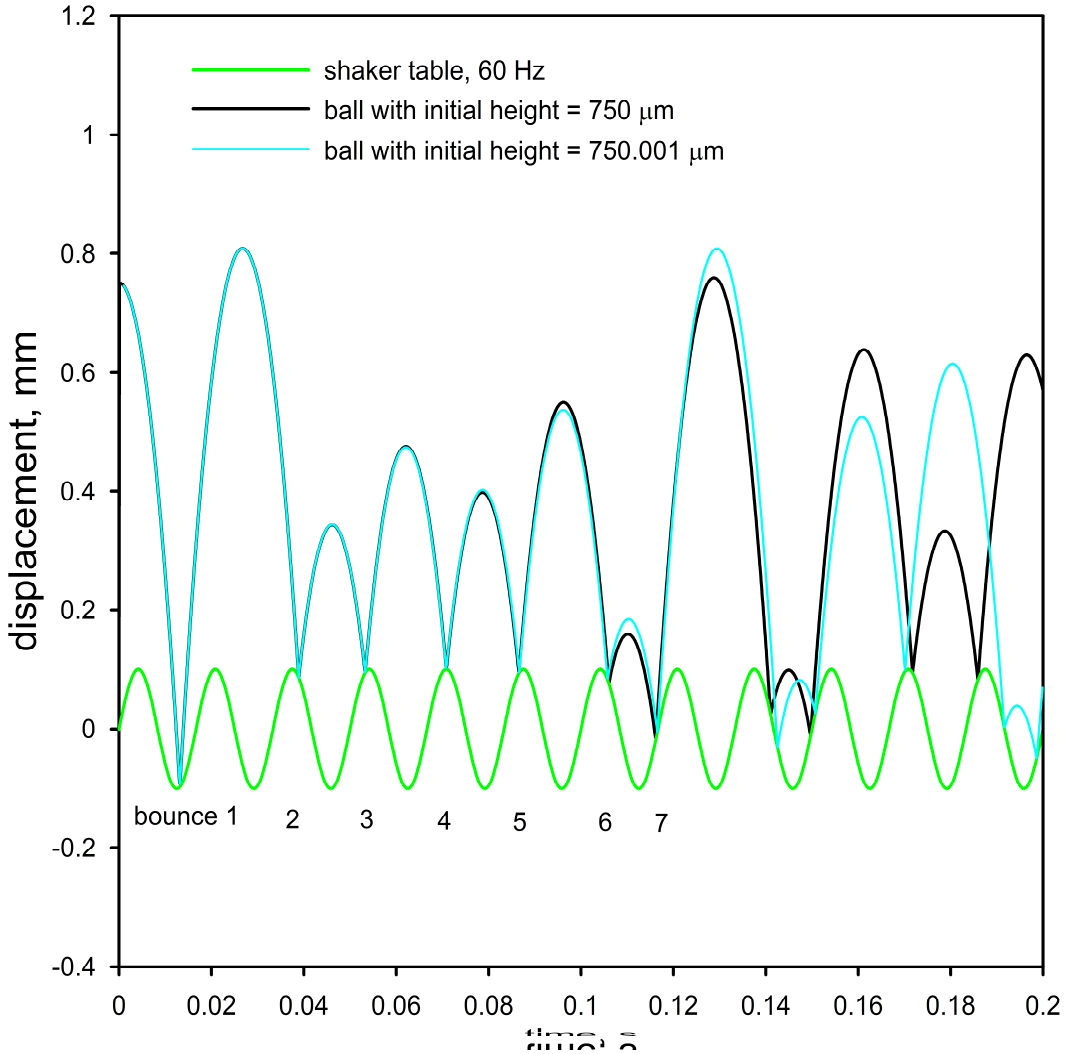

Height between Bounces

bounce 1,2,3, and 4

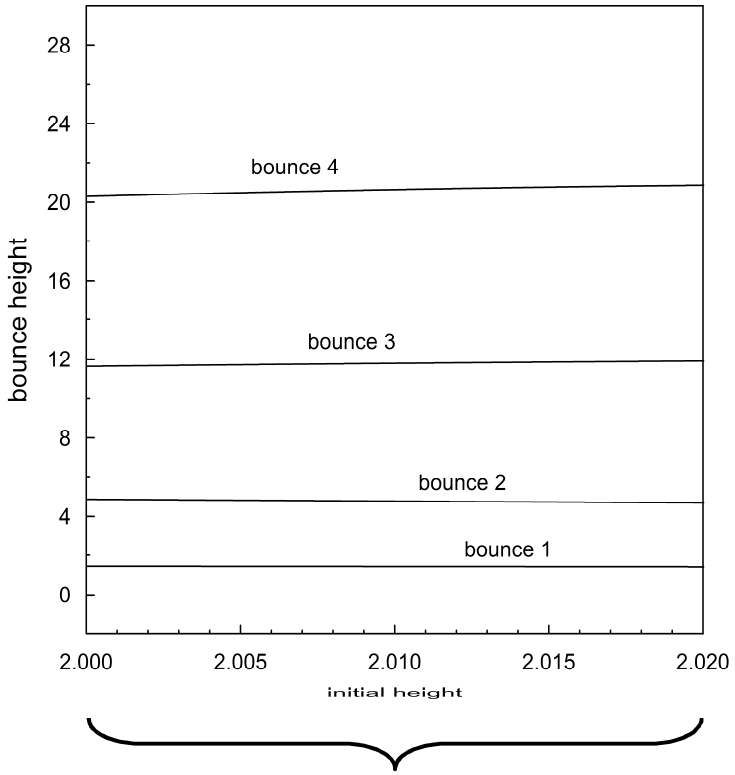

bounce 5,6, and 7

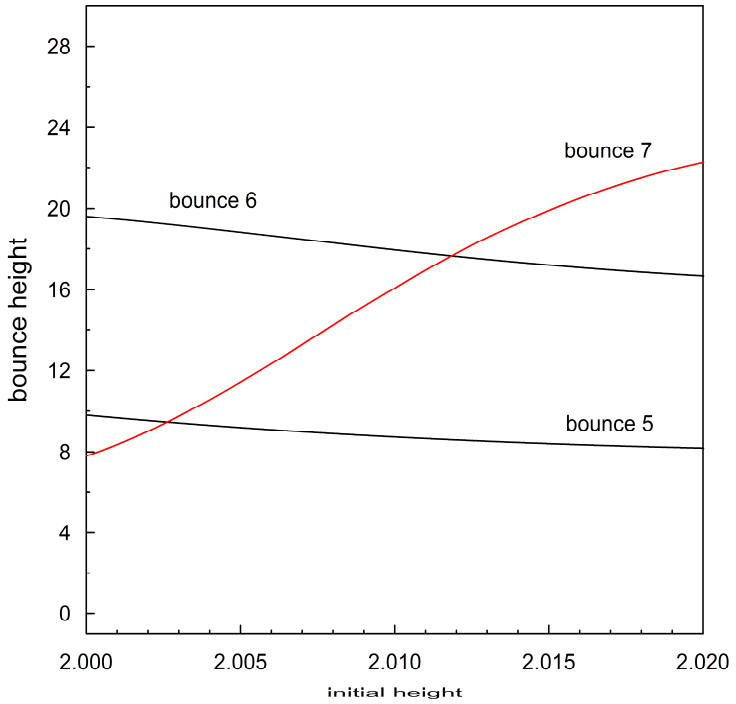

1% variation on initial drop height

Height between Bounces

bounce 8 and 9

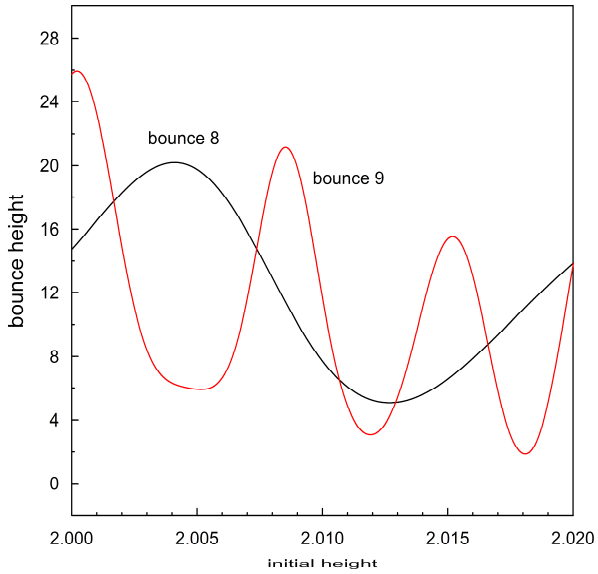

bounce 10

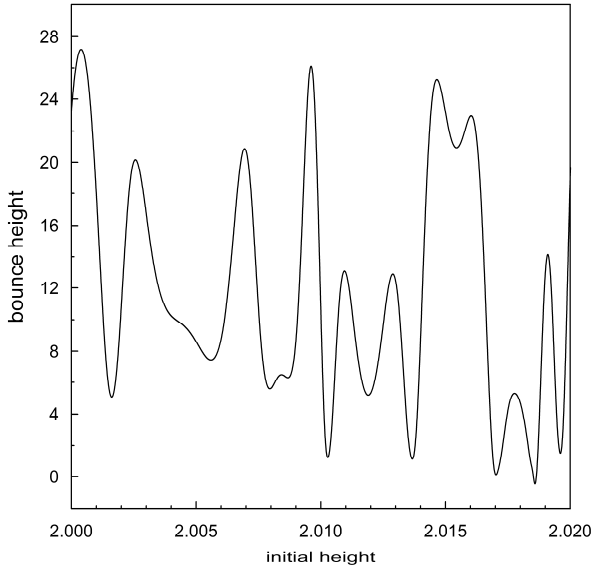

bounce 11

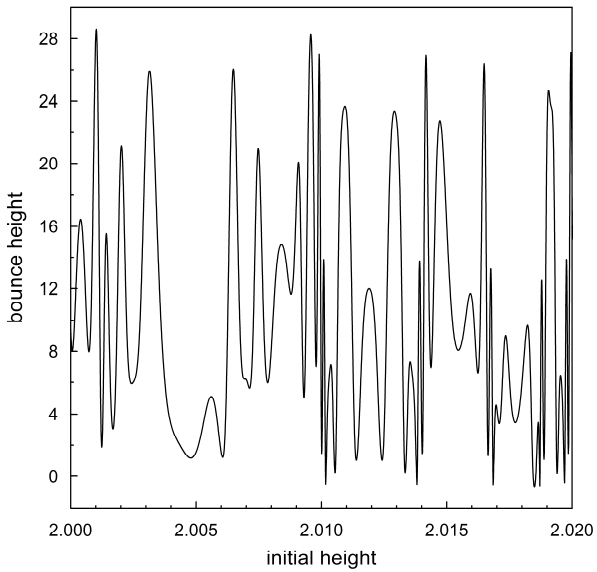

- Each bounce stretches and folds phase space (position and velocity).
- Correlation of bounce height with input height decreases with each bounce.
- Information is lost (entropy is created) with each bounce.
- There exists a deterministic time-horizon beyond which only a statistical description is appropriate.

Single trajectory, 80000 bounces

phase space, density of states

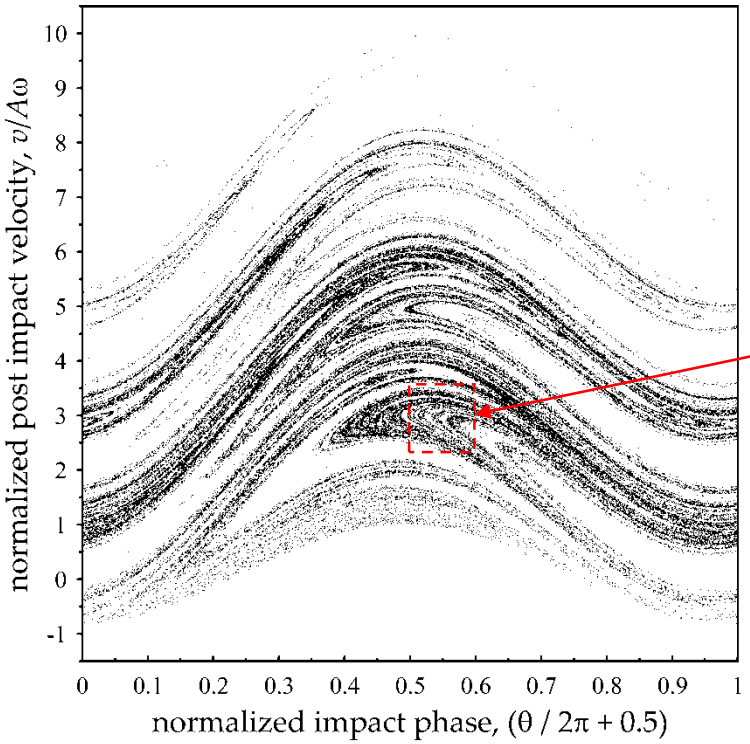

fractal structure

Beyond the predictability horizon, only statistical descriptions are appropriate.

Single trajectory, 80000 bounces

histogram

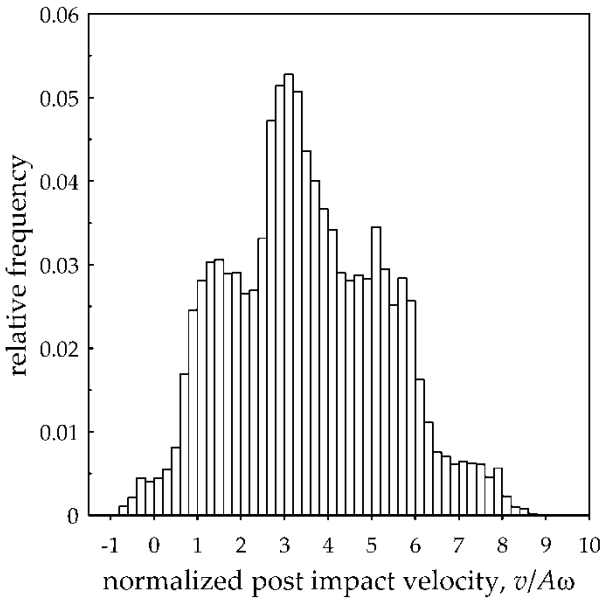

cumulative distribution

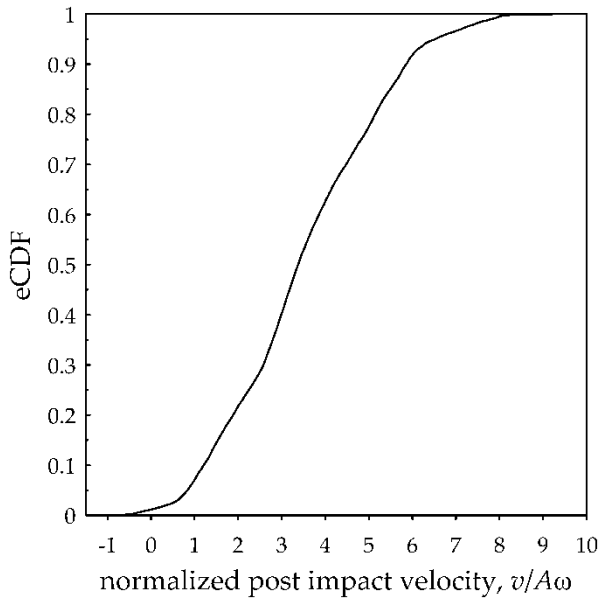

Despite extreme sensitivity to initial conditions, statistical behavior is “stable”.

Review of Probability

X = random variable

(an engineering quantity of interest)

PDF

$f(x)$ probability distribution function

$$f(x) = \frac{dF}{dx}$$

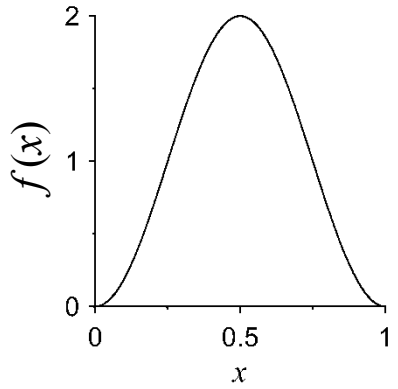

CDF

$F(x)$ cumulative distribution function

$$F(x) = \Pr(X < x)$$

$$F(x) = \int_{-\infty}^{x} f(x')\,dx'$$

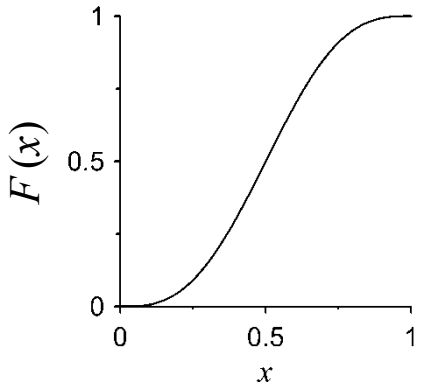

Definitions of Statistical Convergence

almost sure convergence

$$\Pr\left(\lim_{h\to 0} x_h = x\right) = 1$$

convergence in r-mean

$$\lim_{h\to 0} E\left(\left|x_h - x\right|^r\right) = 0$$

convergence in probability

$$\lim_{h\to 0} \Pr\left(\left|x_h - x\right| > \varepsilon\right) = 0$$

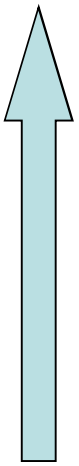

increasing strength

convergence in distribution

$$\lim_{h\to 0} F_h(x) = F(x)$$

Example

sequence of random variables X_n, $n = 1, 2, 3, \ldots$

PDF

$$f_n(x) = 1 - \cos(2\pi n x)$$

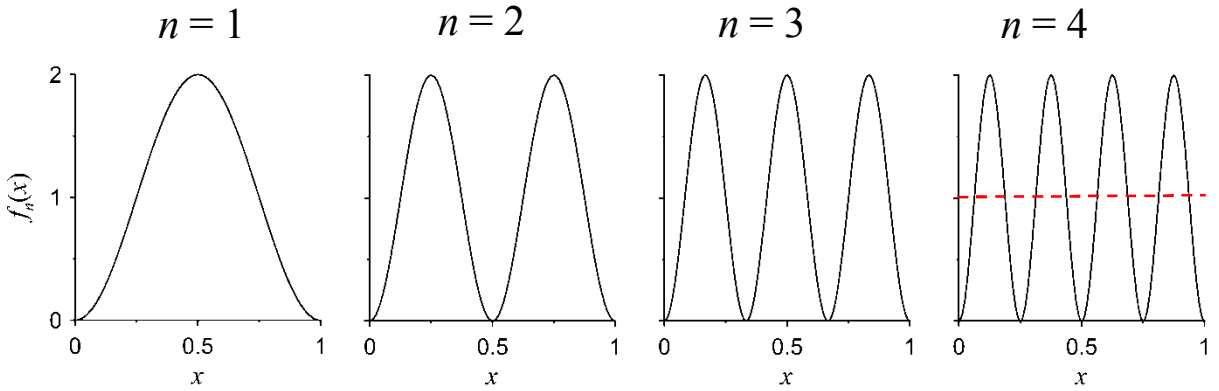

CDF

$$F_n(x) = x - \frac{1}{2\pi n}\sin(2\pi n x)$$

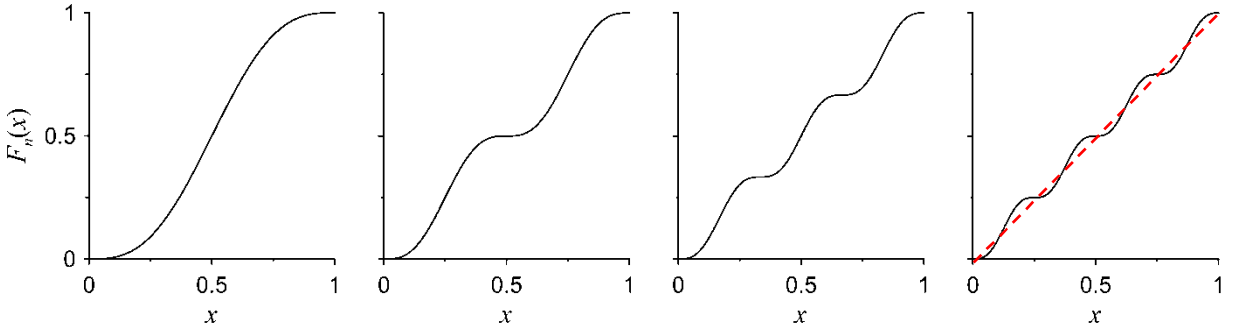

YES convergence-in-distribution: $\lim_{n\to\infty} F_n(x) = x$ for each x (pointwise)

NO convergence-in-probability: $\lim_{n\to\infty} \Pr\left(|X_n - X| > \varepsilon\right) \stackrel{?}{=} 0$ $\Pr\left(|X_n - X| > \varepsilon\right) = \frac{2}{\pi} + O(\varepsilon)$

for all n

How to Assess Convergence-in-Distribution?

$$\lim_{h \to 0} F_h(x) \stackrel{?}{=} F(x)$$

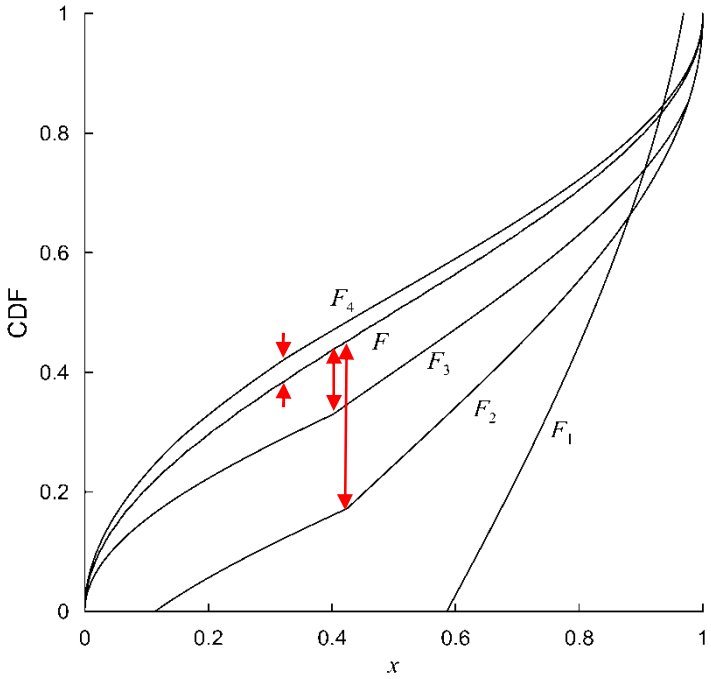

engineering quantity-of-interest

use L_∞ norm: $L_\infty(F_h, F) = \sup_x |F_h(x) - F(x)|$

What about finite sampling effects?

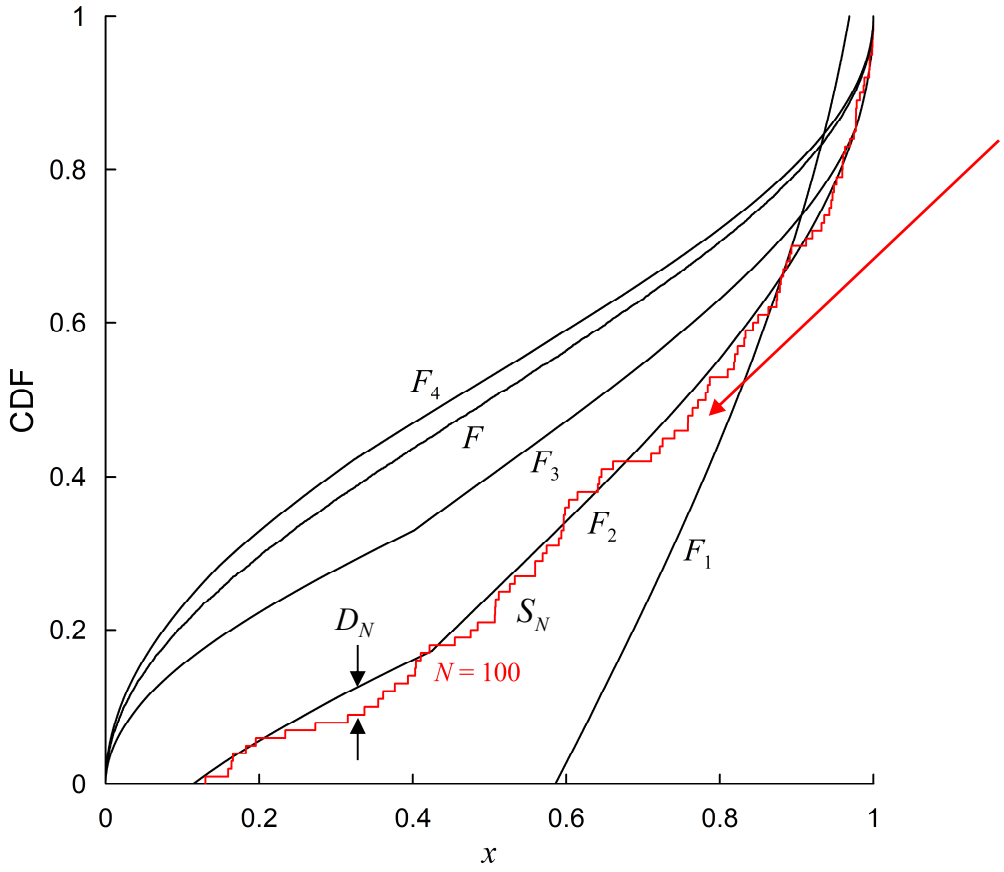

empirical CDF, $S_N(x)$

$$S_N(x) \equiv \begin{cases} 0, & x < x_1 \\ \dfrac{r}{N} & x_r < x < x_{r+1} \quad r = 1, \ldots, N-1 \\ 1 & x_N < x \end{cases}$$

Strong Law of Large Numbers:

$$\lim_{N \to \infty} S_N(x) = F(x) \quad \text{(almost surely)}$$

Finite Sampling Fluctuations in CDF

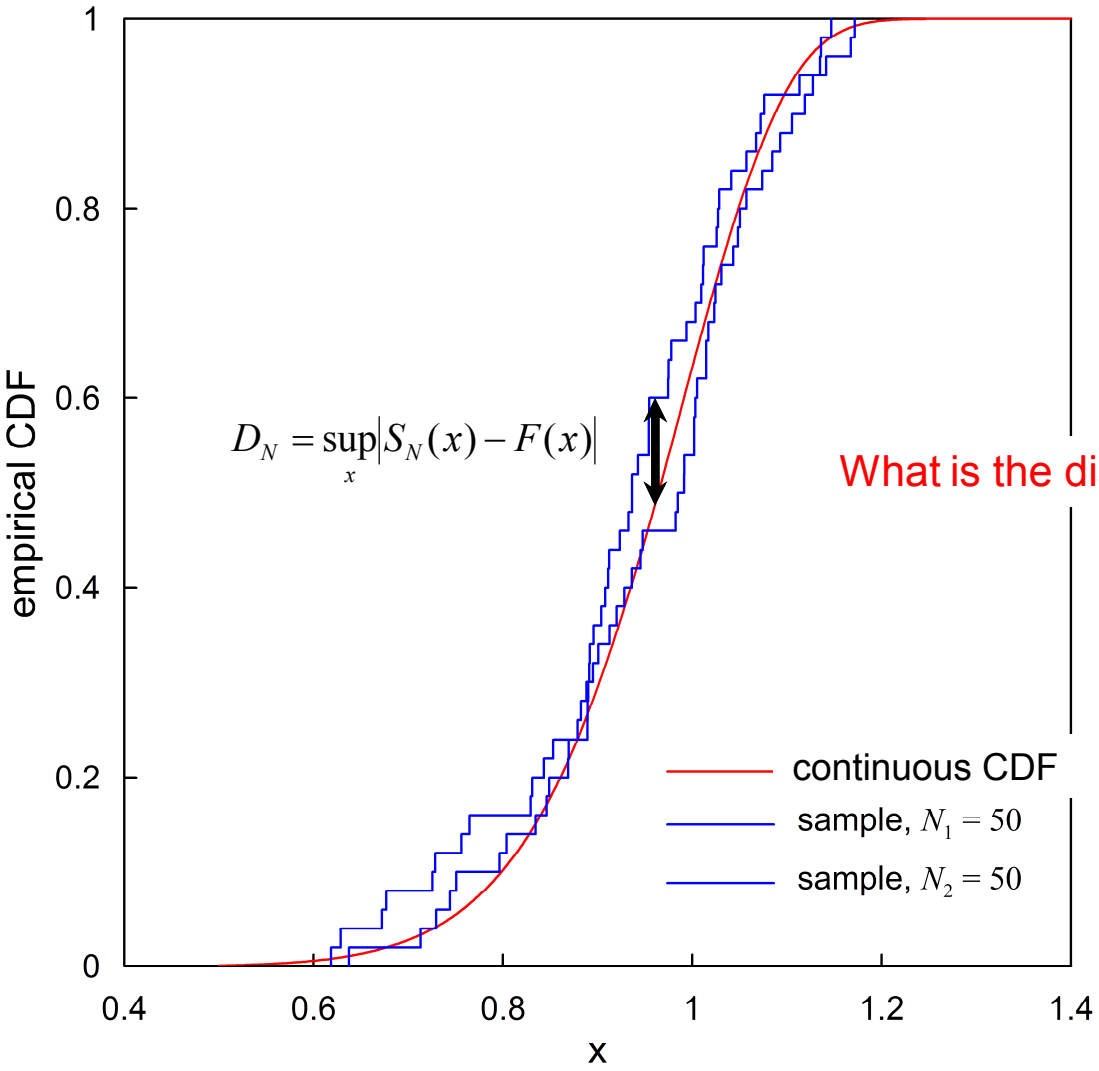

What is the distribution for D_N?

Kolmogorov-Smirnov Statistic

$$D_N = \sup_x \left| S_N(x) - F(x) \right|$$

$$\lim_{N\to\infty} \Pr\left(D_N < z/\sqrt{N}\right) = 1 - 2\sum_{j=1}^{\infty} (-1)^{j-1} \exp(-2j^2 z^2) \equiv p(z)$$

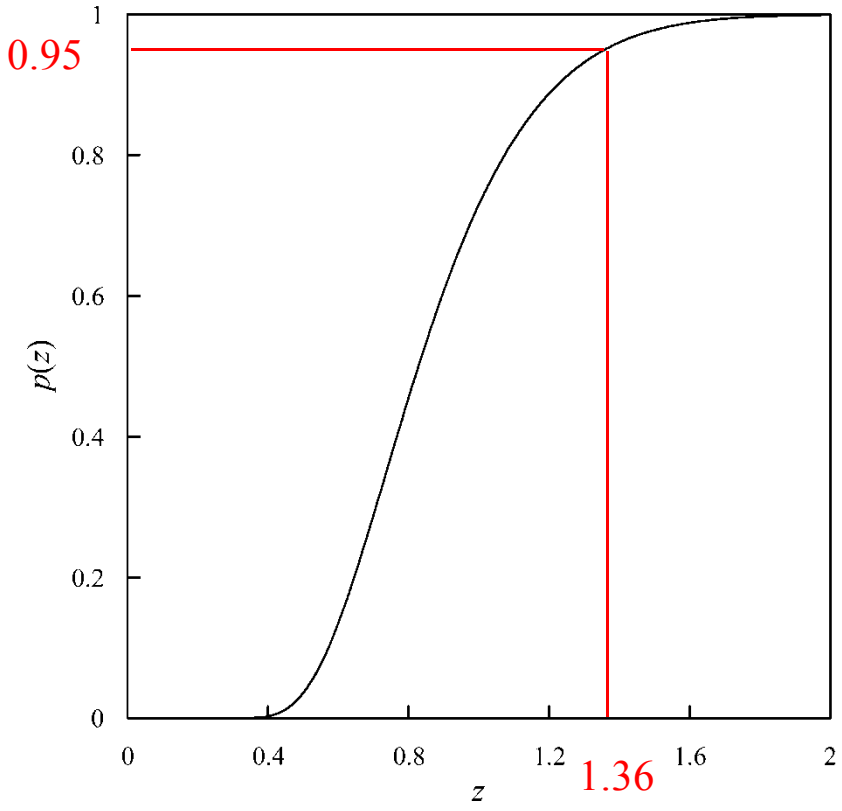

$$\Pr\left(D_N < \frac{1.63}{\sqrt{N}}\right) = 99\%$$

$$\Pr\left(D_N < \frac{1.36}{\sqrt{N}}\right) = 95\%$$

$$\Pr\left(D_N < \frac{1.19}{\sqrt{N}}\right) = 90\%$$

confidence bounds

- independent of distribution
- only for continuous CDFs

(conservative to within 2% for $N > 50$)
(tabulated for $N < 50$)

Kolmogorov-Smirnov Statistic

95% confidence bounds

N = 50

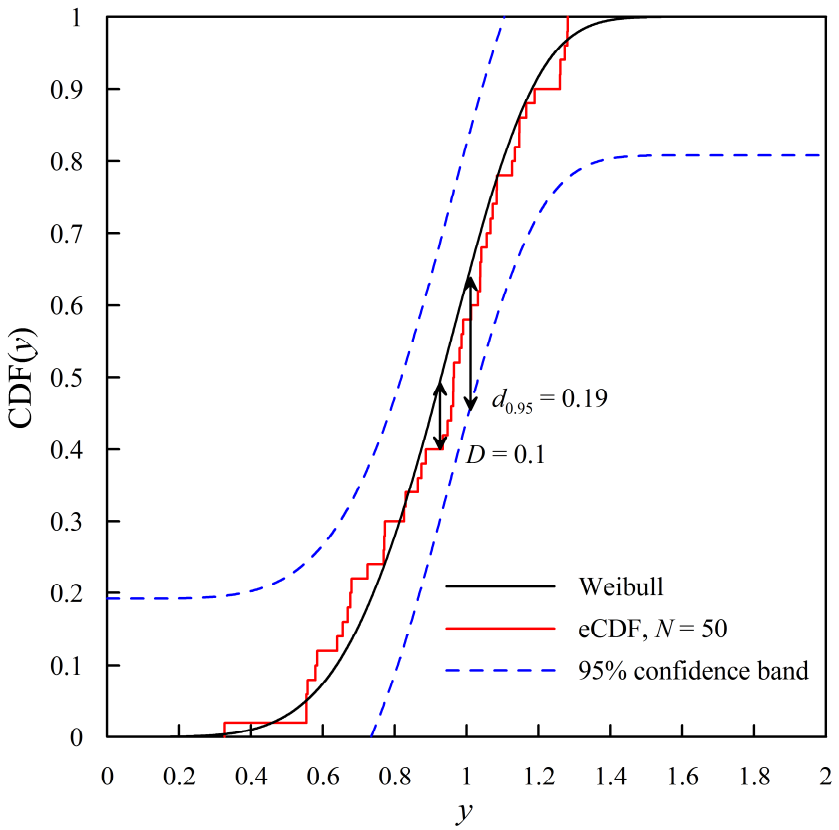

N = 500

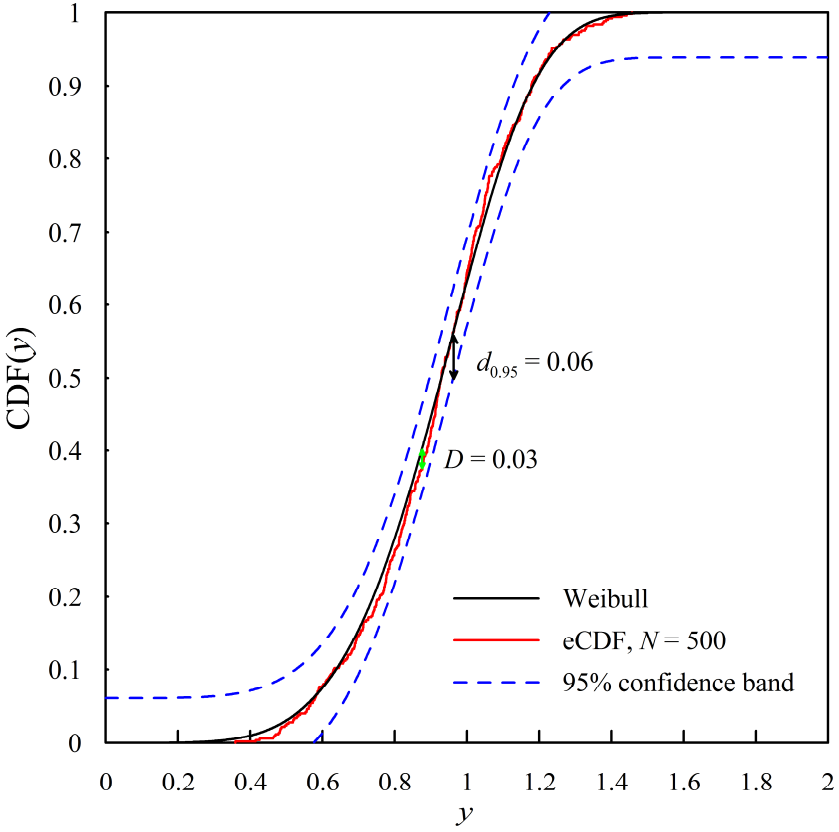

How to use KS-statistic to assess convergence-in-distribution with finite sample sizes?

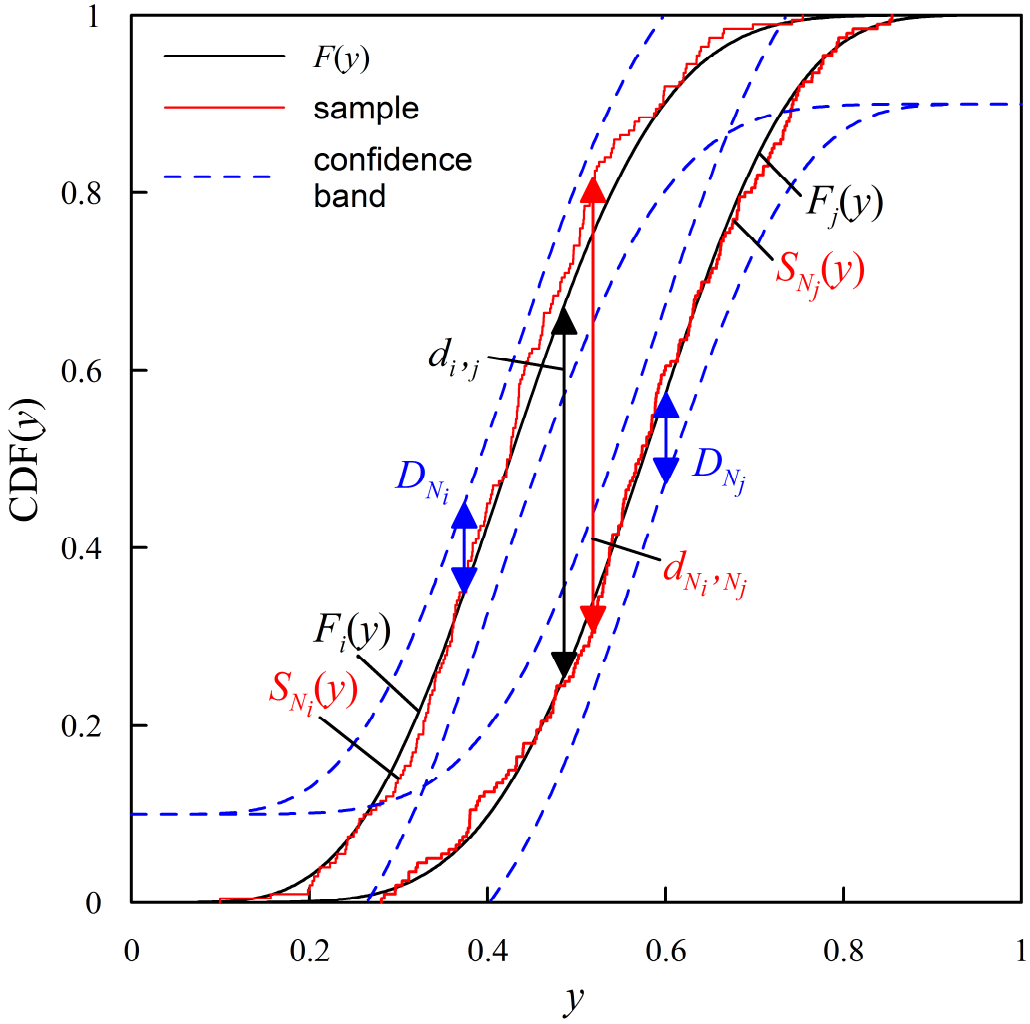

$$\left| d_{i.j} - d_{N_i,N_j} \right| \le D_{N_i} + D_{N_j} = \frac{z_i}{\sqrt{N_i}} + \frac{z_j}{\sqrt{N_j}}$$

Also, joint probability reduces confidence level.

Sandia National Laboratories

Outline

1. Pervasive fracture and fragmentation
2. Random meshes and a polyhedral finite-element formulation
3. Assessing mesh convergence in a probabilistic sense
4. Example of statistical convergence using dynamic ring expansion
5. What is material variability?
6. Summary

Example: Ductile Thin Ring Expansion

Grady, D. and D. Benson,1983, "Fragmentation of metal rings by electromagnetic loading." *Experimental Mechanics* **23**(4): 393-400.

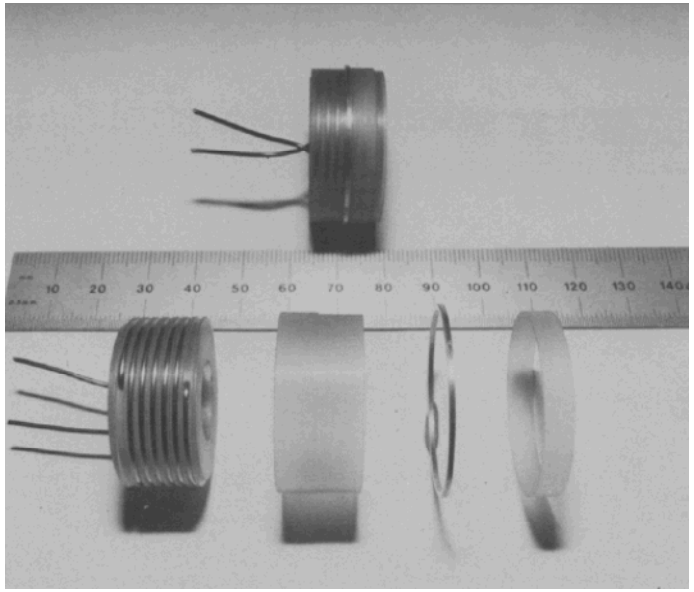

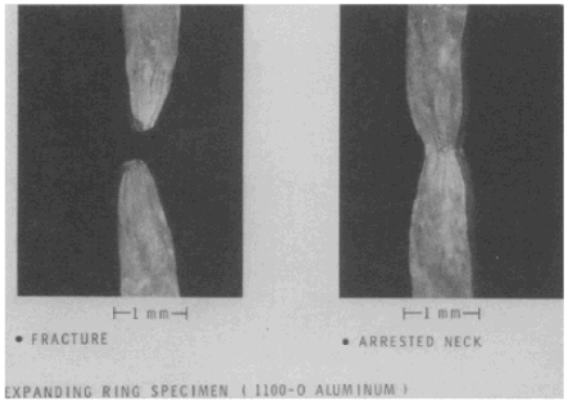

Fig. 5—Photograph of fracture and arrested-neck region from dynamic expansion of an aluminum ring

Simulation

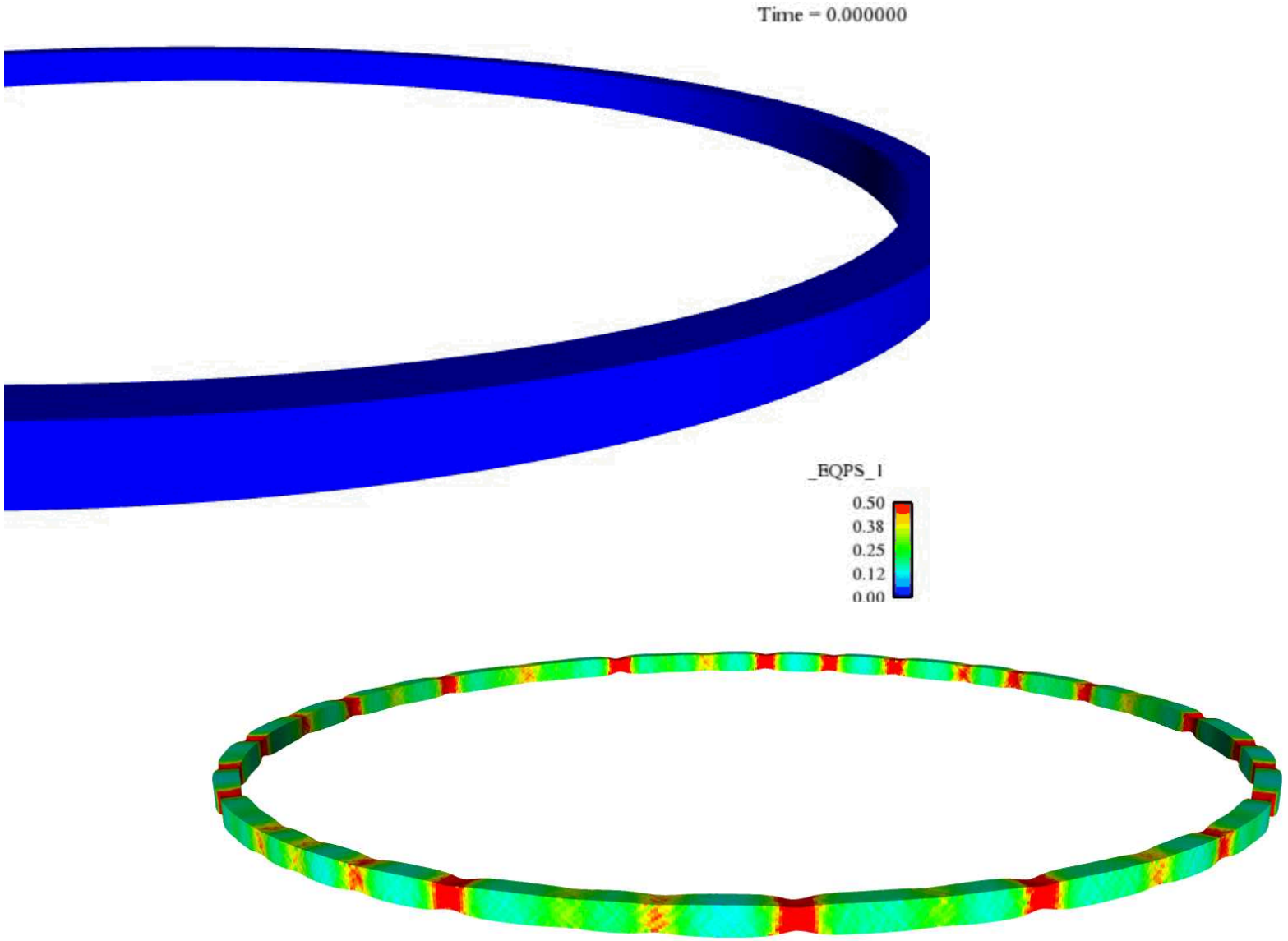

Four Levels of Mesh Refinement

R0

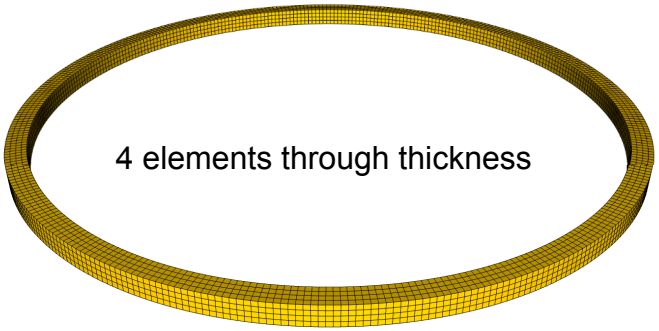

R2

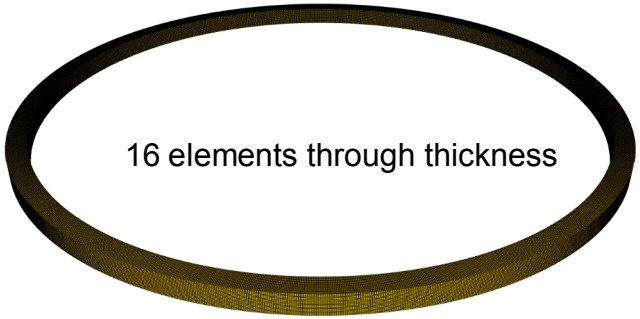

R1

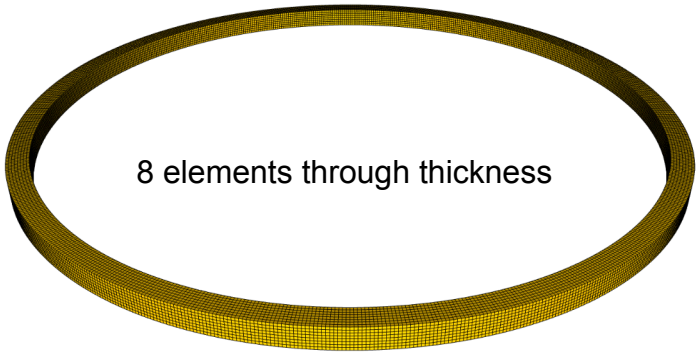

R3

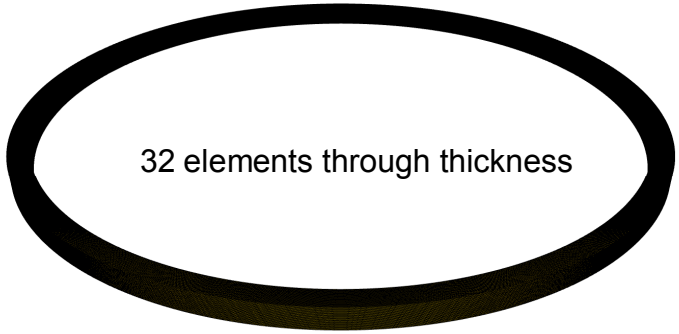

Spatial Material Variability in Initial Yield Stress

(power-law hardening)

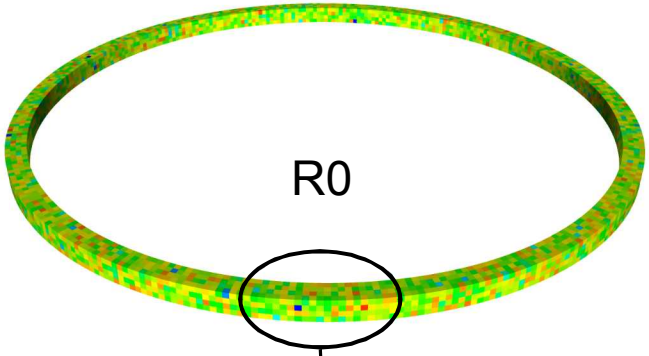

Weibull Probability Density

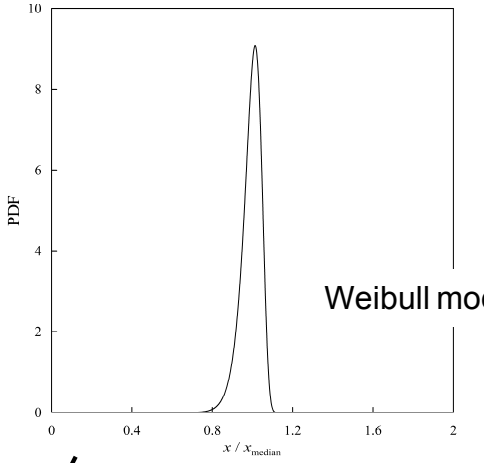

Weibull modulus = 25

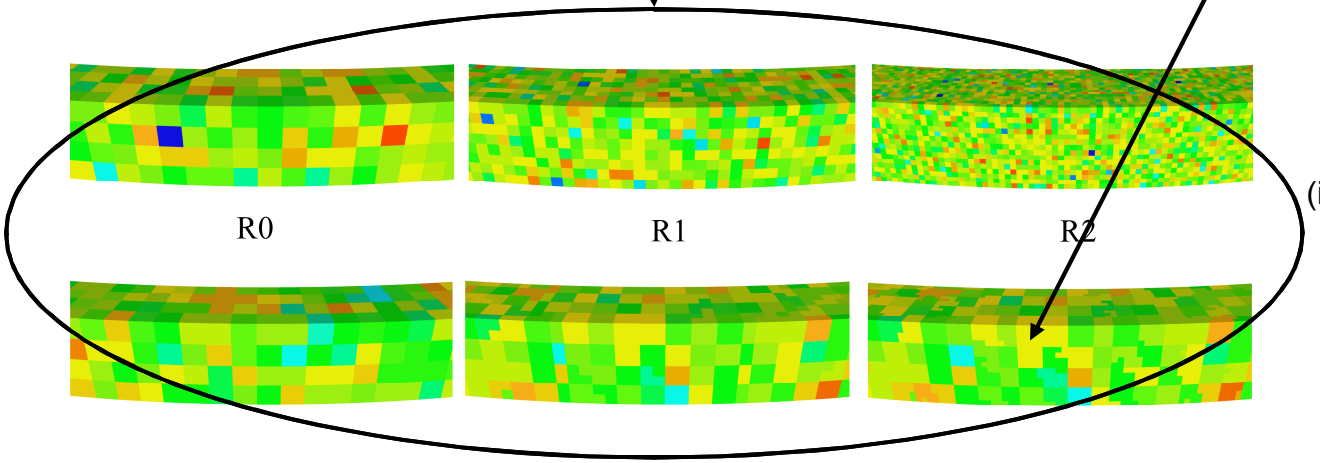

without texture

each *element* is iid

(independent, identically distributed)

with texture

each "*cell*" is iid

Cross-Sectional Area

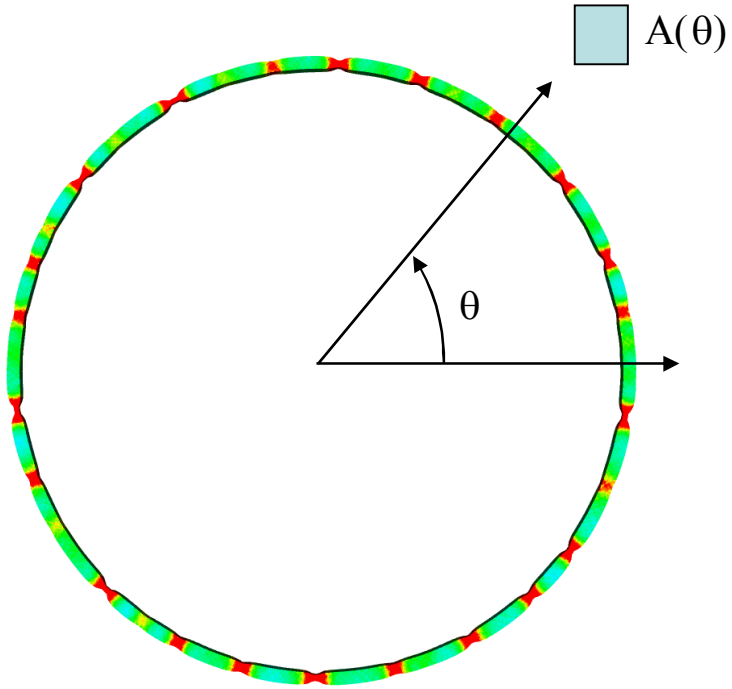

Reduce 3D random field to 1D random field.

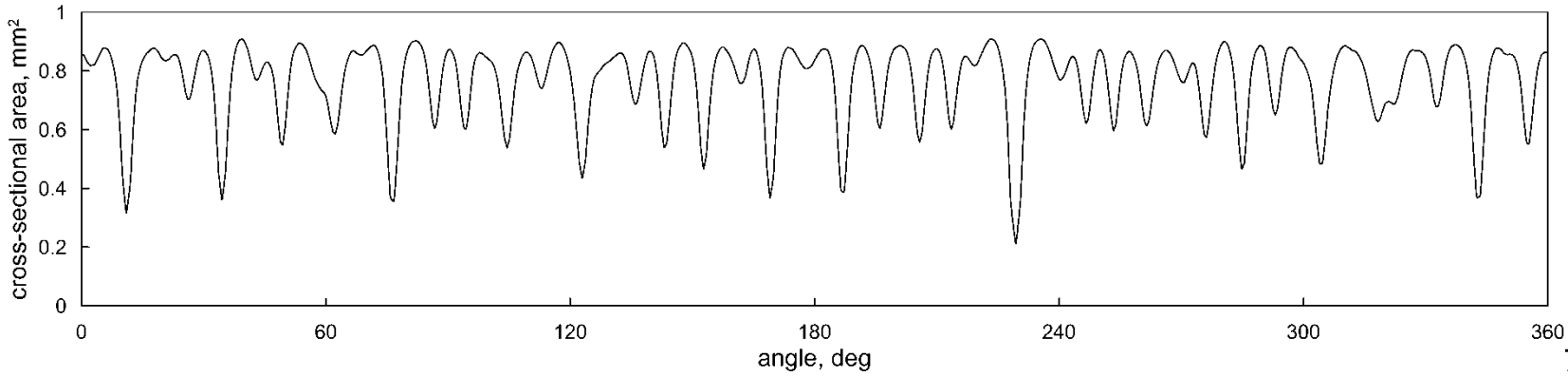

Neck Identification

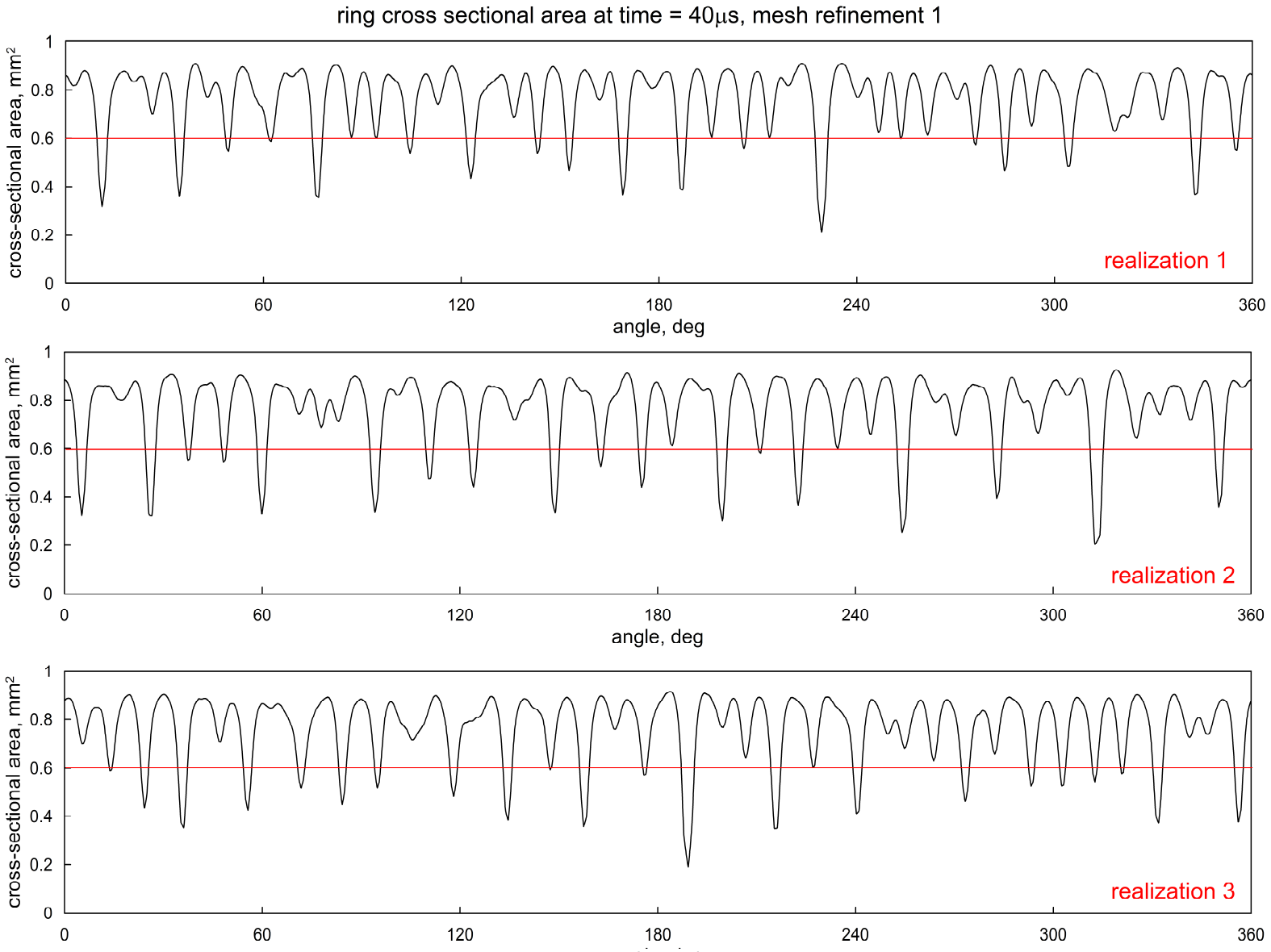

Convergence-in-Distribution?

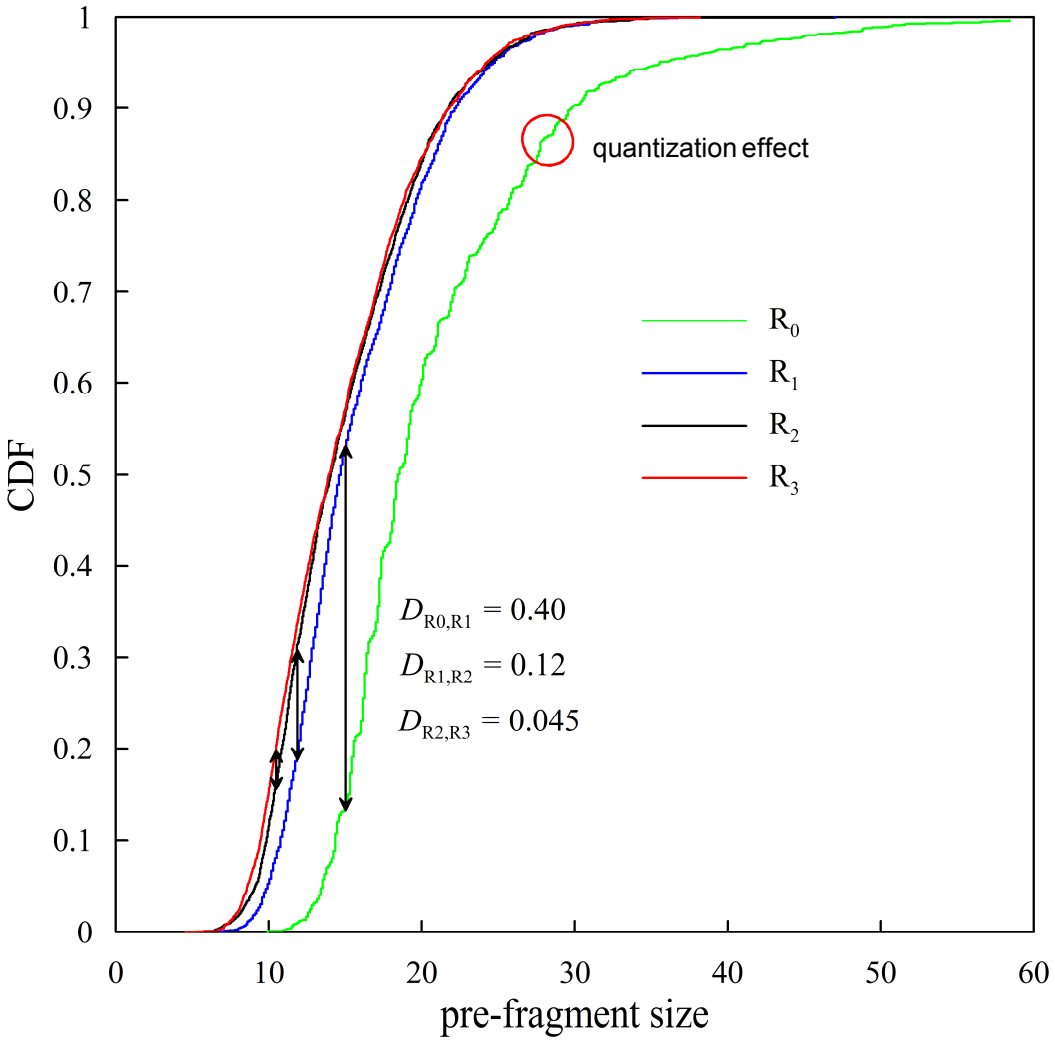

100 simulations
ensemble statistics

number of pre-fragments
(sample sizes)

$N_0 = 1714$
$N_1 = 2274$
$N_2 = 2386$
$N_3 = 2421$

Convergence-in-Distribution?

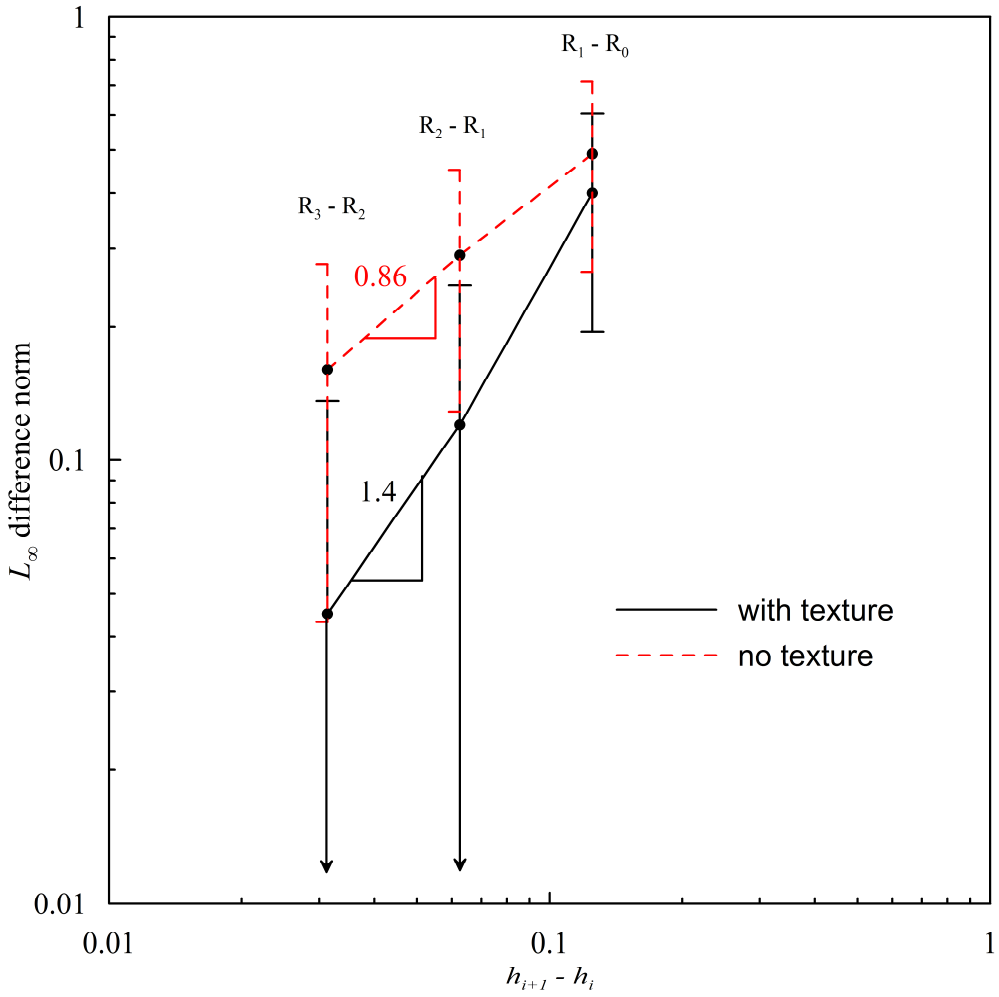

Sandia National Laboratories

Outline

1. Pervasive fracture and fragmentation
2. Random meshes and a polyhedral finite-element formulation
3. Assessing mesh convergence in a probabilistic sense
4. Example of statistical convergence using dynamic ring expansion
5. What is material variability (multi-scale)?
6. Summary

Summary

1. Presented a finite-element method for modeling pervasive fracture in materials and structures based on random meshes.
2. Presented a polyhedral finite-element formulation for both convex and nonconvex elements.
3. If engineering quantities-of-interest are extremely sensitive to initial conditions and system parameters, need to embrace a probabilistic description.
4. Presented a statistical-method for verifying and validating nonlinear dynamical systems in this regime including pervasive fracture.

Bishop, J., 2009, "Simulating the Pervasive Fracture of Materials and Structures using Randomly Close Packed Voronoi Tessellations," *Computational Mechanics*, 44, p. 455-471.

Bishop, J. and Strack, O., 2011, "A Statistical Method for Verifying Mesh Convergence in Monte Carlo Simulations with Application to Fragmentation," *International Journal for Numerical Methods in Engineering*, 88, p. 279-306.

Bishop, J., VanGoethem, D., Sweetser, J., (submitted) "On the Propagation of Uncertainty in Nonlinear Dynamical Systems," *International Journal for Uncertainty Quantification*.

Bishop, J., Martinez, M., Newell, P. (submitted) "A Finite-Element Method for Modeling Fluid-Pressure Induced Discrete-Fracture Propagation using Random Meshes," *46th US Rock Mechanics / Geomechanics Symposium*